Investigating the Modulating Effects of Afriplex GRT^{TM} Extract on Vascular Function and Antioxidant Status in Obese Wistar Rats

by
Zimvo Maqeda

Thesis presented in fulfilment of the requirements for the degree of Master of Science in the Faculty of Medicine and Health Science at Stellenbosch University

Supervisor: Dr Shantal Windvogel
Co-supervisor: Prof. Barbara Huisamen

March 2018

DECLARATION

By submitting this thesis electronically, I declare that the entirety of the work contained therein is my own, original work, that I am the sole author thereof (save to the extent explicitly otherwise stated), that reproduction and publication thereof by Stellenbosch University will not infringe any third party rights and that I have not previously in its entirety or in part submitted it for obtaining any qualification.

Zimvo Maqeda

Date: March 2018

Abstract

Introduction

Obesity is associated with the development of metabolic syndrome, a conglomerate of cardiometabolic risk factors, which synergistically result in cardiovascular diseases (CVDs), the major leading cause of death worldwide. The indigenous South African plant Rooibos (*Aspalathus linearis*), contains polyphenolic phytochemicals such as aspalathin, which is unique to Rooibos and has been associated with its health promoting properties. These include antidiabetic, anti-inflammatory, antioxidant, anti-obesity and cardiovascular benefits. Not much is known about the health promoting properties of Afriplex GRT^{TM}, an aspalathin-rich Rooibos extract. It is hypothesised that Afriplex GRT™ may ameliorate the development of hypertension, vascular dysfunction and oxidative stress in a model of obese Wistar rats.

Aim

To investigate the ameliorative effect of Afriplex GRT™ extract on blood pressure, vascular function and oxidative stress in diet-induced obese Wistar rats.

Methods

Adult male Wistar rats were randomly divided into 5 experimental groups (n=10/group) and fed a Control or high-fat-diet (HFD), to induce obesity over a period of 16 weeks. Rats in the HFD and Control groups received the aspalathin-rich extract supplemented at 60 mg/kg/day from week 10 to 16. A Captopril (50 mg/kg/day) group was included as a positive control. Food and water intake, body weight, blood glucose, blood pressure, intraperitoneal (IP) fat mass, liver weight, leptin levels and vascular reactivity was measured. Western blotting of proteins involved in vascular function such as eNOS, AMPK and PKB were performed in aortic tissue. Antioxidant status and oxidative stress were determined in the liver tissue of experimental groups. This was done by measuring the activities of the primary antioxidant enzymes superoxide dismutase (SOD), catalase (CAT), glutathione peroxidase (GPx), and performing the thiobarbituric reactive substances (TBARS) assay which measures malondialdehyde as an indicator of lipid peroxidation.

Results and Discussion

HFD animals presented with increased food intake, leptin levels, body weight, glucose levels, IP fat and liver mass compared to Control animals. Furthermore, HFD animals had decreased

fluid intake and increased blood pressure vs the Control animals. Additionally, they presented with a downregulation in total and phosphorylated PKB and AMPK expression. HFD rats also had reduced SOD, CAT and GPx activity, increased malondialdehyde (MDA) levels and phosphorylated eNOS levels vs Control animals. Supplementation with GRT extract significantly decreased body weight, leptin levels, IP fat, liver mass and improved glucose metabolism. Furthermore, it increased vasodilation, total eNOS expression, AMPK phosphorylation according to the AMPK ratio, whereas it decreased blood pressure. Additionally, it upregulated SOD, CAT and GPx activity and decreased MDA levels in the liver. Captopril decreased blood pressure, increased vasodilation and upregulated PKB, AMPK and eNOS expression. Therefore, supplementation with GRT extract alleviated the plethora of cardiovascular risk factors presented by the HFD animals.

Conclusion

The HFD model demonstrated detrimental effects on cardiovascular health. Treatment with the Afriplex GRT^{TM} extract improved glucose metabolism, vascular function and antioxidant status in the HFD animals. Therefore, Afriplex GRT™ extract may be a potential therapeutic agent against obesity-related vascular dysfunction, impaired glucose homeostasis, elevated blood pressure and oxidative stress.

Opsomming

Inleiding

Vetsug word geassosieer met die ontwikkeling van metaboliese sindroom, 'n konglomeraat van kardiometaboliese risikofaktore, wat sinergisties lei tot kardiovaskulêre siektes (CVD's), die grootste oorsaak van die dood wêreldwyd. Die inheemse Suid-Afrikaanse plant, Rooibos (*Aspalathus linearis*), bevat polifenoliese fitochemikalieë soos aspalatien, wat uniek is aan Rooibos en geassosieer word met sy gesondheidsbevorderende eienskappe. Dit sluit in antidiabetiese, anti-inflammatoriese, antioksidant, anti-vetsug en kardiovaskulêre voordele. Nie veel is bekend oor die gesondheidsbevorderende eienskappe van Afriplex GRT™, 'n aspalatienryke Rooibos-ekstrak, nie. Daar word gepostuleer dat Afriplex GRT™ die ontwikkeling van hipertensie, vaskulêre disfunksie en oksidatiewe stres kan verbeter in 'n model van vetsugtige Wistar-rotte.

Doelstelling

Om die verbeterende effekte van Afriplex GRT™ ekstrak op bloeddruk, vaskulêre funksie en oksidatiewe stres in dieet-geïnduseerde vetsugtige Wistar-rotte te ondersoek.

Metodes

Volwasse manlike Wistar-rotte is lukraak verdeel in 5 eksperimentele groepe (n = 10 / groep) en is ‘n Kontrole of hoëvet-dieet (HFD) gevoer om vetsug oor 'n tydperk van 16 weke te veroorsaak. Rotte in die HFD- en Kontrole groepe het die aspalatien-ryke ekstrak as aanvulling ontvang vanaf week 10 tot 16 teen 60 mg / kg / dag. 'n Captopril (50 mg / kg / dag) groep is as 'n positiewe kontrole ingesluit. Voedsel- en waterinname, liggaamsgewig, bloedglukose, bloeddruk, intraperitoneaal (IP) vetmassa, lewergewig, leptienvlakke en vaskulêre reaktiwiteit is gemeet. Westerse klad tegnieke is uitgevoer om die uitdrukking van proteïene betrokke by vaskulêre funksie, soos eNOS, AMPK en PKB, in aortiese weefsel te bepaal. Antioksidant status en oksidatiewe stres is bepaal in die lewerweefsel van eksperimentele groepe. Dit is gedoen deur die aktiwiteite van die primêre anti-oksidant ensieme- superoksied dismutase (SOD), katalase (CAT), glutatioonperoksidase (GPx) te meet, en die tiobarbituursuur reaktiewe stowwe (TBARS) te toets wat malondialdehied meet as 'n aanduiding van lipiedperoksidasie.

Resultate en Gevolgtrekking

HFD-diere het verhoogde voedselinname, leptienvlakke, liggaamsgewig, basale glukosevlakke, IP-vet en lewermassa in vergelyking met Kontrole-diere getoon. Verder het HFD-diere verminderde vloeistofinname, en verhoogde bloeddruk teenoor die Kontrole diere gehad. Daarbenewens het hulle 'n onderdrukking in totale en gefosforileerde PKB en AMPK uitdrukking getoon. HFD rotte het ook verlaagde SOD, CAT en GPx aktiwiteit, sowel as verhoogde malonaldialdehied (MDA) en gefosforileerde eNOS vlakke teenoor Kontrole diere getoon. Aanvulling met GRT ekstrak het tot beduidend verminderde liggaamsgewig, leptienvlakke, IP-vet, lewermassa en verbeterde glukose metabolisme gelei. Verder het dit vasodilatasie, totale eNOS-uitdrukking, sowel as AMPK-fosforilering volgens die AMPK-verhouding verhoog, terwyl dit bloeddruk verlaag het. Daarbenewens het dit SOD, CAT en GPx aktiwiteit opreguleer en MDA-vlakke in die lewer verminder. Captopril het bloeddruk verminder, vasodilatasie bevorder en PKB-, AMPK- en eNOS-uitdrukking verhoog. Aanvulling met die GRT ekstrak het dus die oorvloed van kardiovaskulêre risikofaktore waarmee die HFD-diere gepresenteer het, verlig.

Afsluiting

Die HFD-model het nadelige uitwerking op kardiovaskulêre gesondheid getoon. Behandeling met die Afriplex GRT™ ekstrak het glukose metabolisme, vaskulêre funksie en antioksidante status in die HFD diere verbeter. Die Afriplex GRT™ ekstrak mag dus 'n potensiële terapeutiese middel wees teen die behandeling van vetsugverwante vaskulêre disfunksie, verswakte glukose homeostase, verhoogde bloeddruk en oksidatiewe stres.

Acknowledgements

A special thanks to my supervisor, Dr Shantal Windvogel, for her continuous support, patience and guidance throughout my postgraduate journey. I am deeply honoured to have worked with her.

My sincere gratitude to my co-supervisor, prof. Barbara Huisamen for her invaluable input and advice.

A special thanks to my parents (Simphiwe and Nomvulo Maqeda), my sisters (Latisa, Nandile, Zezethu Maqeda), my brother (Aviwe Maqeda) and aunt (Zanele Keto), for their love, continuous support encouragement and for always being there for me in sunshine and in rain throughout this project.

A special thanks to my colleagues in the Department of Medical Physiology, especially Michelle Smit-van Schalkwyk, Mignon van Vuuren, Marlow Kroukamp, Claudine Manirafasha and Lorenzo Bennie for their assistance in the lab.

A sincere gratitude a good friend of mine, Adetayo Emmanuel Obasa, for his continuous support and encouragement throughout this project.

Lastly, I would like to thank the Almighty God, the loving Father for seeing me through and making it possible for me to complete my thesis.

Table of Contents

Abstract iii

Opsomming v

Acknowledgements vii

List of Figures xiii

List of Tables xvi

Appendices xvi

List of Abbreviations xvii

Units of Measurement xxi

Symbols xxi

Chapter 1. Introduction and Literature Review 1

1.1 Introduction 1

1.2 Cardiovascular Disease (CVD) 2

1.2.1 Overview of CVD and Risk Factors 2

1.3 Epidemiology 3

1.4 Obesity as an Independent Risk Factor for Mortality and Morbidity 4

1.4.1 Overview and Epidemiology 4

1.4.2 Assessment and classification 4

1.5 Obesity and the Metabolic Syndrome 5

1.6 Obesity and Adipose Tissue 6

1.7 Obesity and Insulin Resistance 8

1.7.1 AMP-activated protein kinase 10

1.8 Obesity and NAFLD 10

1.9 The Endothelium 11

1.9.1 Endothelial Function 11

1.10 Endothelium-Derived Factors 12

1.10.1 Nitric Oxide (NO) 12

1.10.2 Endothelin-1 (ET) 15
1.10.3 Angiotensin II (Ang II) 15
1.11 Endothelial dysfunction 16
1.11.1 Endothelial dysfunction and Hypertension 16
1.11.2 Endothelial Dysfunction and Oxidative Stress 17
1.12 Hypertension 17
1.12.1 Overview and Epidemiology 17
1.12.2 Primary Causes of Hypertension 18
1.12.3 Secondary Causes of Hypertension 18
1.13 Activation of Renin-Angiotensin-System 20
1.14 Oxidative Stress 20
1.14.1 Overview 20
1.14.2 ROS 21
1.14.3 Antioxidants 22
1.14.3.1 Endogenous Antioxidant Enzymes 23
1.14.3.2 Exogenous Antioxidant Enzymes 23
1.15 Lipid Peroxidation 24
1.16 Rooibos (*Aspalathus linearis*) 24
1.16.1 Overview 24
1.17 Health Promoting Medicinal Effects Rooibos 26
1.18 Conclusion 28
1.19 Motivation of the study and Origin of the GRT Extract 28
1.20 Research Question 29
1.21 Research Aim 29
1.22 Research Objectives 29
Chapter 2. Materials and Methods 30
2.1 Materials 30

2.2 Methods 32
2.3 Animals and Diets 32
2.4 Administration of the treatment 33
2.5 Oral Glucose Tolerance Test (OGTT) 34
2.6 Blood Pressure Measurements 34
2.7 Sample and Blood Collection 35
2.8 Vascular contraction/relation studies 35
2.8.1 Drug Preparation 36
2.8.2 Dissection and Mounting of the Aortic Ring 36
2.9 Initial Round of Stabilization 37
2.9.1 Initial Round of Contraction/Relaxation 37
2.9.2 Second Round Stabilisation 38
2.9.3 Second Round Cumulative Contraction/Relaxation 38
2.10 Western Blot Analysis 39
2.10.1 Tissue Homogenate Preparation 39
2.10.2 Protein Concentration 40
2.10.3 Protein Separation 41
2.10.4 Protein Transfer 41
2.10.5 Immunoblot Analysis 42
2.10.6 Stripping of membranes 43
2.11 ELISA Assay 43
2.11.1 Leptin Assay 43
2.12 Antioxidant Enzyme Analysis 44
2.12.1 Lysate Preparation 44
2.12.2 Determination of Protein Concentration 44
2.13 Catalase (CAT) 45
2.14 Superoxide dismutase (SOD) 45

2.15 Glutathione Peroxidase (GPx) 46
2.16 Thiobarbituric acid reactive substances (TBARS) Assay 47
2.17 Statistical Analysis 49
Chapter 3. Results 50
3.1 Overview 50
3.2 Baseline Studies: Biometric and Blood Pressure Measurements 52
3.2.1 Mean Food and Water Intake 52
3.2.2 Initial Mean Body Weight 54
3.2.3 Blood Glucose: Oral Glucose Tolerance Test (OGTT) 54
3.3 Blood Pressure 57
3.4 Results During and after the 16-Week Treatment Period 59
3.4.1 Biometric Measurements 59
3.4.2 Mean Food Intake 59
3.4.3 Mean Water Intake 60
3.4.4 Body Weight 61
3.4.5 Weekly Body Weight Gain 62
3.4.6 IP Fat Weight 63
3.4.7 Liver Weight 64
3.4.8 Blood Glucose: OGTT 65
3.5 Leptin Assay 67
3.6 Blood Pressure 67
3.7 Vascular Reactivity 70
3.7.1 Phenylephrine Induced Vascular Cumulative Contraction 70
3.7.2 Acetylcholine Induced Vascular Cumulative Relaxation 71
3.8 Western Blot Analysis 72
3.8.1 Example of How the Western Blots Were Calculated 72
3.8.2 AMPK 74

3.8.3 PKB 77
3.8.4 eNOS 80
3.9 Antioxidant status 82
3.9.1 SOD 82
3.9.2 CAT 83
3.9.3 GPx 84
3.9.4 TBARS 85
Chapter 4. Discussion 87
4.1 Biometric Parameters 87
4.1.1 Food and Water Intake 87
4.1.2 Body Weight/Gain 88
4.1.3 IP Fat Weight 89
4.1.4 Liver Weight 89
4.1.5 Blood Glucose 90
4.2 Leptin levels 92
4.3 Blood Pressure 93
4.4 Vascular Function/Reactivity 95
4.5 Western Blot Analysis 97
4.6 Antioxidant Status 99
4.7 Summary of the Main Findings 101
Chapter 5. Conclusion 103
5.1 Final Conclusion 103
5.2 Study Limitations 103
5.3 Future Directions 103
Appendix A: HPLC Analysis of GRT extract 105
Appendix B: Preparation of the strawberry jelly/gelatine blocks for the animals 106
Chapter 6. Bibliography (Stellenbosch Harvard Referencing style) 107

List of Figures

Figure 1.1 Classification of the CVD risk factors. 2
Figure 1.2 Global percentage distribution of NCD deaths that occurred before the age of 70. 3
Figure 1.3 Association of obesity with metabolic syndrome and atherosclerotic cardiovascular disease.. 6
Figure 1.4 Role of the enlarged adipose tissue in the development of CVD risk factors. 8
Figure 1.5 Insulin signalling pathway in the adipose tissue.. 9
Figure 1.6 The production of endothelial nitric oxide and its function in the smooth muscle cell. 14
Figure 1.7 Mechanisms associated with development of hypertension in obese state. 19
Figure 1.8 Fermented (**A**) and unfermented rooibos (**B**). 25
Figure 2.1 Treatment groups (n=8-10/group) for a total duration of 17 weeks. 33
Figure 2.2 Measurement of blood pressure in adult male Wistar rats using non-invasive Coda® system.. 35
Figure 2.3 Aortic segments with PVAT, after removing the clotted blood from the lumen. .36
Figure 2.4 Aortic ring mounted between two stainless steel hooks submerged in the organ bath filled with warm KHB. 37
Figure 2.5 Graphical illustration summary procedure for the aortic ring studies experimental protocol 39
Figure 2.6 Example of a Rat Leptin standard curve with absorbance read at 450 nm. 44
Figure 2.7 Enzymatic coupled reaction used to determine glutathione peroxidase activity. ..47
Figure 2.8 Formation of the MDA-TBA adduct under high temperatures and acidic conditions. 48
Figure 3.1 Summary of the measurements performed throughout the study. 51
Figure 3.2 Mean food intake of the HFD vs Control animals over 10 weeks. 53
Figure 3.3 Mean water intake of the HFD vs Control animals over 10 weeks 53
Figure 3.4 Mean body weight of the HFD vs Control animals in week 10. 54
Figure 3.5 A) Glucose levels (mmol/L) and **B**) AUC representation of glucose tolerance in the HFD vs Control group. **A**) Blood glucose levels (mmol/L) of the HFD vs Control animals. .56
Figure 3.6 Mean systolic blood pressure of the HFD vs Control group. 57
Figure 3.7 Mean diastolic blood pressure of the HFD vs Control group. 58
Figure 3.8 Mean arterial pressure of the HFD vs Control group 58

Figure 3.9 Mean food intake of the HFD vs Control group (GRT treated and untreated). 60
Figure 3.10 Mean water intake of the HFD vs Control group (GRT treated and untreated). .61
Figure 3.11 Body weight measured in week 16 of the HFD vs Control group (GRT treated and untreated). 62
Figure 3.12 Weekly body weight measured over the 16-week period....63
Figure 3.13 IP fat weight of the HFD vs Control group (GRT treated and untreated). 64
Figure 3.14 Liver weight of the HFD vs Control (GRT treated and untreated). 65
Figure 3.15 A) Glucose tolerance (mmol/L) and **B**) AUC analysis for the HFD vs Control group (GRT treated and untreated). 66
Figure 3.16 Leptin levels of the HFD vs Control group (GRT treated and untreated). 67
Figure 3.17 Mean systolic blood pressure of the HFD vs Control group (GRT treated and untreated). 68
Figure 3.18 Mean diastolic blood pressure of the HFD vs Control group (GRT treated and untreated). 69
Figure 3.19 Mean arterial blood pressure of the HFD vs Control group (GRT treated and untreated). 70
Figure 3.20 Cumulative Phenylephrine induced vascular contraction of the HFD vs Control group (GRT treated and untreated). 71
Figure 3.21 Cumulative Acetylcholine induced vascular relaxation of the HFD vs Control group (GRT treated and untreated). 72
Figure 3.22: A 26-well Pre-Cast gel depicting successful protein separation. 73
Figure 3.23: Membrane picture depicting successful protein transfer from the 26-well pre-cast gel. 73
Figure 3.24: Blot depicting bands of the speficic protein probed for. 74
Figure 3.25 T-AMPK expression in the aortic rings of the HFD vs Control group (GRT treated and untreated)....75
Figure 3.26 P-AMPK levels in the aortic rings of the HFD vs Control group (GRT treated and untreated). 76
Figure 3.27 AMPK P:T ratio in the aortic rings of the HFD vs Control group (GRT treated and untreated). 77
Figure 3.28 T-PKB expression in the aortic rings of the HFD vs Control group (GRT treated and untreated)....78
Figure 3.29 P-PKB levels in the aortic rings of the HFD vs Control group (GRT treated and untreated) 79

Figure 3.30 P:T PKB ratio in the aortic rings of the HFD vs Control group (GRT treated and untreated). 79
Figure 3.31 T-eNOS expression in the aortic rings of the HFD vs Control group (GRT treated and untreated).....80
Figure 3.32 P-eNOS expression in the aortic rings of the HFD vs Control group (GRT treated and untreated).....81
Figure 3.33 P: T eNOS ratio in the aortic rings of the HFD vs Control group (GRT treated and untreated). 82
Figure 3.34 SOD activity in the liver of the HFD vs Control group (GRT treated and untreated).. 83
Figure 3.35 Catalase activity in the liver of the HFD vs Control group (GRT treated and untreated).. 84
Figure 3.36 GPx activity in the liver of the HFD vs Control group (GRT treated and untreated). 85
Figure 3.37 TBARS levels in the liver of the HFD vs Control group (GRT treated and untreated). 86

List of Tables

Table 1.1 Obesity classification in relation to health risk 5
Table 1.2 An overview of the endothelin-derived vasoactive factors. 13
Table 1.3 Reactive oxygen species and reactive nitrogen species 21
Table 1.4 Sources of pro-oxidants 22
Table 1.5 Classification of antioxidant defence system components 22
Table 2.1 Cumulative concentrations of Phe and ACh 38
Table 2.2 BSA standard dilutions, done in duplicate 40
Table 2.3 Summary of the western blot protein analysis 42
Table 2.4 BSA standard preparation 45
Table 2.5 MDA standard preparation 49
Table 3.1 Mean food and water intake per rat per day together with the mean body weight gain of the HFD vs Control group before treatment with the GRT extract 52
Table 3.2 OGTT in HFD vs Control animals 55
Table 3.3 Mean systolic, diastolic and arterial pressure of the Control vs HFD group 57
Table 3.4 Summary of the biometric measurements during and after the 16-week treatment period 59
Table 3.5 Mean systolic, diastolic and arterial pressure of the HFD vs Control group, GRT treated and untreated 68

Appendices

Table A.1: HPLC analysis of the GRT extract used in the study 105

List of Abbreviations

6-OHD	-	6-hydroxydopamine
ACE	-	Angiotensin converting enzyme
Ang II	-	Angiotensin II
ACh	-	Acetylcholine
AMPK	-	AMP-activated protein kinase
ADRF	-	Adipocyte-derived relaxing factor
ANOVA	-	Analysis of variance
BCA	-	Bicinchoninic acid
BHT	-	Butylated hydroxytoluene
BMI	-	Body mass index
BSA	-	Bovine serum albumin
cGMP	-	Cyclic guanosine monophosphate
CAT	-	Catalase
CO_2	-	Carbon dioxide
Cu	-	Copper
cGMP	-	Cyclic guanosine-3,5-monophosphate
Cu-Zn	-	Copper-zinc-superoxide dismutase
CVD	-	Cardiovascular Disease
deiH_2O	-	Deionized water
ECL	-	Enhanced chemiluminescence
EDTA	-	Ethylenediaminetetraacetic acid
EDCF	-	Endothelium-derived contracting factors
EDRF	-	Endothelium derived relaxing factors
ED	-	Endothelial dysfunction
EGTA	-	Ethylene-bis(oxyethylenenitrilo)tetraacetic acid

ET-1	-	Endothelin-1
ELISA	-	Enzyme-linked immunosorbance assays
eNOS	-	Endothelial nitric oxide synthase
ETC	-	Electron transport chain
Fe	-	Iron
FFA	-	Free fatty acid
GPx	-	Glutathione peroxidase
GC	-	Guanylate cyclase
GLUT4	-	Glucose transporter 4
GR	-	Glutathione reductase
GRE	-	Green rooibos extract
GRT extract	-	Afriplex GRT^{TM} extract
GSSG	-	Oxidised glutathione
GSH	-	Reduced glutathione
H_2O	-	Water
H_2O_2	-	Hydrogen peroxide
HDL	-	High density lipoprotein
HFD	-	High-Fat-Diet
HPLC	-	High performance liquid chromatography
HRP	-	Horse radish peroxidase
IL	-	Interleukin
IL-1β	-	Interleukin-1 Beta
iNOS	-	inducible nitric oxide synthase
IP fat	-	Intra-peritoneal fat
IRS	-	Insulin receptor substrate
K^+	-	Potassium

KHB	-	Krebs-Henseleit buffer
LDL	-	Low density lipoprotein
MAP	-	Mitogen-activated protein
MDA	-	Malondialdehyde
Mn	-	Manganese
Mn-SOD	-	Manganese superoxide dismutase
N	-	Sample Size
NADPH	-	Nicotinamide adenine dinucleotide phosphate
NaCl	-	Sodium chloride
NAFLD	-	Non-alcoholic fatty liver disease
NCD	-	Non-communicable disease
NF-κβ	-	Nuclear factor kappa beta
nNOS	-	neuronal nitric oxide synthase
NO	-	Nitric oxide
NOS	-	Nitric oxide synthase
Nox	-	NADPH oxidase
$O_2^{\bullet-}$	-	Superoxide
O_2	-	Oxygen
Ob	-	Obese
OGTT	-	Oral glucose tolerance test
Phe	-	Phenylephrine
PMSF	-	Phenylmethylsulfonyl Flouride
PI3K	-	Phosphoinositide 3-kinase
PIP3	-	Phosphoinositide (3,4,5) trisphosphate
PKB	-	Protein kinase B
PPAG	-	Phenylpyruvic acid-2-O-glucoside

PVAT	-	Perivascular adipose tissue
RAAS	-	Renin angiotensin aldosterone system
RNS	-	Reactive nitrogen species
ROS	-	Reactive oxygen species
RSA	-	Republic of South Africa
SEM	-	Standard error of the mean
sGC	-	soluble Guanylyl Cyclase
SOD	-	Superoxide dismutase
SDS	-	Sodium dodecyl sulfate
SNS	-	Sympathetic nervous system
T2DM	-	Type 2 diabetes mellitus
TBA	-	Thiobarbituric acid
TBS	-	Tris-buffered saline
TBARS	-	Thiobarbituric acid reactive substances
TNF-α	-	Tumor necrosis factor alpha
USA	-	United States of America
UK	-	United Kingdom
UV	-	Ultraviolet
VEGF	-	Vascular endothelial growth factor
VPR	-	Volume-pressure recording
VSMC	-	Vascular smooth muscle cells
WHO	-	World Health Organisation
Zn	-	Zinc

Units of Measurement

%	-	Percentage
°C	-	Degrees Celsius
µg	-	Microgram
µmol	-	Micro molar
µl	-	Microliter
µM	-	Micro molar
mmol	-	Millimole
mmHg	-	Pressure
nmol	-	Nano molar
g	-	Gram
m^2	-	Square meter
kg	-	Kilogram
mg	-	Milligram
min	-	Minutes
ml	-	Millilitre
L	-	Litre

Symbols

α	-	alpha
β	-	beta
γ	-	gamma

Chapter 1. Introduction and Literature Review

1.1 Introduction

Obesity is a major leading global health problem, more especially in the developing countries. It is mostly prevalent in the adult population, particularly in women (Baleta & Mitchell, 2014). Obesity is associated with the development of several non-communicable diseases (NCDs), such as cardiovascular diseases (CVDs). Risk factors for CVDs include hypertension, stroke, diabetes, dyslipidaemia, stroke, raised blood glucose, tobacco smoking, a sedentary lifestyle, ethnicity, ageing and a family history of CVDs (World Health Organization, 2017). Amongst the NCDs, CVDs contribute a large percentage of the global deaths annually, rapidly increasing in the low-to-middle income countries, increasing the health and socio-economic burden. Obesity prevalence is also associated with endothelial dysfunction (ED) and oxidative stress (World Health Organization, 2014).

Plant and dietary polyphenols, have been shown to have ameliorative effects on the risk factors for CVDs. The Rooibos (*Aspalathus linearis*) plant in particular, has been of great interest as far as its health benefits are concerned and this includes its effect on cardiovascular health. It is characterised by a rich polyphenolic composition, which includes aspalathin, a unique and major active flavonoid compound (Mikami, Tsujimura, Sato, Narasada, Shigeta, Kato, Hata & Hitomi, 2015). An accumulation of studies have shown that rooibos has numerous health promoting properties, such as anti-hypertensive, antidiabetic, anti-inflammatory, antioxidant, anti-cancer and anti-obesity effects (Mazibuko, Joubert, Johnson, Louw, Opoku & Muller, 2015; Mikami *et al.*, 2015; Persson, Persson, Hägg & Andersson, 2010). When the rooibos plant is harvested, it is processed into the fermented and unfermented product, which may be used to make herbal infusions (Ajuwon, Marnewick & Davids, 2015; Chen, Sudji, Wang, Joubert, Van Wyk & Wink, 2013). The polyphenolic composition of the unfermented rooibos is preserved and as a result, it has been used to produce aspalathin-rich rooibos extracts. The Afriplex^{TM} GRT (GRT) extract used in this study, is a spray dried powder prepared from unfermented Rooibos. To date, no studies have been done investigating the relationship

between the ameliorative effects of the GRT extract on the obesity-induced CVD risk factors, therefore, more scientific investigation is needed.

1.2 Cardiovascular Disease (CVD)

1.2.1 Overview of CVD and Risk Factors

CVD is defined as a group of heart and blood vessel disorders. The major contributors to CVD mortality are coronary heart disease (heart attack) and cerebrovascular disease (stroke). Heart attack and stroke occur when there is a blockage that obstructs blood flow to the heart or brain, respectively (World Health Organization, 2011) The blockage is mainly caused by the deposition of fatty material and cholesterol forming a plaque in the inner walls of the blood vessels supplying the heart and brain. Atherosclerosis is the underlying determinant of the development of heart attack and stroke (WHO, Federation & World Stroke Organization, 2011). CVD risk factors can be classified into three categories, namely; social determinants and drivers (non-modifiable), modifiable behavioural risk factors which subsequently result in 2nd cardiometabolic risk factors, if not well managed (***Fig 1.1***) (World Health Organization, 2011).

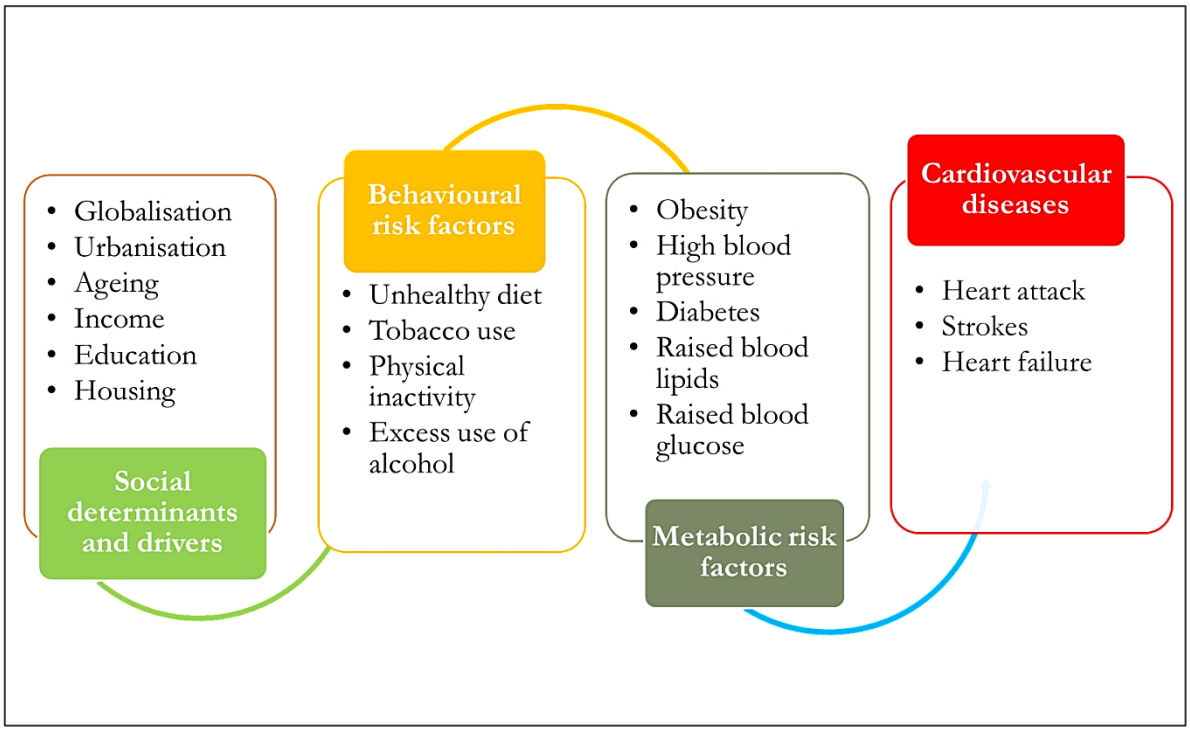

Figure 1.1 *Classification of the CVD risk factors* (World Health Organization, 2011).

1.3 Epidemiology

Non-communicable diseases (NCD) are highlighted as the leading cause of deaths globally, responsible for 40 million deaths (World Health Organization, 2017). It has been estimated that by the year 2030, global deaths due to NCD will increase to 52 million (World Health Organization, 2014). Approximately 16 million of the NCD affect individuals before the age of 70 and over 80% of these deaths occur in low-and-middle income countries and (Al-Mawali, 2015). NCD include CVD (such as stroke and heart attacks), chronic respiratory disease (particularly asthma and chronic pulmonary obstructed disease), cancer and diabetes (Al-Mawali, 2015). CVD are the leading cause of NCD deaths and are accountable for approximately 17.5 million deaths annually. An estimated 7.4 million were as a result of coronary heart diseases and 6.7 million were due to stroke. Secondary cause of NCD deaths is cancer, followed by chronic respiratory diseases and diabetes ***(Fig 1.2***) (Mendis, Puska & Norrving, 2011; World Health Organization, 2017). In South Africa, by the year 2030, deaths due to cardiovascular diseases are expected to have increased by 41% in the working age group (35-64) (Steyn & Fourie, 2007).

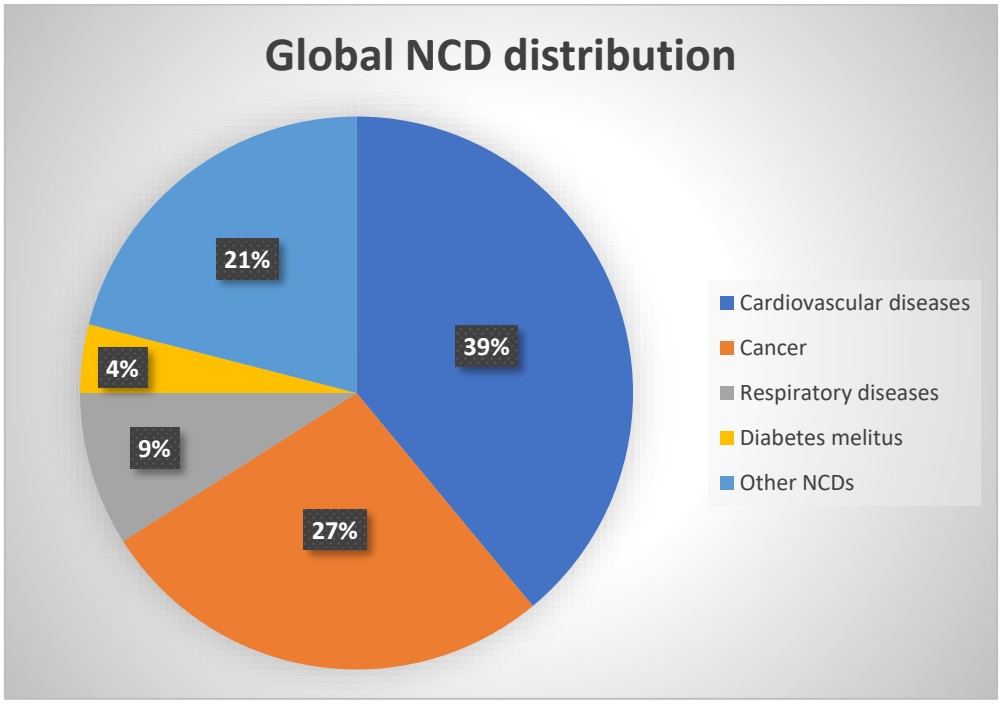

Figure 1.2 *Global percentage distribution of NCD deaths that occurred before the age of 70* (Mendis *et al.*, 2011).

1.4 Obesity as an Independent Risk Factor for Mortality and Morbidity

1.4.1 Overview and Epidemiology

Obesity is defined as the energy imbalance between caloric intake as opposed to that which is expended (Ratzan, 2009). This results in enlarged adipose tissue because of the increased cell size (hypertrophy) and cell number (Hyperplasia) due to excess fat storage (Jo, Gavrilova, Pack, Jou, Mullen, Sumner, Cushman & Periwal, 2009). Excess accumulation of body fat impairs the health of an individual (Mollentze, 2006). Adipose tissue is a connective tissue that stores fat cells or adipocytes and also plays a role as an endocrine organ (Després & Lemieux, 2006).

Obesity is an independent CVD risk factor closely related to the consumption of high-energy dense foods, particularly a diet high in saturated fats, sugars, trans-fat cholesterol coupled with physical inactivity as opposed to low-energy dense foods. Obesity is a modifiable CVD risk factor through changing the diet to a well-balanced healthy diet and increasing physical activity. These changes subsequently reduce coronary heart diseases and other related CVD risk factors. Obesity is a global malady, affecting both adults and the children. In the year 2014, over 1.9 billion adults of 18 years and above were overweight and out of this, more than 600 million were clinically obese. Approximately 42 million children over 5 years were clinically obese in 2013 (Ratzan, 2009). In South Africa in the year 2014, approximately 70% of women and 40 % of men were either obese or overweight (Baleta & Mitchell, 2014).

1.4.2 Assessment and classification

Obesity and overweight can be differentiated according to body mass index (BMI), calculated as body weight (Kg) divided by height (m^2) of the individual (Ratzan, 2009). Obese and overweight persons have a BMI of ≥30 kg/m^2 and >25 kg/m^2, respectively (***Table 1.1***).

Table 1.1 *Obesity classification in relation to health risk* (Seidell & Flegal, 1997).

Category	**BMI (kg/m^2)**	**Heath risk**
Underweight	< 18.5	Increased
Normal weight	18.5-24.9	Normal
Overweight	25.0-29.9	Increased
Class 1 obesity	30.0-34.9	Moderate
Class 2 obesity	35.0-39.9	Severe
Class 3 obesity	40.0-49.9	Extremely high

Although BMI is a clinical method used to identify obese and overweight individuals. The major limiting factor of the BMI method is that, it does not directly measure the fat mass of an individual neither does it differentiate between muscle and fat mass. Therefore, BMI does not accurately measure obesity, especially intermediate obesity. Waist circumference (waist-to-hip ratio), however, is an alternative method that can be used to measure abdominal fat distribution. Definition of abdominal obesity according to waist circumference measurement differs according to gender. Men with a waist circumference greater than 40 (102 cm) are rendered to be abdominal obese and for women, a waist circumference greater than 35 (88 cm) (Seidell & Flegal, 1997). A larger waist circumference is directly proportional to an increased risk of developing multiple CVD risk factors even though BMI is well managed relative to individuals with normal waist circumference.

1.5 Obesity and the Metabolic Syndrome

Obesity, particularly abdominal obesity is associated with the development of metabolic syndrome (MS) and is an independent risk factor for the development of atherosclerotic CVD. MS is defined as a conglomerate of cardiometabolic risk factors that elevates CVD risk and Type 2 Diabetes (T2D) (Després & Lemieux, 2006; Jung & Choi, 2014). MS is characterised by insulin resistance, elevated blood pressure, glucose intolerance, atherogenic dyslipidaemia, and systemic inflammation (***Fig 1.3***) (Després & Lemieux, 2006; Grundy, 2004; Jung & Choi, 2014). Obesity is also strongly associated with ED and the development of oxidative stress, as shown in ***Fig 1.3*** (Todorovic & Mellick, 2015), resulting in atherosclerosis.

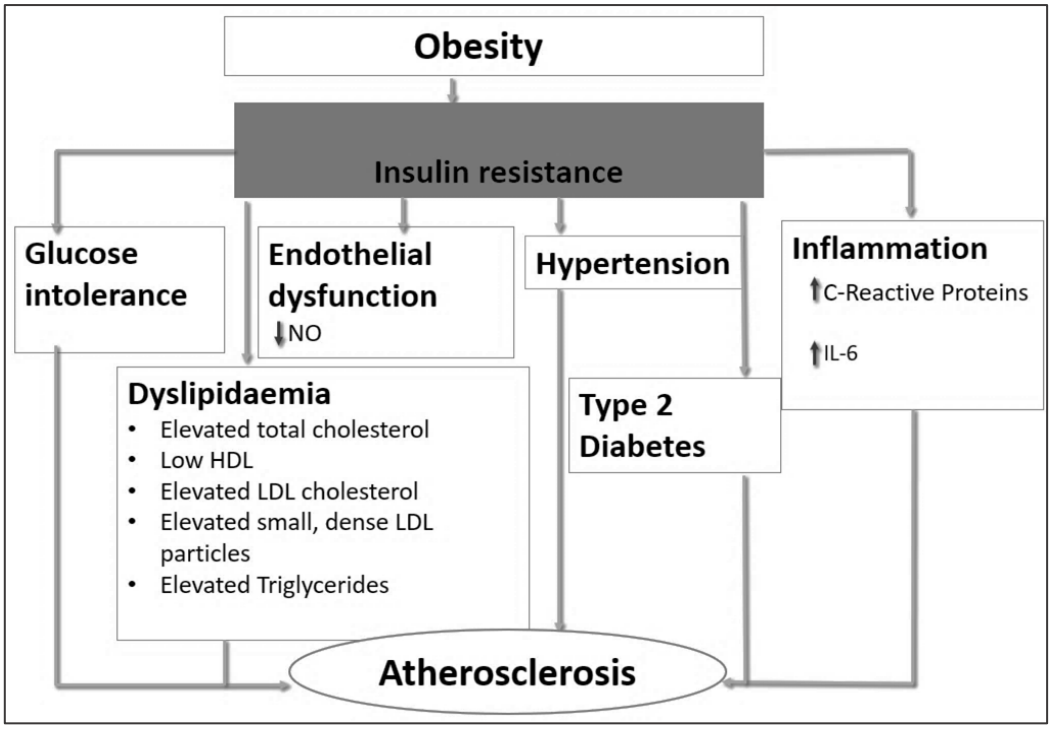

Figure 1.3 *Association of obesity with metabolic syndrome and atherosclerotic cardiovascular disease. Interleukin 6 (*IL-6*), Nitric Oxide (*NO*)* (MacFarlane *et al*., 2001).

The mechanisms underlying the pathogenesis of obesity include modifications in insulin sensitivity, dyslipidaemia, ED and systemic inflammation (Després & Lemieux, 2006). The major driving factors whereby visceral obesity orchestrates the above mentioned metabolic and vascular disorders is through indirect and direct mechanisms. The indirect mechanism is facilitated by the development of insulin resistance (Caballero, 2003; Prieto, Contreras & Sánchez, 2014). Whereas, the direct mechanism, involves the secretion of adipokines such as chemokines, cytokines and hormones by the enlarged and inflamed adipose tissue (Jung & Choi, 2014; Xia & Li, 2017).

1.6 Obesity and Adipose Tissue

Adipose tissue is a connective tissue with dual function. It acts as a major storage site for excess energy in the form of triglycerides but is also considered to be an endocrine organ, secreting chemokines, cytokines and hormones (Jung *et al*., 2014; Kershaw *et al*., 2004). When energy is needed or in a fasting state, the triglycerides are broken down into free fatty acids (FFA) which enter into the various organs a source of energy. In an obese state, there is an increase in the release of pro-inflammatory cytokines, coupled with the downregulation of anti-inflammatory adipokines and release of FFA into the circulation (***Fig 1.4***) (Skurk, Alberti-Huber, Herder & Hauner, 2007). This is attributed to adipocyte hypertrophy as a result of

excess fat accumulation in the adipose tissue. The upregulated pro-inflammatory adipokines include interleukins (IL- 1, 6 & 18), plasminogen activator inhibitor type 1 (PAI-1), tumour necrosis factor alpha (TNF-α), leptin, resistin and angiotensinogen amongst others (Jung & Choi, 2014). The pro-inflammatory production, especially TNF-α, is facilitated by the macrophages and not particularly the adipocytes per se. Accumulation of macrophages is proportional to the adipose hypertrophy and in obesity, there is a macrophage conversion from anti-inflammatory (M2) to pro-inflammatory (M1) macrophages (Jung & Choi, 2014).

The released FFA and pro-inflammatory cytokines, especially TNF-α and IL-1, 6 and 18, enter inside the liver and skeletal muscle and induce modifications in lipid and glucose homeostasis in these metabolic tissues, including modification in the inflammatory responses (Skurk *et al.*, 2007). This consequently induce insulin resistance, inflammation, dyslipidaemia, non-alcoholic fatty liver diseases (NAFLD) and other metabolic syndrome characteristics (Boden, 2008; Kim et al., 2014; Halberg et al., 2008). Additionally, this is also as a result of the impaired production of adiponectin, an insulin sensitizing adipokine that also possess anti-inflammatory effects.

Leptin is a protein produced by the adipose tissue that regulates energy balance and body weight (Kouidhi, Jarboui, Clerget Froidevaux, Abid, Demeneix, Zaouche, Benammar Elgaaied & Guissouma, 2010; Marroquí, Gonzalez, Ñeco, Caballero-Garrido, Vieira, Ripoll, Nadal & Quesada, 2012). It is a hormone that controls appetite, food intake and energy expenditure. However, obese individuals are often at times rendered leptin resistant as a result of the increased circulating levels of leptin and the expression of its mRNA in the adipose tissue (Kouidhi *et al.*, 2010). Leptin has also been shown to play a major role in glucose homeostasis irrespective of the appetite and food intake regulatory action (Marroquí *et al.*, 2012). It improves insulin sensitivity in the liver, skeletal muscle and improves pancreatic β-cell function (Marroquí *et al.*, 2012).

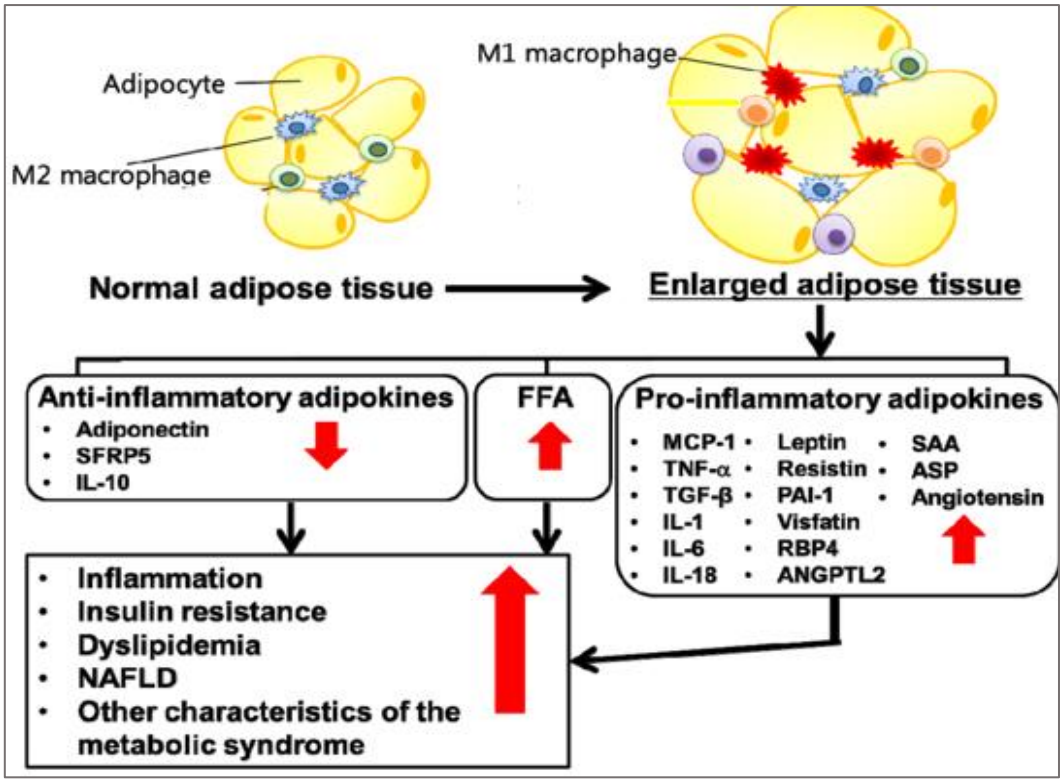

Figure 1.4 *Role of the enlarged adipose tissue in the development of CVD risk factors* (Jung & Choi, 2014). *Monocyte chemoattractant protein-1* (MCP-1), *Plasminogen activator inhibitor-1* (PAI-1), *Retinol binding protein 4* (RBP4), *Angiopoietin Like Protein 2* (ANGPTL2), *Secreted frizzled-related protein 5* (SFRP5), *Serum amyloid A* (SAA), *Severe acute pancreatitis* (ASP) *Tumor necrosis factor alpha* (TNF-α), *Transforming growth factor beta (*TGF-β) *and Interleukin* (IL).

1.7 Obesity and Insulin Resistance

Insulin resistance is defined as the diminished ability of tissues to respond to insulin action (Caballero, 2003; Eringa, Bakker & van Hinsbergh, 2012). It is considered to be the integral feature of the MS, particularly such as T2D. Fig 1 (Muniyappa & Sowers, 2013; Turner, 2013). Insulin modulates glucose and lipid homeostasis by stimulating translocation of the glucose transporter 4 (GLUT4) to the plasma membrane, leading to the upregulation of glucose uptake by tissues, such as adipose tissue, skeletal muscle and the liver (Turner, 2013). In obesity, insulin action is compromised, consequently resulting to insulin resistance. During the insulin resistant state, the activation of downstream signalling pathways is compromised, thus resulting in an inadequate glucose uptake into tissues and a failure to decrease production of glucose by the liver. As a result, the pancreatic beta cells release more insulin into the circulation to compensate for the diminished insulin effectiveness which leads to hyperinsulinaemia, defined as too much insulin in the circulation (Taniguchi, Emanuelli & Kahn, 2006). Obesity-induced-insulin resistance in the adipocytes is linked to the dysregulated

release of pro-inflammatory and anti-inflammatory cytokines by the mature adipocytes and increased FFA production due to lipolysis. This leads to disrupted lipid homeostasis and NAFLD. Therefore, abnormal functioning of the adipose tissue adversely affects the physiological processes of the liver, heart and the skeletal muscle.

Increased FFA in the circulation impairs insulin signalling and obese subjects have been shown to have increased FFA circulating in the plasma as opposed to lean individuals. Therefore, inhibition of lipolysis improves insulin sensitivity, and glucose tolerance in obese individuals. In lean adipose tissue, insulin has anti-lipolytic effects such that it stimulates the hydrolysis of adenosine 3',5'-cyclic monophosphate via activation of phosphodiesterase-3 stimulated by phosphatidyl inositol (PI) 3-kinase (PI3K), thus reducing the release of FFA from the adipocytes. When insulin is released into the circulation, it binds to the insulin receptor on peripheral insulin sensitive tissues and promotes the activation of the insulin receptor substrate (IRS). This leads to the activation of PI3K, subsequently inducing the phosphorylation of the protein kinase B (AKT/PKB kinase) signalling pathway. This pathway is responsible for regulation of glucose and lipid metabolism (***Fig 1.5***) (Taniguchi *et al.*, 2006).

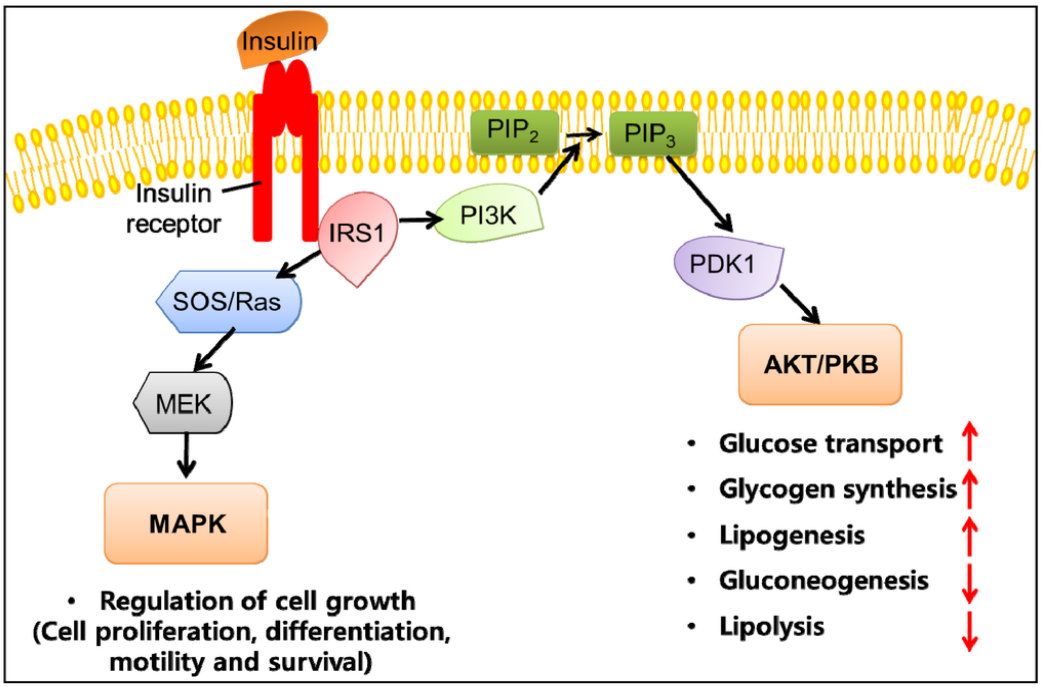

Figure 1.5 *Insulin signalling pathway in the adipose tissue. Insulin binding to its receptor initiates a cascade of signalling events upon phosphorylation of insulin receptor substrate* (IRS) *and AKT/PKB resulting in glucose and lipid metabolism alteration* (Jung & Choi, 2014).

1.7.1 AMP-activated protein kinase

AMP-activated protein kinase (AMPK) is an insulin independent pathway, activated when the Thr172 is phosphorylated on the α-subunit is. Activation of AMPK is induced by nutrient deletion (particularly glucose), ischemia and hypoxic conditions. AMPK can also be activated plant polyphenols such as quercetin and under oxidative stress conditions (Ahn, Lee, Kim, Park & Ha, 2008; Zmijewski, Banerjee, Bae, Friggeri, Lazarowski & Abraham, 2010). When activated, it elicits multiple functions in various organs, such as the liver, skeletal muscle, pancreatic islets and the adipocytes counteracting the pathophysiological-induced metabolic dysfunction. In the liver, it increases fatty acid oxidation, decreases synthesis of cholesterol and lipogenesis. Whereas in the skeletal muscle, it increases glucose uptake and oxidation of fatty acids. In the pancreatic islets it modulates the secretion of insulin and decreases lipogenesis and lipolysis in the adipocytes. Therefore, AMPK is considered an important potential therapeutic target for the treatment of obesity, T2D and cancer (Hardie, 2004; Kim, Jung, Son, Kim, Ha, Park, Jo, Park, Choe, Kim & Ha, 2007; Kim, Yang, Kim, Kim & Ha, 2016; Kim, 2015). It also stimulate the production of NO by inducing the phosphorylation of endothelial nitric oxide synthase (eNOS) in cultured endothelial cells (Zhang, Lee, Kolb, Sun, Lu, Sladek, Kassab, Garland & Shyy, 2006).

1.8 Obesity and NAFLD

NAFLD is categorised into two, steatosis and steatohepatitis, which progress to cirrhosis and liver failure if not reversed. It is one of the chronic liver diseases characterised by an increase in serum aminotransferase (Farrell & Larter, 2006; Kumar & Mohan, 2017). Obesity is regarded as a common cause or primary initiator of NAFLD development. Studies conducted in humans, have shown a positive correlation between the development of steatosis and steatohepatitis and increasing BMI (Choudhary, Duseja, Kalra, Das, Dhiman & Chawla, 2012; Mittendorfer, Magkos, Fabbrini, Mohammed & Klein, 2009; Ruhl & Everharty, 2003).

On the other hand, insulin resistance has been proven to play a significant role in the pathogenesis of NAFLD, especially in obese subjects (Farrell & Larter, 2006). Acute accumulation of triglycerides in the liver is the initial phase to the development of NAFLD. This leads to dysregulation of lipid, glucose and lipoprotein metabolism. Secondly, triglyceride accumulation predispose the liver to inflammation, fibrosis and hepatic injury. The development of the second phase is often characterised by the imbalance in pro-inflammatory and anti-inflammatory cytokine secretion, mitochondrial and oxidative damage and subsequent

lipid peroxidation (Fabbrini, Sullivan & Klein, 2010; Jung & Choi, 2014). An accumulation of studies have shown that NAFLD is strongly associated the development of T2D, dyslipidaemia and hypertension (Adams, Lymp, St. Sauver, Sanderson, Lindor, Feldstein & Angulo, 2005). The development of NAFLD is also driven by genetics, and ethnic background (Adams *et al.*, 2005). NAFLD progression can be effectively reversed by reduction of weight gain, especially visceral obesity and by adopting a healthy lifestyle consequently improving insulin resistance, inflammation, fibrosis, steatosis and hepatic injury.

1.9 The Endothelium

The endothelium is classified as an epithelial tissue lining the interior surface of the blood vessels and plays a major role in vascular homeostasis preventing the development of atherosclerosis (Tang & Vanhoutte, 2010). It also maintains vascular homeostasis by secreting different vasoactive molecules that function to either constrict or dilate the vasculature in response to stimuli (Rajendran, Rengarajan, Thangavel, Nishigaki, Sakthisekaran, Sethi & Nishigaki, 2013; Tang & Vanhoutte, 2010).

1.9.1 Endothelial Function

The endothelium maintains vascular homeostasis through a variety of functions. These include the regulation of vascular tone, vascular growth, inhibition of platelet-leukocyte aggregation, control of vascular inflammation, thrombosis and thrombolysis (Rajendran *et al.*, 2013). These functions are carried out by the endothelium by secreting a variety of endothelium-derived vasoactive factors summarised in ***Table 1.2*** (Mudau, Genis, Lochner & Strijdom, 2012; Rajendran *et al.*, 2013). However, vascular maturity is mediated by the vascular endothelial growth factors (VEGF) secreted by endothelial cells (Rajendran *et al.*, 2013).

The endothelium maintains the vascular tone by secreting vasodilatory factors, nitric oxide (NO) and prostacyclin (PGl_2) (Naruse, Rask-Madsen, Takahara, Ha, Suzuma, Way, Jacobs, Clermont, Ueki, Ohshiro, Zhang, Goldfine & King, 2006; Rajendran *et al.*, 2013). Endothelial cells not only secrete vasodilators but endothelium-derived vasoconstrictors, which include reactive oxygen species (ROS), endothelin-1 (ET-1) and thromboxane A2 (Pober & Sessa, 2007; Vanhoutte, Shimokawa, Tang & Feletou, 2009). These molecules have a positive effect on, the internal alteration of the blood vessel calibre (vasomotion), cell growth and proliferation of endothelial and vascular smooth muscle cells (VSMC) when at normal levels (Pober & Sessa, 2007). In summary, the vasodilatory state entails an enhanced antioxidant activity, an

anti-inflammatory state, thrombolysis and platelet disaggregation. Vasoconstriction on the other hand entails, thrombolysis, adhesion molecules, growth factor, inflammation and increased oxidant activity (Strijdom, Chamane & Lochner, 2009; Strijdom & Lochner, 2009).

1.10 Endothelium-Derived Factors

1.10.1 Nitric Oxide (NO)

Nitric oxide (NO) is a potent endothelium-derived vasodilator of the underlying vascular smooth muscle and was discovered in the 1980's (Sandoo, van Zanten, Metsios, Carroll & Kitas, 2010). It is synthesised by the nitric oxide synthase (NOS) enzyme by converting L-arginine amino acid to NO and L-citrulline. NOS enzyme is comprised of three different isofoms, neuronal (nNOS), inducible (iNOS) and endothelial isoform (eNOS). The neuronal isoform produces NO so to act as a neuronal messenger to stimulate the release of neurotransmitter (Schwartz & Kloner, 2011; Strijdom & Lochner, 2009), inducible isoform expressed only in injured cells which are exposed to inflammatory mediators thus activating macrophages and eNOS produces NO in the blood vessels (Bryan, Bian & Murad, 2009; Strijdom et al., 2009). Dilation of blood vessels is dependent on the activation of eNOS. When inactive, eNOS remains bound to the caveolin-1 protein which is arranged in small caveolae or pockets localised in the cell membrane. eNOS is activated when intracellular calcium levels increase, causing eNOS to detach from the caveolae. The activated eNOS stimulates the release of NO by concerting L-arginine to NO (***Fig 1.6***) (Bae, Kim, Cha, Park, Jo & Jo, 2003).

Activation of eNOS can also be elicited by NO agonists which stimulate the release of calcium from the endoplasmic reticulum. These agonists include; bradykinin, acetylcholine, adenosine tri-phosphate (ATP), adenosine di-phosphate (ADP), cyclic guanosine monophosphate (cGMP). Another mechanism that leads to NO production through eNOS activation is sheer stress (Boo & Jo, 2003). Sheer stress ensures NO production via two processes; it initiates phosphorylation of eNOS via PKB, guanylate cyclase (cGC) and cGMP and through activation of the specialised calcium channels that cause an efflux of the K^+ ions and an influx of Ca^{2+} (Boo, Sorescu, Boyd, Shiojima, Walsh, Du & Jo, 2002). The NO produced diffuses from the endothelial cell to the underlying VSMC and activates the soluble cyclic guanylyl cyclase enzyme ***(Fig 1.6)***.

Table 1.2 *An overview of the endothelin-derived vasoactive factors* (Mudau, Genis, Lochner & Strijdom, 2012).

Endothelium-derived factors	Physiological effects	Enzymatic source and mechanism of action
NO	• Potent vasodilator. • Inhibits inflammation, VSMC proliferation and migration, platelet aggregation and adhesion, and leukocyte adhesion. • Regulates myocardial contractility. • Regulates cardiac metabolism. • Cardioprotective during ischaemia-reperfusion injury.	• It is synthesised by the enzymes: eNOS, nNOS and iNOS, with eNOS being the major source of NO during physiological conditions in the endothelium. • Diffuses from endothelial cells to underlying VSMCs where it binds to an enzyme, soluble guanylyl cyclase, leading to a cascade of events that ultimately result in vascular relaxation.
Prostacyclin (PGI_2)	• Vasodilatory agent. • Inhibits platelet aggregation.	• Derived from arachidonic acid by enzyme cyclooxygenase-2 (COX-2).
Endothelium-derived hyperpolarising factor (EDHF)	• Exerts vasodilatory effects, particularly in small arteries of diameter ≤ 300 µm.	• Its identity is still under suspicion with proposed candidates such as potassium ions and, hydrogen peroxide. • Causes relaxation of VSMCs by means of membrane hyperpolarisation.
Endothelin-1 (ET-1)	• A potent vasoconstrictor.	• Synthesised by endothelin-converting enzyme. • Exerts its effects via two receptors: ET_A expressed on endothelial cells and ET_B on VSMCs. ET_A receptors promote vasoconstriction, whereas ET_B receptors promote NO production and ultimately reduction in ET-1 production.
Thromboxane A (TXA_2)	• A potent vasoconstrictor.	• Derived from arachidonic acid by enzyme COX-1.
Angiotensin II	• A potent vasoconstrictor.	• Synthesised by angiotensin converting enzyme. • Elicits its effects via two receptors: AT_1 which promotes vasoconstriction and cell proliferation, and AT_2 which antagonises the effects of AT_1.

When activated, it enhances the conversion of the guanosine triphosphate (GTP) to cGMP, which leads to the vasodilation of VSMC (***Fig 1.6)*** (Bae, Kim, Cha, Park, Jo & Jo, 2003).

Low calcium levels lead to the dissociation of eNOS from the calcium-calmodulin complex thus binding to the caveolae and becomes inactive. eNOS and iNOS are calcium dependent enzymes. This is in contrast to nNOS, which is calcium-independent and produces NO constitutively in low levels (Strijdom, Chamane & Lochner, 2009). nNOS produces high levels of NO, relatively about 1000-fold more than iNOS and eNOS. This in turn can be dangerous for the cell as NO can bind to the $O_2^{\bullet-}$ free radical, producing peroxynitrite, a highly reactive free radical (Strijdom *et al.*, 2009).

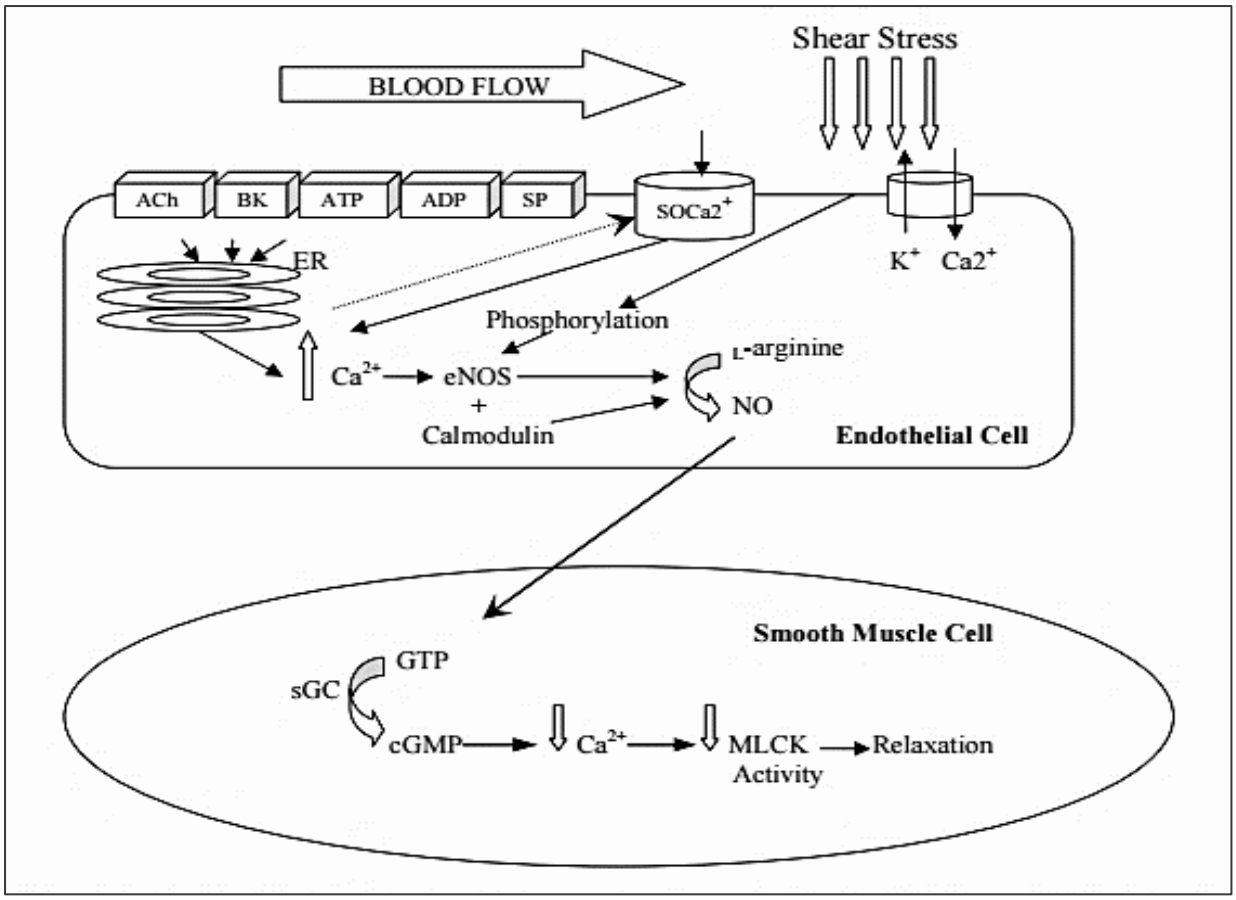

Figure 1.6 The production of endothelial nitric oxide and its function in the smooth muscle cell (Sandoo, van Zanten, Metsios, Carroll & Kitas, 2010). *Acetylcholine* (ACh), *adenosine triphosphate* (ATP), *adenosine diphosphate* (ADP), *bradykinin* (BK), *cyclic guanosine-3', 5-monophosphate* (cGMP), *endothelial nitric oxide* (eNOS), *endoplasmic reticulum* (ER), *soluble guanylyl cyclase* (sGC), *Guanosine-5'-triphosphate* (GTP), *myosin light chain kinase* (MLCK), *nitric oxide* (NO), *store-operated* Ca^{2+} *channel* ($SOCa^{2+}$), *substance P* (SP).

1.10.2 Endothelin-1 (ET)

Endothelin (ET) is classified as a potent vasoconstrictor of the endothelium and has 3 isoforms; ET-1, ET-2 and ET-3. ET-1 is however, the only endothelin which is expressed in the endothelium. The three types of ET-1 receptors are located in the endothelium (ET_{B1}) and in the smooth muscle cell (ET_A and ET_{B2}). ET-1 release and production is regulated by inflammatory cell mediators (TNF-α, interleukin-1 and chemokines) and a decrease in NO However, it has been shown that sheer stress decreases the expression of ET-1 (Böhm & Pernow, 2007). In the normal physiological state, ET-1 binds to ET_A and ET_{B2} receptors causing the calcium smooth muscle channels to open thus allowing an influx of the extracellular calcium into the cells, which leads to vasoconstriction. When ET-1 binds to the ET_{B1} receptors in the endothelium, it elicits a vasodilatory response via the stimulation of NO release (Sud & Black, 2009).

ET-1 is upregulated in cardiovascular risk factors such as and diabetes mellitus obesity (Weil, Westby, Van Guilder, Greiner, Stauffer & DeSouza, 2011). Production of ET-1, a vasoconstrictor, is another underlying cause of ED (discussed in 1.11) in obesity and ET-I is highly expressed in obese individuals with metabolic syndrome (Prieto, Contreras & Sánchez, 2014). In patients with ED (as result of decreased NO bioavailability) it has been shown that blocking the ET_A and ET_{B2} receptors leads to vasodilation. This means that in ED, the ET_{B1} receptors in the endothelium are downregulated while the ET_{B2} are upregulated subsequently resulting in enhanced vasoconstriction (Böhm & Pernow, 2007) An increase in ET-1 expression results in the reduction of eNOS expression which leads to decreased NO production via a protein kinase C (PKC) mechanism (Sud & Black, 2009).

1.10.3 Angiotensin II (Ang II)

Angiotensin II (Ang II) is metabolised from angiotensin I by angiotensin converting enzyme (ACE). It is a potent vasoconstrictor that plays a key role in the development of ED, a common feature of hypertension (Tang & Vanhoutte, 2010). When bound to the angiotensin receptors, it triggers an increase in extracellular calcium, thus mediating vasoconstriction. Ang II also increases the production of ROS through the activation of Nicotinamide adenine dinucleotide phosphate (NADPH) oxidase and the membrane bound NADPH. Furthermore, it directly stimulates the release of endothelin-I, thus aggravating ED (Zhang, Dellsperger & Zhang, 2012).

1.11 Endothelial dysfunction

Endothelial dysfunction (ED) is defined as an imbalance between the production of vasodilatory and vasoconstriction factors acting on the endothelium. ED is considered to be an early predictor or precursor of atherosclerosis and is characterised by a decrease in the bioavailability of NO (Sena, Pereira & Seiça, 2013; Tang & Vanhoutte, 2010).

Development of ED is associated with chronic exposure to CVD risk factors and the harmful stimuli associated with these factors (Mudau, Genis, Lochner & Strijdom, 2012; Sena *et al.*, 2013). The CVD risk factors include hypertension, dyslipidaemia, diabetes mellitus, smoking, physical inactivity, obesity and aging (Yang *et al.,* 2010). The harmful stimuli include the secretion of adipokines, pro-inflammatory cytokines (TNF-α, IL-1, Ang II), increased FFA, including oxidised low-density lipoprotein (LDL), hyperglycaemia and ROS (Mudau *et al.*, 2012).

ED is the most common feature in obese and overweight individuals. The inflamed adipose tissues in an obese state release proinflammatory cytokines in large amounts, which consequently interferes with insulin signalling in endothelial cells and downregulation of NO signalling (eNOS phosphorylation) (Aghamohammadzadeh, Unwin, Greenstein & Heagerty, 2016). Reduction of eNOS enzyme expression, eNOS uncoupling (due to reduction in substrate availability) and increased NO scavenging by $O_2^{\bullet-}$ anions are the underlying mechanisms responsible for the reduction of NO production (Bakker, Eringa, Sipkema & van Hinsbergh, 2009; Kobayasi, Akamine, Davel, Rodrigues, Carvalho & Rossoni, 2010). The development of oxidative stress has been shown to be one of the causes of ED in obese individuals due to elevated $O_2^{\bullet-}$ production which binds with NO forming peroxynitrite, a highly reactive free radical responsible for eNOS uncoupling (Li & Förstermann, 2013; Li, Horke & Förstermann, 2014; Wolin, 2000).

1.11.1 Endothelial dysfunction and Hypertension

In the hypertensive state, the balance between the production of the vasodilators and vasoconstrictors produced by the endothelium is disturbed. This includes the NO pathway and subsequently vasoconstriction factors like ET-1 dominate, resulting in elevated high blood pressure (Bernatova, 2014; Lobato, Filgueira, Akamine, Tostes, Carvalho & Fortes, 2012). Anti-hypertensive drugs, that act to inhibit the ACE such as Captopril can improve vascular function, oxidative stress and stimulate the secretion of bradykinin in order to increase NO bioavailability (Franzini, Ardigò, Valtueña, Pellegrini, Del Rio, Bianchi, Scazzina, Piatti,

Brighenti & Zavaroni, 2012; Rizos, 2014). Patients with diabetes have characteristically low NO bioavailability, resulting from increased oxidative stress levels (Li & Förstermann, 2013; Li, Horke & Förstermann, 2013). Studies have shown a positive correlation between the intake of ACE inhibitors and endothelial function, through an increase in NO bioavailability and a decrease in oxidative stress in type 1 diabetic patients (Gillespie, White, Kardas, Lindberg & Coleman, 2005; Li, Heran & Wright, 2014). Patients with hypertension have low NO levels, high expression of the vasoconstriction factors (ET-1, Ang II and TXA2) and elevated ROS production (Tang & Vanhoutte, 2010). Upon vasodilatory stimuli (acetylcholine and bradykinin), patients with hypertension had poor forearm mediated blood flow and this also indicated ED (Tang et al., 2010). A study showed an impairment in the PKB independent activation of eNOS in a hypertensive rat model (Iaccarino, Ciccarelli, Sorriento, Cipolletta, Cerullo, Iovino, Paudice, Elia, Santulli, Campanile, Arcucci, Pastore, Salvatore, Condorelli & Trimarco, 2004).

1.11.2 Endothelial Dysfunction and Oxidative Stress

Amongst the CVD risk factors, oxidative stress is the major leading cause of ED which is characterised by increased production of ROS, particularly the $O_2^{\bullet-}$. NADPH oxidase, xanthine oxidase and the mitochondria and are the well-known ROS sources and ROS production results in VSMC growth (thickening of the vascular wall) and apoptosis of the endothelium (Iaccarino *et al.*, 2004).The $O_2^{\cdot}$ free radical is scavenged by the superoxide dismutase (SOD) endogenous antioxidant enzyme to H_2O_2 (Pennathur & Heinecke, 2007). Increased production of the $O_2^{\cdot}$ overwhelms the SOD antioxidant enzyme and tends to couple with NO produced, forming peroxynitrite, a highly reactive nitrogen species (RNS). This process is defined as eNOS uncoupling, whereby eNOS acts as a free radical generator in the presence of high O_2^{-} levels. The O_2^{-} has high affinity with NO compared to SOD, which perpetuates the production of peroxynitrite. Increased levels of peroxynitrite in turn damages the cell DNA, lipids and proteins (Landmesser, Harrison & Drexler, 2006).

1.12 Hypertension

1.12.1 Overview and Epidemiology

Hypertension occurs when the blood pressure is greater or equal to ≥140/90 mmHg, systolic and diastolic, respectively. Blood pressure is defined as the force of blood pushing against the walls of the arteries. Hypertension forms part of the CVD risk factors and is often regarded as

a silent killer such that the symptoms are not apparent in the early stages resulting to individuals being undiagnosed. It is most prevalent in the low-and-middle income countries and prevalence increases with age. In 2014, approximately 22% adults (>18 years and above) were hypertensive (WHO, 2014) and 21% adults in South Africa were hypertensive, women contributing a large percentage, relative to men (Steyn, Gaziano, Bradshaw, Laubscher & Fourie, 2001).

1.12.2 Primary Causes of Hypertension

Causes of hypertension can be classified into two categories, primary and secondary. Secondary causes are as a result of the primary causes. The primary causes include behavioural risk factors, such as, sedentary lifestyle, physical inactivity, chronic consumption of alcohol, and tobacco use (***Fig 1.1***). Reduction in salt intake also plays a vital role in preventing the development of hypertension, including the behavioural risk factors especially BMI < 25 kg/m^2 maintenance.

1.12.3 Secondary Causes of Hypertension

The major instigator of hypertension is abdominal obesity (Ritchie & Connell, 2007). Obesity-induced hypertension leads to impaired renal pressure natriuresis mechanism, defined as the relationship between excretion of sodium and mean arterial pressure (Hall, Do Carmo, Da Silva, Wang & Hall, 2015; Hall, Da Silva, Do Carmo, Dubinion, Hamza, Munusamy, Smith & Stec, 2010). In hypertensive patients, it has been shown that this mechanism maintains sodium excretion and water intake, resulting in an increased mean arterial pressure (Jung & Choi, 2014; Lobato, Filgueira, Akamine, Tostes, Carvalho & Fortes, 2012). Several studies have shown that activation of the sympathetic nervous system, activation of the renin angiotensin aldosterone activation system (RAAS) and renal compression, due to accumulation of fat inside and around the kidney impair renal pressure natriuresis (Chandra, Neeland, Berry, Ayers, Rohatgi, Das, Khera, McGuire, De Lemos & Turer, 2014; Thethi, Kamiyama & Kobori, 2012).

Increased leptin levels is another mechanism that elevates blood pressure via activation of the sympathetic nervous system, thus inducing renal failure. Activation of the sympathethic nervous system and fat accumulation inside the kidneys have also been associated with RAAS activation. A deficiency in the natriuretic peptide has been correlated with the poor sodium and water excretion (Asferg, Nielsen, Andersen, Linneberg, Møller, Hedley, Christiansen, Goetze, Esler & Jeppesen, 2013). Previous studies have documented a deficiency in the atrial natriuretic

peptide in hypertensive obese individuals when compared to lean normotensive individuals (Wang, Larson, Levy, Benjamin, Leip, Wilson & Vasan, 2004). Human studies have shown a positive correlation between visceral, renal adiposity and hypertension (Chandra *et al.*, 2014; Chughtai, Morgan, Rocco, Stacey, Brinkley, Ding, Nicklas, Hamilton & Hundley, 2010).

Ang II plays a major role in mediating hypertension by stimulating sodium reabsorption. Previous studies done in diet-induced obese animals have shown an attenuated response in increased blood pressure and sodium retention when ACE is inhibited (Boustany, 2005). In addition, inhibition of the RAAS system may serve as potential therapeutic strategy for hypertension, dyslipidaemia and impaired glucose homeostasis (Putnam, Shoemaker, Yiannikouris & Cassis, 2012).

Other pathophysiological causes of the obesity-induced hypertension, subsequently resulting to renal injury include insulin resistance, dylipidemia, glucose intolerance and inflammation (Engeli, 2005). In an obese state, the inflamed adipocytes release adipocytokines in significant amounts, which subsequently induce the development of hypertension and metabolic syndrome via different pathways as that depicted in ***Fig 1.7.*** (Katagiri, Yamada & Oka, 2007)**.**

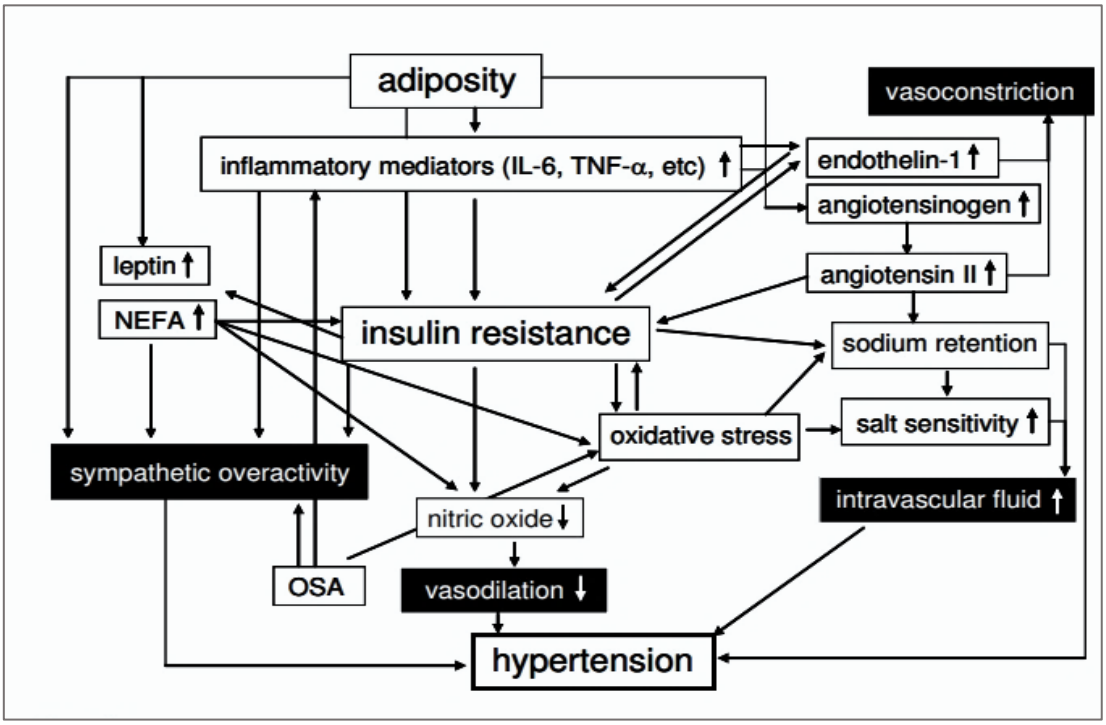

Figure 1.7 *Mechanisms associated with development of hypertension in obese state. interleukin*-6 (IL-6); *non-esterified fatty acids* (NEFA), *obstructive sleep apnea* (OSA*) and tumor necrosis factor-α* (TNF-α), (Yanai, Tomono, Ito, Furutani, Yoshida & Tada, 2008).

1.13 Activation of Renin-Angiotensin-System

Activation of the RAS is common in obesity and it plays a major role in blood pressure regulation and fluid homeostasis (Thethi *et al*, 2012). RAAS activation is stimulated by the production of adipocytokines (angiotensinogen), sympathetic stimulation, hyperinsulinemia and structural changes in the kidney, as well as adverse changes in sodium retention (Thethi *et al*., 2012). Angiotensinogen is highly expressed in adipocytes which results in increased levels of angiotension II production (Engeli, Schling, Gorzelniak, Boschmann, Janke, Ailhaud, Teboul, Massiéra & Sharma, 2003). Hence studies have found a high expression of ACE and angiotensin type 1 receptor in adipose tissues (Engeli *et al*., 2003).

1.14 Oxidative Stress

1.14.1 Overview

Oxidative stress occurs when there is an imbalance between the normal cellular production of pro-oxidants and endogenous antioxidant enzymes and plays a major role in the pathogenesis of numerous diseases such as CVD and risk factors thereof, such as ED (Ajuwon, Marnewick & Davids, 2015).

Pro-oxidants are primarily composed of free radicals, defined as ions or atoms that have a non-paired electron on the outer orbital, thus rendered to be highly reactive. The highly reactive and unstable nature of the free radicals lead to generation of more free radicals. This occurs when they bind to macromolecules in search for electrons to complete the outer orbital, resulting to oxidation of the macromolecules. Sources of free radicals are; oxygen, nitrogen, chlorine and sulphur. When they react with oxygen and nitrogen, they form ROS and RNS, respectively. ROS and RNS are essentially produced as by-products by aerobic organisms during normal metabolism, their examples are listed in ***Table 1.3*** (Ajuwon, Oguntibeju & Marnewick, 2014).

Table 1.3 *Reactive oxygen species and reactive nitrogen species* (Ajuwon, Marnewick & Davids, 2015; Dhawan, 2014).

ROS	**RNS**
Radicals	
Superoxide: $O_2^{\cdot-}$ Hydroxyl: OH· Peroxyl: ROO· Alkoxyl: RO· Hydroperoxyl: HOO·	Nitric oxide: $NO^{\cdot}$ Nitrogen dioxide: $NO_2^{\cdot}$
Non-radicals	
Hydrogen peroxide: H_2O_2 Hypochlorous acid: HOCL Hypobromus acid: HOBr Peroxynitrite: $ONOO^-$ Ozone: O_3	Peroxynitrite: $ONOO^-$ Alkyl peroxynitrites: ROONO Nitrogen dioxide: NO_2 Nitrosonium cation: $\cdot NO_2$ Nitroxyl anion: NO^- Nitronium anion: NO_2^+

1.14.2 ROS

ROS are exceptionally reactive species containing oxygen and their production can be triggered by a variety of sources classified as endogenous or exogenous as listed in ***Table 1.4.*** ROS are primarily produced by the mitochondria via the mitochondrial electron transport chain, complex I and III being the major production sites. These complexes produce ROS in the mitochondrial matrix in the form of $O_2^{\bullet-}$ radical, during energy transduction. Other important production sites for ROS include xanthine oxidase, NADPH oxidase and eNOS uncoupling (Dhawan, 2014).

The ROS have both beneficial and harmful effects depending on the concentration status. When produced in normal or moderate physiological concentrations ROS exert beneficial effects, such as, acting as signalling molecules, protect against environmental pathogens by functioning as mediators of inflammation and they play a role in maintaining vascular tone via cGMP (Dröge, Granner & Boveris, 2002; Li, Horke & Förstermann, 2014; Pourova, Kottova, Voprsalova & Pour, 2010; Valko, Leibfritz, Moncol, Cronin, Mazur & Telser, 2007). However, when the mitochondrial electron transport chain is impaired, primarily due to a pathophysiological condition, excess ROS is generated as a by-product. Excess production of ROS in the biological system often induce oxidative stress which results in the degradation of lipids, membranes, proteins and nucleic acids (Scherz-Shouval & Elazar, 2011).

Table 1.4 *Sources of pro-oxidants* (Ajuwon, Marnewick & Davids, 2015).

Exogenous	**Endogenous**
High-calorie diet Excessive alcohol intake Tobacco smoke Radiation (UV and X-rays) Environmental pollutants (heavy metals, N-containing compounds Strenuous exercise and psychological stress	Mitochondrial electron transport chain Phagocytosis Neutrophils and macrophages during inflammation Xanthine oxidase NADPH oxidase eNOS uncoupling Oxidation of haemoglobin Enzyme activity including cytochrome P450 system

1.14.3 Antioxidants

Antioxidants play a role in anti-oxidant defence system by regulating the balance between ROS production and their elimination. They can either be endogenous or exogenous produced and further classified as enzymatic or non-enzymatic substances (***Table 1.5***).

Table 1.5 *Classification of antioxidant defence system components* (Ajuwon *et al.*, 2015).

Endogenous	**Exogenous**
Non-enzymatic	
Thiols (glutathione, lipoic acid, N-acetyl cysteine) Ubiquinones (coenzyme Q10) Uric acid Bilirubin Transferrin Albumin	Carotenoids (β-carotene) Vitamin C Vitamin E Vitamin A Plant phenols (flavonoids and other polyphenol types) Metals (copper, manganese, selenium and Zinc)
Enzymes	
Superoxide dismutase (SOD) Catalase (CAT) Glutathione peroxidase (GPx) Glutathione reductase (GR)	

1.14.3.1 Endogenous Antioxidant Enzymes

Endogenous enzymes are localised in different areas, functioning to protect the cells against oxidative damage. These innate antioxidant enzymes can be classified as SOD, catalase (CAT), glutathione peroxidase (GPx) and glutathione reductase (GR) (***Table 1.5***).

$O_2^{\cdot-}$ is considered a primary and highly reactive ROS radical produced by the mitochondria during energy transduction. Other sources of $O_2^{\cdot-}$ include uncoupled eNOS, xanthine and NADPH oxidase. $O_2^{\cdot-}$ radical is converted by the SOD into a less reactive compound, hydrogen peroxide (H_2O_2). SOD can be classified in to 3 main types; Mitochondrial SOD (MnSOD), cytosolic copper/zinc (Cu/Zn) SOD and extracellular SOD. The extracellular SOD is localised in the interstitial spaces of tissues and extracellular fluids, primarily responsible for the SOD activity in the plasma. They function to dismutate the $O_2^{\cdot-}$ radical in various areas to protect the cells from oxidative damage (Pamplona & Costantini, 2011).

H_2O_2 is further metabolised into H_2O and oxygen by the CAT enzyme and also by the glutathione coupled enzyme reaction. The glutathione coupled enzyme reaction consist of GPx, GR and glutathione. Glutathione is the most abundant thiol found in all the cells. In most cells, it exist as reduced glutathione (GSH) and functions to detoxify hydroperoxides. Increased GSH cellular levels may be an indicator of the pathophysiological changes. The glutathione coupled enzyme reaction hydrolyses H_2O_2 by using the GSH as a substrate and is oxidised to glutathione disulphide (GSSG) by GPx. GSH is in turn regenerated via NADPH oxidation by the GR. This reaction is rendered the most important pathway in H_2O_2 metabolism in most cells and provides protection against oxidation of lipids (Pamplona & Costantini, 2011).

1.14.3.2 Exogenous Antioxidant Enzymes

Excessive ROS production including other free radicals tend to overwhelm the innate antioxidant enzyme system, as result, additional exogenous antioxidant defence system is often required (Ajuwon, Marnewick & Davids, 2015). Examples of the exogenous antioxidants, often derived from the diet, include vitamin C (ascorbate), E, A and carotenoids (***Table 1. 5***). Vitamin C is the most abundant non-enzymatic antioxidant in the cells and is often compared glutathione. Ascorbate opposes accumulation of ROS and free radicals by donating an electron to their outer orbital, forming an ascorbate radical (Asc^-). Asc^- is later converted to its former state by NADH- and NADPH-dependent dehydroascorbate reductase and GSH-dependent dehydroascorbate reductase (Wells & Xu, 1994). Vitamin E and carotene protect the cells

against lipid oxidative damage by decreasing the formation of peroxyl to hydroperoxides groups, thus inhibiting the propagation of lipid peroxidation (Brigelius-Flohe & Traber, 1999; Esterbauer, Schaur & Zollner, 1991; Pamplona & Costantini, 2011). Plant phenolics also play a major role in the exogenous antioxidant defence system by protecting the cells against oxidative damage. Their numerous health effects are mainly attributed to their polyphenolic content (Liu, 2003). These polyphenols are mostly found in teas, fruits, vegetables, spices and have been proven to possess ameliorative effects on the CVD risk factors and cancer (Weng & Yen, 2012).

1.15 Lipid Peroxidation

Lipid peroxidation is an oxidative degradation of lipids that occurs when the ROS bind to lipids on the cellular membrane by removing the lipid bound hydrogen molecule, resulting in cellular injury. These ROS include $O_2^{\cdot -}$, ONOO, and OH. They form lipid radicals by binding to the double-carbonated fatty acids on the cell membrane. To stabilise themselves, they bind to oxygen forming peroxyl radical, which later oxidises the neighbouring fatty acids turning into a stable lipid hydroperoxide. The oxidised neighbouring fatty acids propagate the process by oxidising lipids across the cell membrane thus forming multiple lipid hydroperoxides (Jomova, Jenisova, Feszterova, Baros, Liska, Hudecova, Rhodes & Valko, 2011; Valko, Rhodes, Moncol, Izakovic & Mazur, 2006). The generation of these lipid peroxidation is later converted to unstable conjugated dienes that give rise end products that are stable, malondialdehyde (MDA). MDA is the most common example of oxidative stress biomarker and is often used to quantify and access oxidative damage in the cell (Dalle-Donne, Rossi, Colombo, Giustarini & Milzani, 2006).

1.16 Rooibos (*Aspalathus linearis*)

1.16.1 Overview

Rooibos (*Aspalathus linearis*) is a leguminous shrub indigenous to the Cederberg Mountains of the Western Cape, South Africa (Mikami, Tsujimura, Sato, Narasada, Shigeta, Kato, Hata & Hitomi, 2015). In comparison to *Camelia sinensis* teas (black and green tea), it is a caffeine-free herbal infusion/tisane, low in tannin levels (Joubert & de Beer, 2012; Ku, Kwak, Kim & Bae, 2014). Rooibos is known for its flavonoid composition, particularly the unique flavonoids,

aspalathin and aspalalinin. Aspalathin is a C-C linked dihydrochalcone glucoside and aspalalinin, a cyclic dihydrochalcone. Nothofagin, a 3-dehydroxydihydrochalcone glucoside is amongst the flavonoids isolated from rooibos, with vitexin and iso-vitexin as its flavone derivatives. Other flavonoids detected in rooibos include, orientin and iso-orientin. The list of flavonols detected in rooibos include luteolin, rutin, isoquercitrin, quercetin, and catechin (Ku *et al.*, 2014; Snijman, Swanevelder, Joubert, Green & Gelderblom, 2007).

After harvest, rooibos is processed into two different herbal infusions, fermented and unfermented as shown in ***Fig 1.10*** (Olawale *et al.*, 2015). The stems and leaves are bruised and fermented yielding traditional rooibos, red in colour. The latter product is unfermented; thus, its colour is preserved and is classified as green rooibos (Olawale *et al.*, 2015). During the processing of green rooibos, the oxidation step is kept to a minimum. The rooibos shoots are immediately dried at low temperatures and air humidity before being shredded to a certain moisture content (De Beer and Joubert, 2002; Krafczyk and Glomb, 2008).

A   **B**

Figure 1.8 *Fermented* (**A**) *and unfermented rooibos* (**B**).

Thereafter, the shoots are further dried in controlled temperatures until the desired moisture is reached (Van Der Merwe, De Beer, Joubert & Gelderblom, 2015). The traditional rooibos has a sweet aromatic profile and occasionally a caramel note, whilst green rooibos has a hay-like and grassy aroma (Schulz, Joubert & Schütze, 2003).

The fermentation process reduces the polyphenolic content of rooibos and consequently resulting in a major decrease in aspalathin levels, the major bioactive compound in rooibos (Villaño, Pecorari, Testa, Raguzzini, Stalmach, Crozier, Tubili & Serafini, 2010). As a result, high levels of polyphenols, flavonoids and non-flavonoids have been quantified in unfermented green rooibos relative to the fermented red rooibos (Villaño *et al.*, 2010). Studies have proven that the aspalathin content in unfermented green rooibos is 50X higher compared to the

fermented rooibos (Bramati, Minoggio, Gardana, Simonetti, Mauri & Pietta, 2002). The process of fermentation also affects the antioxidant activity as a result of low total polyphenolic content (Awoniyi, Aboua, Marnewick & Brooks, 2012).

The unfermented rooibos is the most commonly used product to generate aspalathin-rich extracts as opposed to the fermented rooibos, as a result of the high phenolic content. To elaborate, powered extracts, such as an aspalathin-enriched green rooibos extract (GRE) and the pure aspalathin have been produced from the unfermented green rooibos and have been used in extensively in experimental studies to study their health benefits (Van Der Merwe, De Beer, Joubert & Gelderblom, 2015).

Unfermented rooibos has been of interest in investigating its beneficial health effects in obesity related cardiovascular risk factors and diabetic related conditions. The combination of rooibos polyphenols ensures effective dose delivery as opposed to one isolated antioxidant (Marnewick, Rautenbach, Venter, Neethling, Blackhurst, Wolmarans & Macharia, 2011).

1.17 Health Promoting Medicinal Effects Rooibos

Marnewick and colleagues (2011), documented an inverse correlation between high flavonoid consumption and cardiovascular risk (heart attack, stroke). A daily consumption of 6 cups of rooibos in 6 weeks yielded a maximum health benefit (Marnewick *et al.*, 2011). This was mainly attributed to its polyphenolic constituents (Pandey *et al*, 2009).

Rooibos has been proven to possess anti-oxidant properties (Van Der Merwe *et al.*, 2015), anti-hypertensive (Persson, Josefsson & Andersson, 2006; Persson, Persson, Hägg & Andersson, 2010), anti-mutagenic, anti-inflammatory (Baba, Ohtsuka, Haruna, Lee, Nagata, Maeda, Yamashiro & Shimizu, 2009) and anti-diabetic effects (Muller, Joubert, De Beer, Sanderson, Malherbe, Fey & Louw, 2012; Son, Minakawa, Miura & Yagasaki, 2013). Studies have further shown that it inhibits lipid peroxidation (Cullere, Hoffman & Zotte, 2013) and lowers blood glucose levels and has cancer modulating effects (Kawano, Nakamura, Hata, Minakawa, Miura & Yagasaki, 2009; Mikami, Tsujimura, Sato, Narasada, Shigeta, Kato, Hata & Hitomi, 2015; Muller *et al.*, 2012; Son *et al.*, 2013). GRE has also been shown to possess protective effects against DNA damage caused by free radicals, thus inhibiting the oxidation of cholesterol which results in clogged arteries, heart attack and stroke and preventing development of cancer (anti-cancer effects) (Gelderblom, Joubert, Gamieldien, Sissing, Malherbe & Maritz, 2017).

The health benefits of aspalathin are equivalent to its bioavailability or how it is metabolised by the body. Therefore, absorption of this flavonoid has been quantified in humans in order to evaluate its biological importance. The plant flavonoids have radical scavenging capabilities (Snijman, Swanevelder, Joubert, Green & Gelderblom, 2007). Chronic high consumption of plant phytochemicals results in improved redox status due to their anti-oxidant activity (Chu *et al*., 2014).

In a study done by Chen (2013), aspalathin exhibited potent protective effects against oxidative stress in *Caenorhabditis elegans* subjected to high glucose concentration compared to fermented rooibos. Furthermore, aspalathin attenuates H_2O_2 the anions and other free radical species (Chen, Sudji, Wang, Joubert, Van Wyk & Wink, 2013)

Oxidative stress has been show to impair insulin action and glucose uptake in myotubes is reduced (Kawano *et al*., 2009). High levels of ROS trigger insulin resistance and suppression of oxidative stress has been shown to improve insulin sensitivity and increase glucose homeostasis (Houstis *et al*., 2006).

A study done by Kamakura (2015) showed intracellular ROS scavenging ability of GRE by reducing the advanced glycation end products (AGEs)-induced ROS levels in cultured RIN-5F pancreatic cells thus protecting them from oxidative stress (Kamakura, Son, de Beer, Joubert, Miura & Yagasaki, 2015).

In vitro studies have shown the effects of GRE and aspalathin to enhance glucose uptake in cultured muscles cells (L6 myotubes) and cultured RIN-5F pancreatic beta cells in the absence of insulin (Kawano *et al.,* 2009; Kamakura *et al*., 2015). It also promotes the uptake of glucose by stimulating the translocation of GLUT4 into the plasma membrane by inducing phosphorylation of AMPK and PKB (Kamakura *et al*, 2015; Son *et al.*, 2013). Furthermore, studies done *in vivo* using a type 2 diabetic model KK-Ay and db/db mice have shown the suppressive effects of GRE and aspalathin have on the increases in fasting blood glucose levels, thus reducing glucose intolerance (Kamakura *et al.,* 2015; Kawano *et al.,* 2009).

Aspalathin has also been proven to decrease blood glucose levels in streptozotocin (STZ)-induced diabetic rats (Muller *et al*., 2012) and increases the production of insulin by the pancreatic beta cells (Kawano *et al*., 2009). According to a study done by Kamakura and colleagues (2015), the fermented rooibos extract was not effective in reducing the plasma glucose levels, due to its low aspalathin content.

1.18 Conclusion

Obesity is a modifiable cardiovascular risk factor, strongly associated with the development of insulin resistance, T2D and hypertension. It is characterised by endothelial dysfunction (ED) via a reduction in nitric oxide bioavailability and an increase in oxidative stress and inflammation, disrupting vascular homeostasis. Individuals with the comorbidities induced by obesity are at a high risk of developing CVDs, such as atherosclerosis, stroke and myocardial infarction. CVDs are the major contributors to mortality. The emerging CVD related mortality can be reversed by effectively controlling CVD behavioural risk factors, such as obesity and lack of physical activity. Additionally, adaptions to lifestyle changes reverse the early stages before manifesting to irreversible chronic damage. Plant polyphenols have been shown to have ameliorative effects against the obesity-induced CVD risk factors, especially polyphenols derived from the rooibos plant. Rooibos (*Aspalathus linearis*), is rich in polyphenols such as aspalathin, and is well-known for its numerous health promoting properties. These include antidiabetic, anti-inflammatory, antioxidant, anti-obesity and cardiovascular benefits. Therefore, Rooibos may have potential in order to counteract the deleterious effects of obesity on cardiovascular health.

1.19 Motivation of the study and Origin of the GRT Extract

CVD are the leading cause of death worldwide, accountable for 17.7 million deaths annually (World Health Organization, 2011). Obesity is a major risk factor for the development of CVD and is associated with the development of insulin resistance, hypertension, increased leptin levels, impaired glucose and lipid homeostasis (Kim, Després & Koh, 2016; Lteif, Han & Mather, 2005; Rader, 2007; Xia & Li, 2017). In South Africa, obesity is more prevalent in women than in men (Baleta & Mitchell, 2014). Obesity is also characterised by ED via a reduction in NO bioavailability, and an increase in oxidative stress and inflammation, which disrupts vascular homeostasis (Prieto, Contreras & Sánchez, 2014).

Rooibos (*Aspalathus linearis*), particularly the unfermented green rooibos, is rich in polyphenols such as aspalathin and nothofagin and its health promoting properties include antidiabetic, anti-hypertensive, anti-inflammatory, antioxidant and anti-obesity effects. These health benefits are attributed to the flavonoid content, especially aspalathin.

Afriplex^{TM} GRT (GRT) extract, an aspalathin-rich *Aspalathus linearis* extract, used in this study is a spray-dried powder produced from unfermented green rooibos. The GRT extract was

prepared and standardized by the Afriplex (Pty) Ltd pharmaceutical company in Paarl, South Africa. To date, there is no information available on the effects of GRT extract on obesity-induced cardiovascular risk factors, such as insulin resistance, hypertension, impaired glucose tolerance, vascular function and oxidative stress. Further research into the cardiovascular benefits of the GRT extract were thus deemed necessary in order to elucidate its potential for use in the amelioration of obesity-related cardiovascular effects.

1.20 Research Question

Does the GRT extract alleviate elevated blood pressure, vascular dysfunction and oxidative stress in diet-induced obese Wistar rats?

1.21 Research Aim

To investigate the ameliorative effects of the GRT extract and the mechanisms involved, on elevated blood pressure, vascular dysfunction, and oxidative stress in diet-induced obese Wistar rats.

1.22 Research Objectives

I. To establish an *in vivo* Wistar rat model receiving treatment for 16 weeks with a high-fat-diet to induce hypertension and obesity.

II. To determine vascular reactivity in diet-induced obese and age matched Control Wistar rats using thoracic aorta with perivascular adipose tissue (PVAT).

III. To determine antioxidant status by measuring the activities of the primary antioxidant enzymes, and determine oxidative stress by measuring lipid peroxidation in diet-induced obese and age matched control Wistar rats.

IV. To determine cardiovascular risk by measuring blood pressure, glucose tolerance in the diet-induced obese and age matched Control Wistar rats.

V. To determine the ameliorative effects of the GRT extract on vascular reactivity, antioxidant status, and cardiovascular risk factors in diet-induced obese and age matched Control Wistar rats.

Chapter 2. Materials and Methods

2.1 Materials

Abcam (Pty) Ltd (Cambridge, USA): Rat Leptin ELISA Kit (ab100773)

AEC Amersham (Buckinghamshire, United Kingdom (UK)): Horseradish peroxidise-linked Anti-Rabbit Immunoglobulin Gene (IgG; Secondary Antibody) and Enhanced Chemiluminescence (ECL) Detection Reagent

Bayer (Pty) Ltd. (Isando, Gauteng, RSA)*:* Eutha-naze (Sodium pentobarbital; $C_{11}H_{17}N_2NaO_3$)

Bio-Rad Inc. (Hercules, California, USA): Criteron™ TGX (Tris Glycine eXtended) stain-Free™ precast gels

Boehriger Mannheim, Cat.127744: Glutathione (GSH; $C_{10}H_{17}N_3O_6S$, Cat. 127744)

Cell Signaling Technologies (Beverly, Massachusetts, USA): Antibodies: Total- and Phosphorylated AMPK, Total- and Phosphorylated PKB/AKT, Total- and Phosphorylated eNOS

Cipla MedPro (Pty) Ltd. (Bellville, Western Cape, RSA): GlucoPlus™ (Conventional glucose meter ***Classical Academy (Colorado Springs, US):*** Trichloroacetic acid (TCA; $C_2HCl_3O_2$)

Dunedin, New Zealand: LabChart 7 Software

Fluka Chemie, Switzerland: Butylated hydroxytoluene (BHT)

Greiner Bio-One Inc. (Monroe, North Carolina, USA): Cryo Vials

Merck (Pty) Ltd. (Darmstadt, Germany)*:* Sodium Chloride (NaCl), Formaldehyde (CH_2O), Ethanol (C_2H_6O). Acrylamide (C_3H_5NO) and Enzyme-linked Immunosorbent Assay (ELISA) kit For Rat/Mouse Insulin. Tris (hydroxylmethyl aminomethane), Methanol (CH_4O) and Polyvinylidene Difluoride (PVDF) Membrane (Immobilon™-P)

San Diego, CA, USA*:* GraphPad Prism® 6 software

Scientific Group (Pty) Ltd. (Milnerton, Western Cape, RSA): Blood Collection Tubes (SGVac Tubes) and Storage Eppendorf

Sigma (St. Louis, MO, USA): Phenylephrine, Acetylcholine, Bicinchoninic Acid (BCA) Protein Assay Kit, Bovine Serum Albumin (BSA), 2-Thiobarbituric acid (TBA; $C_4H_4N_2O_2S$), Phenylmethylsulfonyl Flouride (PMSF; $C_7H_7FO_2S$), Ethylene-bis(oxyethylenenitrilo)tetraacetic acid (EGTA; $C_{14}H2_4N_2O_{10}$), Ethylenediaminetetraacetic Acid (EDTA; $C_{10}H_{16}N_2O_8$), β-glycerophosphate ($C_3H_7Na_2O_6P$), Sodium Orthovanadate (Na_3VO_4), Sodium Dodecyl Sulfate (SDS; $C_{12}H_{25}NaO_4S$), Triton® X-100 ($C_{18}H_{28}O_5$), Mercaptoethanol (C_2H_6OS), Ponceau Red ($C_{18}H_{14}N_2Na_2O_7S_2$), Ammonium Persulfate (APS; $H_8N_2O_8S_2$), Commassie Brilliant Blue ($C_{37}H_{34}N_2Na_2O_9S_3$), Aprotinin ($C_{284}H_{432}N_{84}O_{79}S_7$), Leupeptin ($C_{20}H_{38}N_6O_4$), Polyethylene Glycol Sorbitan Monolaurate (Tween® 20; $C_{58}H_{114}O_{26}$), 1,2-Bis(dimethylamino) ethane (TEMED), Bromophenol blue ($C_{19}H_{10}Br_4O_5S$), Captopril, 6-hydroxydopamine (6-OHD; $C_8H_{11}NO_3$: Catalogue number (Cat) H8523), Potassium dihydrogen phosphate (KH_2PO_4), Perchloric Acid ($HCLO_4$), Diethylenetriaminepentaacetic Acid (DETAPAC; $[(HOOCCH_2)2NCH_2CH_2]2NCH_2COOH$; Cat D6518), Triton X-100 ($C_{18}H_{28}O_5$), Hydrogen Peroxide (H_2O_2), Glutathione Reductase, Cat. G3664) Nicotinamide adenine dinucleotide phosphate (NADPH; $C_{21}H_{29}N_7O_{17}P_3$, Cat. N1630) Sodium Bicarbonate ($NaHCO_3$), Sodium Hydroxide (NaOH), tert-butyly Hydroperoxide, Sodium Azide (NaN_3 Cat. B2633), Monopotassium Phosphate (KH_2PO_4), Dipotassium Phosphate (K_2HPO_4), Sodium Phosphate (Na_3PO_4), 2,2,2-Trichloroethanol ($C_2H_3Cl_3O$), Secondary SignalBoost™ Immunoreaction Enhancer For Secondary Signal Enhancement, Hamilton syringe, BRAND® standard disposable PMMA (semi-micro) cuvettes, TBS (Tris-buffered saline),

Thermo Scientific (Lithuania, European Union): Molecular Marker For Western Blot (PageRuler Prestained Protein Ladder)

2.2 Methods

2.3 Animals and Diets

Ethical clearance for this study was obtained from the Stellenbosch University Animal Ethics Committee (Ethical Number: SU-ACUM15-00102). The study was conducted according to "The Revised South African National Standard for the animal care and use for Scientific Purposes" (South African Bureau of Standards, SANS 10386, 2008). Adult male Wistar rats weighing between 150-210 g and ± 7-8 weeks old were obtained from the Central Animal Facility of the Faculty of Medicine and Health Sciences at Stellenbosch University, for the purposes of this study. They were housed in stainless steel cages containing 4 rats per cage and maintained under a 12-hour day and 12-hour night cycle at 24-25 °C. A total of 48 adult male Wistar rats were randomly divided into the high-fat-diet (HFD) and Control groups (8-10 rats/ group). The animals were placed on the diet for a total duration of 16 weeks and were on treatment for the last 6 weeks of the 16-week diet regime (***Fig 2.1***). The age-matched control group received standard Epol^{TM} rat chow and the diet group received HFD, containing the following contents per kg of food; 390 g Epol^{TM} rat chow + 200 millilitre (ml) water, 100 g fructose, 10 g cholesterol, 600 g holsum cooking fat, 100 g casein (added to equalize protein levels) and two tins of condensed milk (Huisamen, George, Dietrich & Genade, 2013). The HFD diet was specifically adapted to induce high blood pressure (Huisamen *et al.*, 2013). Food and fluid intake were measured thrice weekly and the animals were weighed once a week.

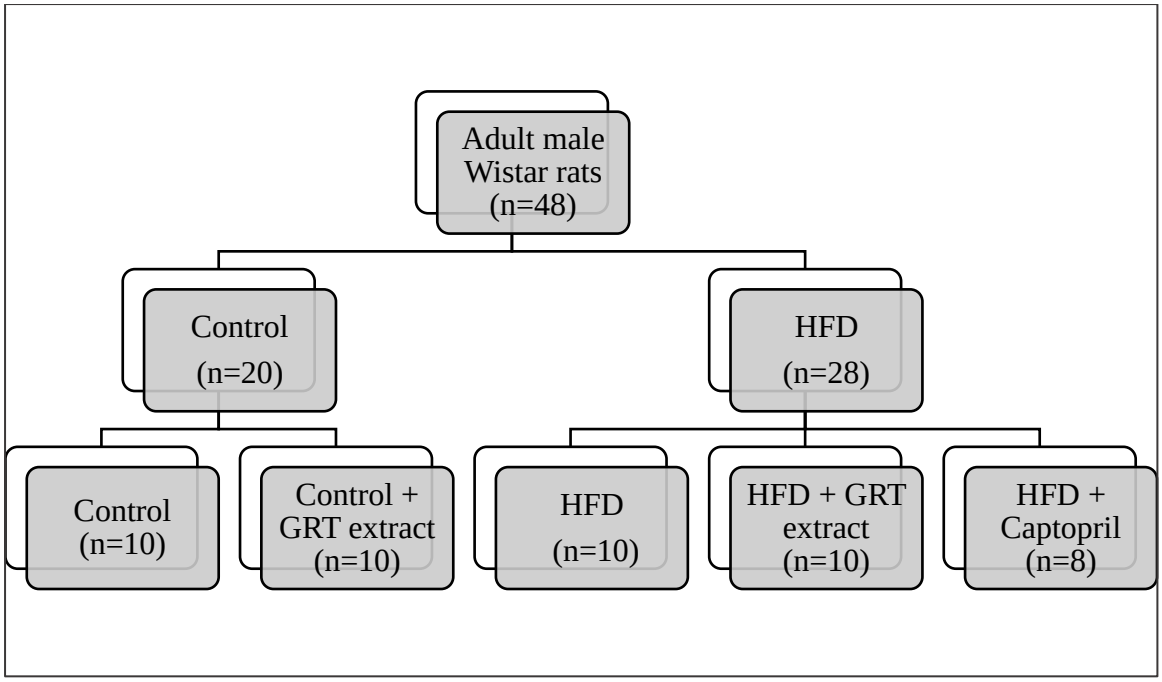

Figure 2.1 *Treatment groups (n=8-10/group) for a total duration of 17 weeks.*

2.4 Administration of the treatment

The GRT extract was kindly supplied by the South African Medical Research Council (SAMRC) coupled with the total polyphenolic composition analysis, performed using the High performance liquid chromatography (HPLC) method (see Appendix A) (Beelders, 2012). The administered GRT extract dose calculation was deduced from available literature on similar extracts (Kamakura, Son, de Beer, Joubert, Miura & Yagasaki, 2015; Muller, Joubert, De Beer, Sanderson, Malherbe, Fey & Louw, 2012). There is currently no evidence on the exact dosage of this specific product. The Captopril dosage was previously used in our laboratory, and used as a positive control in the same rat model (Huisamen *et al.*, 2013). A total of 10 rats per group in both the HFD and the Control group were treated with 60 mg/kg/day of GRT extract. An additional HFD group was included which served as a positive control (n= 8) for blood pressure effects, and were treated with Captopril (50 mg/kg/day), an ACE inhibitor and anti-hypertensive drug (***Fig 2.1***). The GRT extract and Captopril treatments were prepared in the form of strawberry jelly/gelatine blocks and were given to each animal, individually according to their body weight (see Appendix B). The untreated groups (without GRT extract or Captopril supplementation), were given normal strawberry jelly/gelatine blocks to normalise for the additional sugar content present in the jelly/gelatine.

2.5 Oral Glucose Tolerance Test (OGTT)

The OGTT is an experimental procedure that measures the clearance of a glucose load in the body (Stern, Williams & Haffner, 2002). This test was done to examine the insulin sensitivity of the animals. The OGTT's were performed in the week before treatment (week 10) and a week before sacrifice (week 16) in both the Control and HFD groups. The animals were fasted overnight, and had free access to drinking water.

Fasting blood glucose levels were determined using a Glucoplus^{TM} glucometer after a tail prick with a lancet at the tail tip. The animals were anaesthetized by an intraperitoneal injection of 0.1 µl Eutha-naze (53 mg/kg Sodium Pentobarbital) and baseline (0 min, fasting level) glucose levels were taken. The animals were gavaged with 1 g/kg of a sucrose solution (50 %), and the disappearance of glucose in the blood was monitored for 2 hours, with blood glucose readings taken at 3 min, 5 min, 10 min, 15 min, 20 min, 30 min, 45 min, 60 min, 90 min and 120 min, respectively using a glucometer. After the OGTT procedure, the animals were left to recover for a week from this metabolic insult, prior to sacrifice.

2.6 Blood Pressure Measurements

The blood pressure of each animal was measured using a CODA® non-invasive blood pressure acquisition system (Kent Scientific), which utilises a volume pressure recording (VPR) tail-cuff system. The CODA® system measures blood pressure by determining the blood flow in the tail (***Fig 2.2***). Prior to the actual study, the animals were acclimatized to the apparatus (for a period of 2 weeks. Blood pressure was then monitored on a weekly basis for 16-weeks, and baseline levels determined for 2 weeks prior to treatment. In each session, 10 readings of both the systolic and diastolic blood pressure were taken per animal and used to calculate the mean systolic and diastolic pressures.

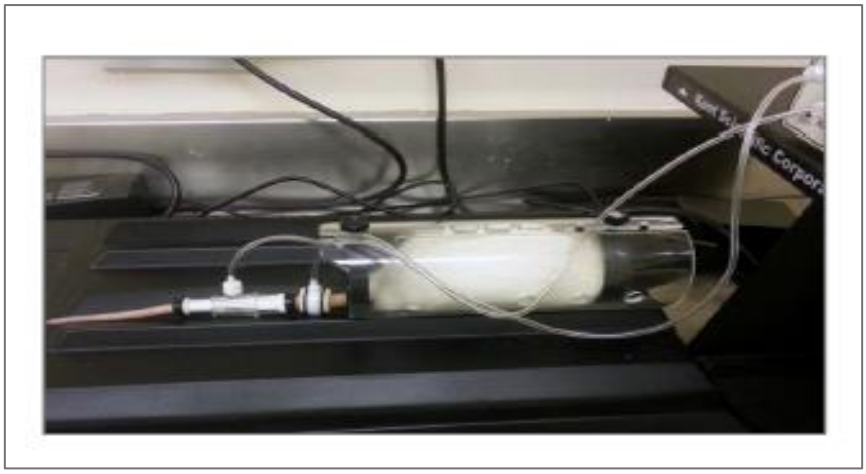

Figure 2.2 *Measurement of blood pressure in adult male Wistar rats using non-invasive Coda® system. Rat on the warming platform with an Occlusion and V-cuff attached to the tail.*

2.7 Sample and Blood Collection

Animals were weighed prior to sacrifice and euthanised with an overdose of Eutha-naze (160 mg/kg body weight, intra-peritoneally). To ensure that the animals were in deep-sleep, thus showing no responses before opening their chest cavity, a foot-pinch (pedal reflex) and an eye-reflex test was performed. Following this, non-fasting plasma glucose levels were determined via a tail prick, measured using a Glucoplus® glucometer. Non-fasting blood was collected from all the animals. It was transferred to vacutainer tubes (SGVac) and allowed to clot at room temperature (25°C). Thereafter, the blood was centrifuged at 1200 x g for 10 min at 4 ˚C. The serum was collected and aliquoted accordingly and stored at -80 ˚C for further analysis. After 30 min, the blood was centrifuged at 1200 g for 10 min at 4˚C. The serum was collected and aliquoted accordingly and stored at -80˚C for further analysis.

The liver, kidney, pancreas and the intra-peritoneal (IP) fat, were removed, rinsed, weighed and snap-frozen in liquid nitrogen and stored at -80 ˚C for future experimental procedures. For the purposes of this study only the liver and IP fat was used for downstream experimental procedures. The thoracic aorta was gently excised from the thoracic cavity of the male Wistar rats, in presence of the PVAT. The aortic ring was then immediately prepared and used for vascular contraction/relaxation experimentation.

2.8 Vascular contraction/relation studies

The vascular contraction/relaxation studies were assed in all the groups using the aortic ring with PVAT. This was done to determine the endothelial function of these animals. PVAT is

the fat surrounding the aortic tissue. In healthy individuals it exerts vasodilatory effects by releasing mediators responsible for vasodilation, such as NO. However, in obese individuals, the vasodilatory effects of PVAT are diminished as a result of macrophage infiltration and oxidative stress, causing compromising the vascular system (Aghamohammadzadeh, Greenstein, Yadav, Jeziorska, Hama, Soltani, Pemberton, Ammori, Malik, Soran & Heagerty, 2013; Aghamohammadzadeh, Unwin, Greenstein & Heagerty, 2016).

2.8.1 Drug Preparation

Phenylephrine (Phe) and Acetylcholine (ACh) stocks were prepared in a 0.9 % saline solution. Phe stock (0.002 g Phe in 10 ml 0.9 % saline) with a final concentration of 1 mM was prepared (Eppendorf tube covered with foil-light sensitive reagent). ACh stock (0.0182 g in 10 ml 0.9 % saline) with a final concentration of 10 mM was prepared and labelled as stock A. Thereafter, stock A was diluted (1 ml of stock A in 9 ml 0.9 % saline) to a final concentration of 1 mM stock B. Finally, stock B was also diluted (1 ml stock B in 9 ml of 0.9 % saline) to a final concentration of 100 µM stock C.

2.8.2 Dissection and Mounting of the Aortic Ring

The aortic ring was removed by initially grabbing hold of the proximal aortic opening (where the heart was cut off), using tweezers and gently cutting horizontally against the spine and the aorta. The clotted blood was carefully removed from the lumen of the aorta before cutting it into 3-4 mm piece, without removing the PVAT (***Fig 2.3***).

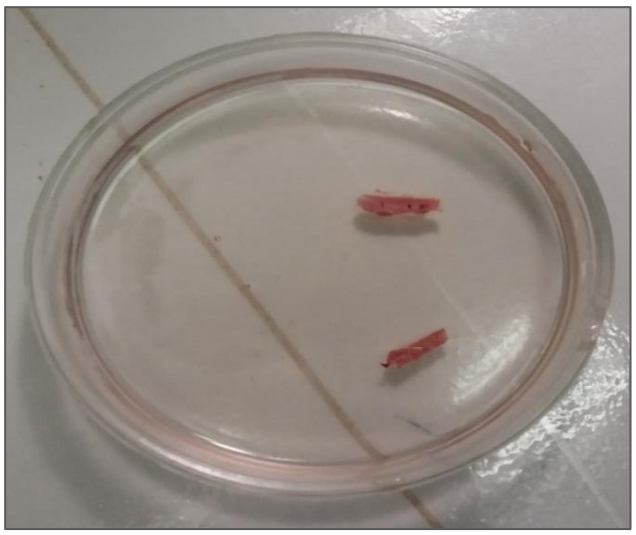

Figure 2.3 *Aortic segments with PVAT, after removing the clotted blood from the lumen.*

The aortic ring was carefully mounted onto two stainless steel hooks (***Fig 2.4***) and slowly submerged inside the organ bath (AD Instruments, Bella Vista, New South Wales, Australia) filled with Krebs-Henseleit buffer (KHB composition in mM: 119 NaCl, 25 $NaHCO_3$, 4.75 KCl, 1.2 KH_2PO_4, 0.6 $MgSO_4.7H_2O$, 0.6 Na_2SO_4, 1.25 $CaCl_2.H_2O$ and 10 glucose) at 37 °C optimum temperature. The organ bath was gassed with 95 % oxygen (O_2) and 5 % carbon dioxide (CO_2). The tension was slowly adjusted to 0.2 g ensuring that the aorta did not fall off during insertion inside the organ bath. The remaining aortic ring was stored at -80 °C for western blot analysis.

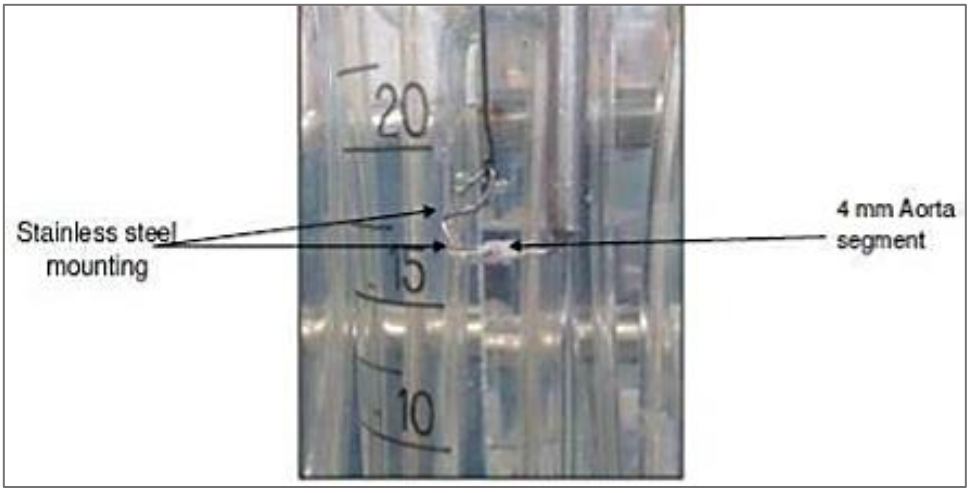

Figure 2.4 *Aortic ring mounted between two stainless steel hooks submerged in the organ bath filled with warm KHB (From Loubser D, MSc thesis, Stellenbosch University, April 2014).*

2.9 Initial Round of Stabilization

The aortic ring (inside the organ bath) was stabilised for a period of 40 min, and the tension was well monitored, changing the buffer after every 10 min. For the first 20 min, the tension was slowly adjusted to 0.8 g. Thereafter the tension was gradually increased to 1.5 g and after 40 min the KHB was changed.

2.9.1 Initial Round of Contraction/Relaxation

After 40 min, the organ bath was adjusted to exactly 25 ml, followed by addition of 100 nM Phe (2.5 µL of 1 mM stock), whereby maximum contraction was observed prior to adding the ACh. ACh (25 µL of stock A) with a concentration of 10 µM was added to the organ bath for maximal dilation. To determine whether to proceed with the downstream experiment, the percentage relaxation of the aortic ring needed to be at least 70 % indicating an intact, fully

functional preparation. The organ bath was rinsed 3 times with pre-warmed KHB, to flush out the drugs and refilled up to 25 ml.

2.9.2 Second Round Stabilisation

The tension was stabilised at 1.5 g for a period of 30 min and the KHB was changed after very 10 min during the 30 min period.

2.9.3 Second Round Cumulative Contraction/Relaxation

After 30 min, cumulative concentrations of Phe (to induce contraction) and ACh (to induce relaxation) were added, respectively, as shown in ***Table 2.1***. After adding the drugs, the data was saved and the aortic ring was measured with a ruler and weighed to ensure that the length was between 3-4 mm. The organ bath was thoroughly rinsed with boiled distilled water (4 times) including the string and the steel hooks. The general outline summary of the experimental protocol procedure is shown in ***Fig 2.5***, modified from Privett, Kunert, and Lombard (2013), vascular reactivity experimental protocol.

Table 2.1 *Cumulative concentrations of Phe and ACh.*

Phenylephrine	Acetylcholine
2.5 µl of stock (100 nM Phe)	7.5 µl of stock C (30 nM ACh)
5 µl of stock (300 nM Phe)	17.5 µl of stock C (100 nM ACh)
5 µl of stock (500 nM Phe)	42.5 µl of stock B (1 µM ACh)
7.5 µl of stock (1 µM Phe)	14.3 µl of stock B (1 µM ACh)
5 µl of stock (1 µM Phe)	220 µl of stock B (10 µM ACh)

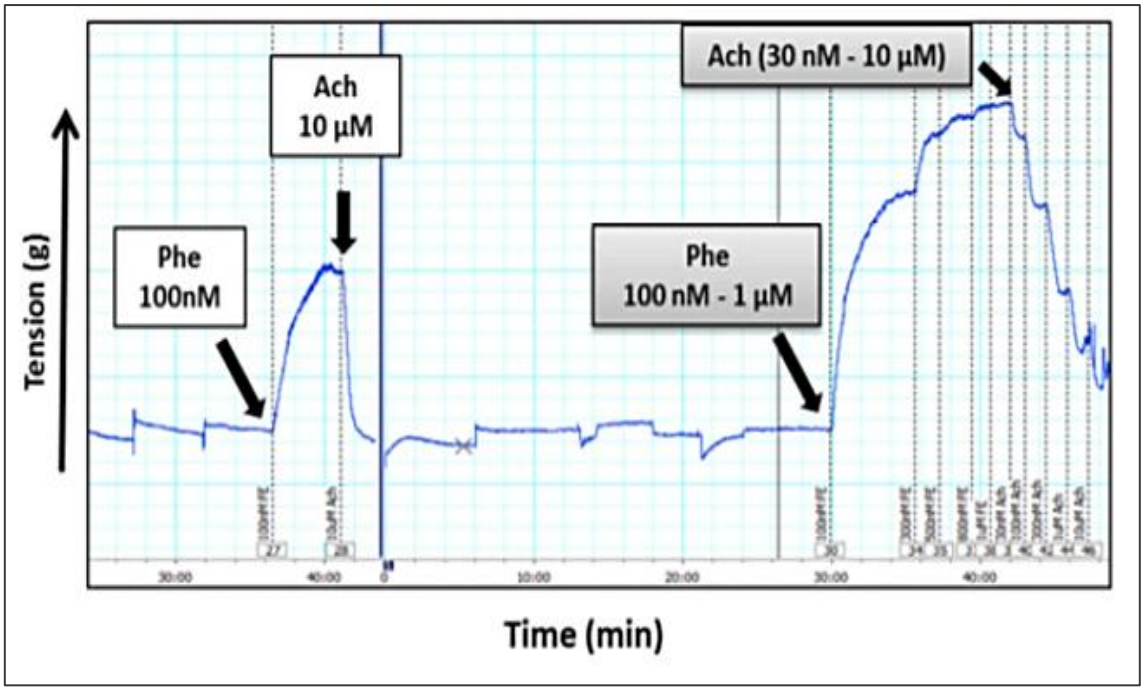

Figure 2.5 *Graphical illustration summary procedure for the aortic ring studies experimental protocol (From Vascular Reactivity: Aortic ring protocol, Laboratory Manual, Stellenbosch University, Westcott C, 2017).*

2.10 Western Blot Analysis

Western blotting was carried out on aortic tissue to determine the expression and activation of proteins involved in endothelial health. These proteins included; AMPK, PKB and eNOS.

2.10.1 Tissue Homogenate Preparation

The frozen sections of the aortic tissue were pulverized in a liquid nitrogen pre-cooled mortar and pestle. The pulverized aortic tissue (40-50 mg) was transferred into a microcentrifuge tube filled with 600 µl of lysis buffer (Composition in mM: 20 Tris-HCl (pH 7.5), 1 Ethylene-bis(oxyethylenenitrilo)tetraacetic acid (EGTA), 1 Ethylenediaminetetraacetic Acid (EDTA), 150 NaCl, 1 β-glycerophosphate, 2.5 Sodiumpyrophosphate, 1 Na_3VO_4, 50 nM NaF, 10 µg/µl leupeptin, 10 µg/ml Aprotinin, 0.1 % Sodium dodecyl sulfate (SDS), 1% Triton X-100 and 50 µg/ml Phenylmethylsulfonyl Flouride (PMSF) which was added last. Stainless steel beads (1.6 mm) were added to the Eppendorf tubes and the samples were homogenised in a Bullet blender® 24 (Next Advance, Inc. New York) at speed 8 for 1 min at 4 °C, for a total period of 3 min with 5 min rest in-between cycles. The samples were allowed to stand on ice for 15 min, thereafter they were centrifuged at 15000 rpm for 20 min at 4 °C. The supernatant was then transferred into clean Eppendorf tubes.

2.10.2 Protein Concentration

The protein concentration of each sample was determined using the Bradford method (Bradford, 1976), immediately after the tissue homogenate preparation step. The supernatant of each sample was diluted in two dilution steps: (A) 10 X dilution (10 µl supernatant + 90 µl dH_20) followed by (B) 5 X dilution (20 µl of (A) + 80 µl dH_20) prepared in duplicate. The 10 X dilution was specifically used to ensure that the unknown samples does not interfere with the low pH achieved by the acid in the Bradford reagent, prepared as explained below (Bradford, 1976). Bovine serum albumin (BSA) standard stock (5 mg/ml) was diluted in a ratio of 1:5 (100 µl BSA stock + 400 µl dH_20) and further diluted in duplicate as shown in ***Table 2.2***.

Table 2.2 *BSA standard dilutions, done in duplicate.*

Stock: [µg/ml]	Volume of Stock (µl)	Solvent (dH_20)	Final volume (µl)
0	0 (Blank)	100	100
1.25	5	95	
2.5	10	90	
5	20	80	
10	40	60	
15	60	40	
20	80	20	

The Bradford reagent containing: 500 mg Commassie Brilliant Blue G-250 protein stain, 250 ml 95 % ethanol and 500 ml phosphoric acid was prepared in a 1:5 dilution (20 ml Bradford stock reagent in 80 ml dH_2O) and filtered using a double layer of Whatman filter paper. A volume of 900 µl of the diluted Bradford reagent was added to the 100 µl standards and samples (B) respectively and allowed to stand for 15 min in order to allow the colour to change from red to blue, under acidic conditions. The sample absorbances were then read in the spectrophotometer (GENESYS™ 20 Visible Spectrophotometer - Thermo Fisher Scientific) at 595 nm. The standard curve was generated in Microsoft™ Excel by plotting the absorbance readings (Y-axis) against the standard protein concentration on the X-axis, as shown in ***Table 2.2***. The sample (lysate) concentrations calculated using the standard curve were further diluted with lysis buffer to render equal protein concentrations per volume unit. Thereafter, a 3 X Laemmli sample buffer (62.5 mM Tris-HCl (pH 6.8), 4 % SDS, 10 % Glycerol, 0.03 % Bromophenol Blue and 5 % β-mercaptoethanol), was added in a 1:2 ratio (Fanglian, 2011).

The sample dilution was performed to control and ensure equal protein loading per gel well (20 µg/15 µl). The samples were boiled for 5 min and were stored overnight at -80 °C.

2.10.3 Protein Separation

The proteins were separated on a Bio-Rad TGX stain-free ™ precast gels, with 26 wells (4-12%) using a Bio-Rad system. The previously stored (-80 °C) samples were boiled again for 5 min and centrifuged at 5000 rpm for 5 min prior to loading an equal volume of sample in the precast gel using a 25 µl Hamilton® syringe (Sigma-Aldrich, St. Louis, MO, USA). A molecular marker (5 µl) was loaded in the first lane of the gel to identify the molecular weight of the specific proteins of interest and thereafter, the samples were loaded sequentially and accordingly into the gel. The running buffer (25 mM Tris, 192 mM glycine and 0.1 % SDS, pH 8.3) was added in the outer gel compartment of the running system. The proteins were then separated by subjecting the polyacrylamide gel to 100 V, 200 mA for 10 min followed by 200 V, 200 mA for 50 min. After protein separation, the gels were activated using the Bio-Rad ChemiDoc™ MP system and the log or record of the exposed PVDF membrane was stored for future normalisation purposes of proteins transferred into the membrane (discussed in section 2.11.4).

2.10.4 Protein Transfer

Prior to protein transfer, the Polyvinylidene fluoride (PVDF) membrane was activated by wetting it in fresh methanol for 30 sec and then placed in the fridge (4 °C), soaked in transfer buffer. The proteins separated by SD-PAGE were transferred onto a PVDF microporous membrane using a Bio-Rad Midi-transfer system and transfer buffer (25 mM Tris-HCl, 192 mM glycine, and 20 % methanol, pH 8.3), for 1 hour at 200 V, 200 mA. After the transfer, the membrane was placed in methanol for 30 seconds and air dried for 15 min. Successful protein transfer onto the membrane was visualised utilising the Bio-Rad ChemiDoc™ MP system (***Table 2.3***).

Table 2.3 *Summary of the western blot protein analysis.*

Protein	Molecular Size (kDa)	Type of Gel	Primary Antibody dilutions	Secondary Antibody dilutions	Exposure Method
AMPK	62	Precast (26 well)	7.5µl/5ml TBS-Tween	1.25µl/5ml TBS-Tween	Bio-Rad ChemiDoc™ MP System
PKB	56	Precast (26 well)	7.5µl/5ml TBS-Tween	1.25µl/5ml TBS-Tween	Bio-Rad ChemiDoc™ MP System
eNOS	140	Precast (26 well)	7.5µl/5ml primary SignalBoost™	7.5µl/5ml secondary SignalBoost™	Bio-Rad ChemiDoc™ MP System

2.10.5 Immunoblot Analysis

The non-specific sites on all the membranes were blocked with 5 % fat free milk in TBS-Tween (Tris-buffered saline and 0.1 % Tween® 20). When the blocking was completed, the membranes were thoroughly washed with TBS-Tween for 1-2 hour at 25 °C in the shaker (Digisystem laboratory instrument, Inc). Following this, the membranes were incubated overnight at 4 °C in a 7.5 µl polyclonal primary antibody solution, diluted in 5ml TBS-Tween or in primary SignalBoost™ as indicated in ***Table 2.3***. Thereafter, the membranes were washed with TBS-Tween for 30 minutes (3 X 10 min) on a shaker (Digisystem laboratory instrument, Inc). All the membranes were again incubated for 1 hour in 1.25 µl HRP-conjugated secondary antibody diluted with 5 ml TBS-Tween (Amersham life science, Buckinghamshire, UK), except for the eNOS membrane. The secondary antibody for eNOS, was diluted in secondary SignalBoost™ Immunoreaction Enhancer for secondary signal enhancement (Sigma-Aldrich, St. Louis, MO, USA). The secondary antibody was removed by washing the membranes again in TBS-Tween for 30 min (3 x 10 min) on the shaker. The proteins were visualised by incubating the membrane with Enhanced chemiluminescence (ECL) detection reagent (2:2 ml of black and white ECL) for 5 min. The membranes were exposed in the Bio-Rad ChemiDoc™ MP system and analysed with Image Lab ™ 5.2.1 software (***Table 2.3***). The obtained values from the exposed bands of the blot were normalised towards the full protein that was transferred to the PDVF membrane for equal protein loading, as a result Bio-Rad ChemiDoc™ MP system does not need a loading control.

2.10.6 Stripping of membranes

When the membranes were re-probed with a different specific antibody it was accomplished according to the following procedure: Membranes were washed 2 times for 5 min in distilled water (dH_2O), incubated in 0.2 M sodium hydroxide (NaOH) stripping buffer and washed again 2 times for 5 min in dH_2O. Thereafter, the membranes were incubated in 5% fat free milk in TBS-Tween for 2 hours and the procedure described in section 2.10.5 was followed.

2.11 ELISA Assay

A commercially available Millipore Rat/Mouse Enzyme-Linked Immunosorbent Assay (ELISA) kit was utilised for the quantification of Leptin in the serum collected from non-fasted blood of the Control and HFD groups, previously stored at -80 ºC described in section 2.7. The results were analysed using a four-parameter algorithm (4PL) software ELISA program which was used to set up the dose response standard curve (http://www.elisaanalysis.com). This ELISA assay was used to determine the expression of leptin levels in the different treatment groups, as shown in ***Fig 2.1***.

2.11.1 Leptin Assay

A rat leptin antibody coated 96-well plate and other relevant reagents were provided and were allowed to equilibrate at room temperature (25 ºC) prior to use. A standard stock (50 ng/ml) solution was diluted with 1 X assay diluent D and subsequently diluted to concentrations ranging from 8,000 pg/ml to 39.92 pg/ml to yield the leptin standard curve (***Fig 2.6***). A blank composed of only the assay diluent D was included. The samples were diluted with 1 X assay diluent D to bring them within the linear standard value range. Standards and sample (100 µl) were added in duplicate to the appropriate wells and the plate was incubated for 2.5 hours at room temperature with gentle shaking.

After incubation, the plate was washed 4 times by filling the wells with 300 µl of 1 X wash buffer solution. Excess wash buffer after the final wash was aspirated and the plate was dried thoroughly. 100 µl of biotinylated anti-rat leptin antibody was added to all the wells and the plate was incubated for 1 hour at room temperature with gentle shaking. The solution was discarded and the wash step was repeated as described above. Following this, 100 µl of 1 X HRP-Streptavidin solution was added to all the wells and the plate was incubated for 45 min at room temperature in the dark with gentle shaking. The solution was discarded and the plate was thoroughly washed. Thereafter, 100 µl of TMB One-Step Substrate Reagent was added to

all the wells and the plate was incubated for 30 min at room temperature in the dark with mild shaking. The absorbance was read immediately at 450 nm after adding 50 µl of the stop solution to all the wells using a FLOUstar® Omega Microplate Reader.

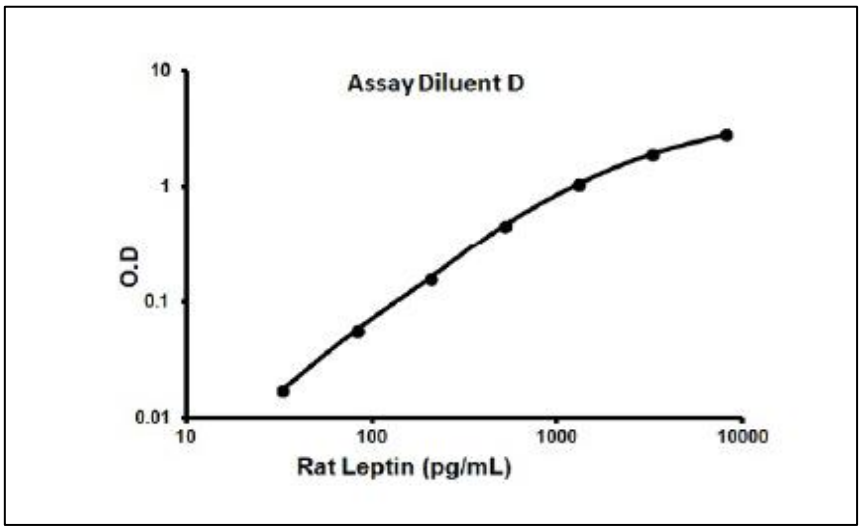

Figure 2.6 *Example of a Rat Leptin standard curve with absorbance read at 450 nm* (Abcam, 2013).

2.12 Antioxidant Enzyme Analysis

2.12.1 Lysate Preparation

Tissue homogenates were prepared from the previously stored liver tissue at -80 ºC, described in Section 2.7. Thin sections of the tissue were cut (± 50 mg) and transferred to microcentrifuge tubes containing an equal amount of 0.5 mm zirconium beads and 2 volumes of ice cold lysis buffer (50 mM Sodium Phosphate, 0.5 % (w/v) Triton X-100, pH 7.5). The samples were homogenised in a Bullet blender® 24 (Next Advance, Inc. New York) at speed 8 for 3 min and speed 9 for 4 min, with 1 min rest in-between cycles. Thereafter, samples were allowed to stand on ice for 30 min and were centrifuged at 15000 rpm for 20 min at 4 ºC. Supernatants were transferred into Eppendorf tubes and stored at -80 ºC for further analysis.

2.12.2 Determination of Protein Concentration

Protein concentration of the prepared tissue homogenates was determined by means of a Bicinchoninic acid (BCA) protein assay kit. BSA was used as a standard with a concentration of 1 mg/ml and was diluted as tabulated in ***Table 2.4***. The samples were diluted with deionised water (deiH_20) to ensure that the protein concentration was within the linear range of the standard protein concentration (200- 1000 µg/ml). A BCA working reagent consisting of

Reagent A (BCA solution and Reagent B (copper (II) sulfate pentahydrate 4 % solution) were prepared in a 50:1 ratio. Into each well of a 96-well microplate, 25 µl of the standards or samples and the blank were assayed in triplicate, followed by 200 µl of the BCA working reagent. The plate was placed on an attachment vortex plate and was shaked (Labnet International, Inc) for 10 seconds. The plate was incubated for 30 min at 37 ºC and the absorbance was read at 562 nm in a FLUOstar® Omega Microplate Reader. All calculations for the subsequent antioxidant enzyme assays (CAT, SOD, GPx and thiobarbituric acid reactive substances: TBARS) were normalised and standardised according to the BCA protein concentration.

Table 2.4 *BSA standard preparation.*

Tube	Stock (mg/ml)	Solvent (deiH$_2$0)	Final Volume (µl)
1 (Blank)	0	100	100
2	20	80	
3	40	60	
4	60	40	
5	80	20	

2.13 Catalase (CAT)

Catalase (CAT, Enzyme Commission number (EC) 1.11.1.6) is a ubiquitous enzyme that catalyses the conversion of two H_2O_2 molecules into non-harmful compounds, oxygen and two water molecules, in mostly aerobic cells (Ellerby & Bredesen, 2000). The liver tissue homogenates were diluted to 0.1 µg/ µl protein in assay buffer (50 mM Potassium Phosphate, 0.5 % Triton X-100, pH 7.0). From the diluted cell lysate, 5 µl was assayed in triplicate in the 96 well ultraviolet (UV) plate, followed by 170 µl of assay buffer. To initiate the reaction, 50 µl of H_2O_2 stock solution was added to all the wells and the absorbance was measured over 5 min to measure the linear decrease over time, at 240nm in a FLUOstar® Omega Microplate Reader. The molar extinction coefficient (43.6 $M^{-1}cm^{-1}$) adjusted for the well pathlength was used to determine catalase activity (µmole H_2O_2 consumed/min/ µg protein).

2.14 Superoxide dismutase (SOD)

Superoxide dismutase (SODs, EC 1.15.1.1) are metalloenzymes that catalyses the dismutation of the reactive superoxide radical (O^-_2) into H_2O_2 and oxygen, according to the following reaction: $2O_2^{\bullet-} + 2H^+ + SOD \rightarrow H_2O_2 + O_2$. SODs form part of the cellular antioxidant defence system. SOD enzymes have been characterised into three types according to their metal

content; Cu/Zn, Mn and Fe. The Cu/Zn and the Mn are localised in the cytosol and mitochondria, respectively. The extracellular SOD, is localised in the interstitial spaces of tissues and extracellular fluid responsible for the SOD activity in the plasma (Marklund, 1980). In this study, only Cu/Zn SOD enzyme was measured, using the cytosolic fraction. SOD activity was determined according to the method modified from Ellerby and Bredesen (2000). This assay method measures the auto-oxidation of 6-OHD (6-hydroxydopamine) and one unit of SOD is defined as the amount of enzyme needed to exhibit 50 % inhibition of auto-oxidation of 6-OHD. Total SOD (using the cytosolic fraction) activity was determined using the liver tissue homogenates prepared as described in section 2.12.1.

The tissue homogenates were diluted to 0.1 ug/µl of protein (using the BCA protein concentrations). 6-OHD, 1.6 mM, was freshly prepared by adding 50 µl of concentrated (70%) perchloric acid ($HCLO_4$) to 10 ml deiH_2O. This solution was purged with nitrogen for 15 min to remove oxygen and 4 mg of 6-OHD was added to this solution, wrapped in foil and kept on ice. The samples (10 µl) and the blank (15 µl SOD assay buffer [50mM Sodium Phosphate, pH 7.4]), were assayed in triplicate. Following this, 170 µl of 0.1 mM Diethylenetriaminepentaacetic acid (DETAPAC), was prepared in SOD assay buffer (1mg in 25 ml), was added to all the wells. Thereafter, 5 µl of the SOD assay buffer was assayed in all the sample wells, excluding the blank well. The reaction was initiated by adding 15 µl of 6-hydroxydopamine (6-OHD) to all the wells of the 96-well plate. The kinetics of the auto-oxidation of 6-OHD was monitored at 490 nm for 5 min at 25 ºC using the FLUOstar Omega® microplate reader. The results were expressed as Units/mg protein.

2.15 Glutathione Peroxidase (GPx)

Glutathione Peroxidase (GPx, EC 1.11.1.9) enzyme catalyses the dismutation of lipids and hydroperoxides, including H_2O_2, by reduced glutathione, thus protecting the cells from oxidative damage (Ellerby & Bredesen, 2000). The enzymatic activity is measured indirectly by a coupled reaction with glutathione reductase (GR, EC 1.8.1.7). Oxidised glutathione (GSSG) produced upon reduction of hydroperoxides by GPx is recycled back to its reduced state by GR and NADPH, as shown in ***Fig 2.7***. The assay was done according to the method modified from Ellerby and Bredesen (2000), in conjunction with that described by (Ajuwon, Katengua-Thamahane, Van Rooyen, Oguntibeju & Marnewick, 2013).

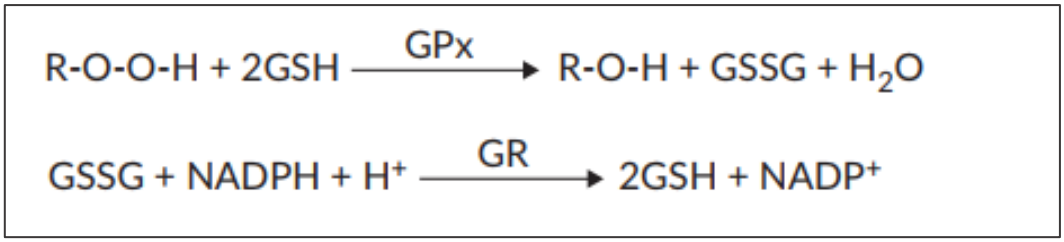

Figure 2.7 *Enzymatic coupled reaction used to determine glutathione peroxidase activity* (Caymen Chemical, 2016).

Liver tissue homogenates were prepared as described in section 2.12.1 were diluted using a 2.5 X dilution (40µl sample: 60µl assay buffer) so that the protein concentration falls between the required range (5-10mg/ml). A cocktail solution consisting of; 210 µl assay buffer (50 mM Potassium Phosphate, 1 mM EDTA, pH 7.0), 2.5 µl GSH solution (30.7 mg/ ml, in deH_2O), 2.5 µl GR (1.6 mg/ml, diluted in assay buffer), 2.5µl of 0.1M Sodium azide to inhibit catalase and lastly and 2.5 µl NADPH (5 mg dissolved in 0.1% $NaHCO_3$) was prepared. Following this, 5 µl of the sample and blank (Assay buffer: 50 mM Potassium Phosphate, 1 mM EDTA, pH 7.0) were assayed in triplicate. Thereafter, 215 µl of the cocktail solution was added in all the wells. The absorbance of NADPH oxidation in the absence of H_2O_2 was measured 3 min with 30 second intervals at 340nm. Thereafter, to initiate the reaction, 25µl of 1.5mM H_2O_2 (3.4µl of 30% stock solution in 20ml assay buffer) was added to the microplate immediately after the first absorbance measurement. The hydroperoxide-dependent linear NADPH oxidation was recorded for 2-5 min in 30 second intervals at the same wavelength. The GPx activity was expressed as µmol NADPH oxidized/min.

2.16 Thiobarbituric acid reactive substances (TBARS) Assay

Measurement of TBARS is a widely used assay method for the determination of lipid peroxidation in tissue homogenates and serves as an indicator of oxidative stress. MDA is a naturally occurring product of lipid peroxidation which forms an adduct with thiobarbituric acid (TBA) under high temperatures (90-100 °C) and acidic conditions (***Fig 2.8***). The TBARS assay method calorimetrically measures the MDA-TBA adduct at 530 nm absorbance. The assay was performed according to the modified method of Esterbauer and Cheeseman (1990).

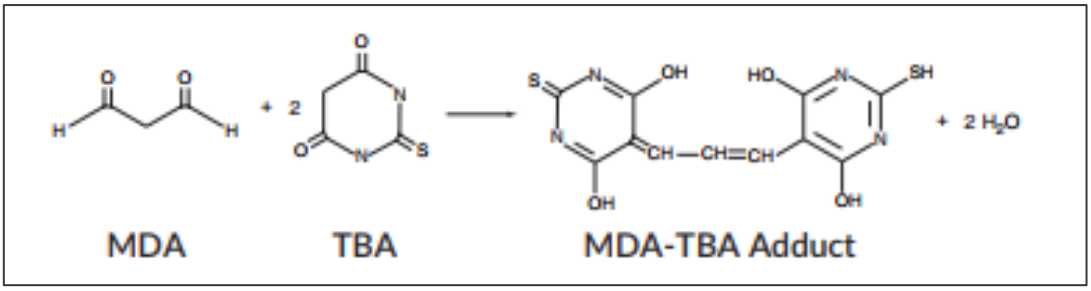

Figure 2.8 *Formation of the MDA-TBA adduct under high temperatures and acidic conditions* (Caymen Chemical, 2014).

The liver tissue was homogenised in 0.01 mM sodium phosphate buffer (pH 7.5) containing 1.15 % KCl. The samples were homogenised in a Bullet blender® 24 (Next Advance, NYC, USA) at speed 8 for 3 min and speed 9 for 4 min, with 1 min rest in-between cycles. Thereafter, the samples were aliquoted and stored at -80 °C. Protein concentration was determined as described in section 2.12.2. The MDA standard solution (500 µM) was prepared by diluting 1.23 µl of the MDA stock solution in 10 ml of deionised water (deiH_2O). Following this, the MDA standard dilution series was prepared according to ***Table 2.5***. Samples and standards (100 µl) were added in glass test tubes followed by 100 µl of 2 % SDS solution and vortexed thoroughly. Thereafter, TCA reagent (10 % TCA, BHT [12.5mM BHT/ 10 ml TCA solution]) and 2ml TBA (0.67 % w/v) solution were added on the side of each tube and the glass tubes, capped with marbles. The tubes were incubated in a water bath at 95 ºC for 1 hour. After incubation, the glass tubes were cooled to room temperature in an ice bath, for 10 min. Following this, the samples were centrifuged at 3000 rpm for 15 min. The supernatant was removed and pipetted into a clean microcentrifuge tube, thereafter, 150 µl was plated in triplicate in a 96 well microplate. The absorbance was then measured at 530 nm using the FLUOstar Omega® microplate reader. The results were normalized using the previously determined protein concentrations and expressed in µmole MDA equivalent/mg protein.

Table 2.5 *MDA standard preparation.*

Tube	MDA standard (µl)	MDA Diluent (µl)	Final Concentration (nmol/ml MDA)
A	0	1000	0
B	2.5	997.5	0.322
C	5	995	0.625
D	10	990	1.25
E	20	980	2.5
F	40	960	5
G	80	920	10
H	200	800	25
I	400	600	30

2.17 Statistical Analysis

All the results were analysed using GraphPad Prism® 6. Statistical analysis was done using one-way or two-way analysis of variance (ANOVA) followed by the Bonferroni post-hoc test for comparison within the groups. The results were expressed as the Mean ± Standard Error of Mean (SEM). A probability of $p < 0.05$ was considered significant.

Chapter 3. Results

3.1 Overview

Male Wistar rats were fed a HFD composed of 390 g standard rat-chow, 200 ml water, 600 g holsum cooking fat, 10 g cholesterol, 100 g fructose, 100 g casein and two tins of condensed milk for 16-weeks, compared to aged-matched chow-fed Controls. The HFD was designed to induce obesity and specifically hypertension. Half of each animal group was treated with GRT extract, given in the form of jelly blocks from week 10 till week 16 (60mg/kg/day). An additional HFD group, treated with Captopril (50 mg/kg/day), served as a positive control against the development of hypertension. Captopril is a known anti-hypertensive drug that exerts its function by inhibiting the ACE. Using both animal models (Control and HFD), the relationship between GRT extract and insulin resistance/hypertension was investigated. All the data was statistically analysed using GraphPad® Prism 6 and data is expressed as mean ± SEM. (***Fig 3.1***).

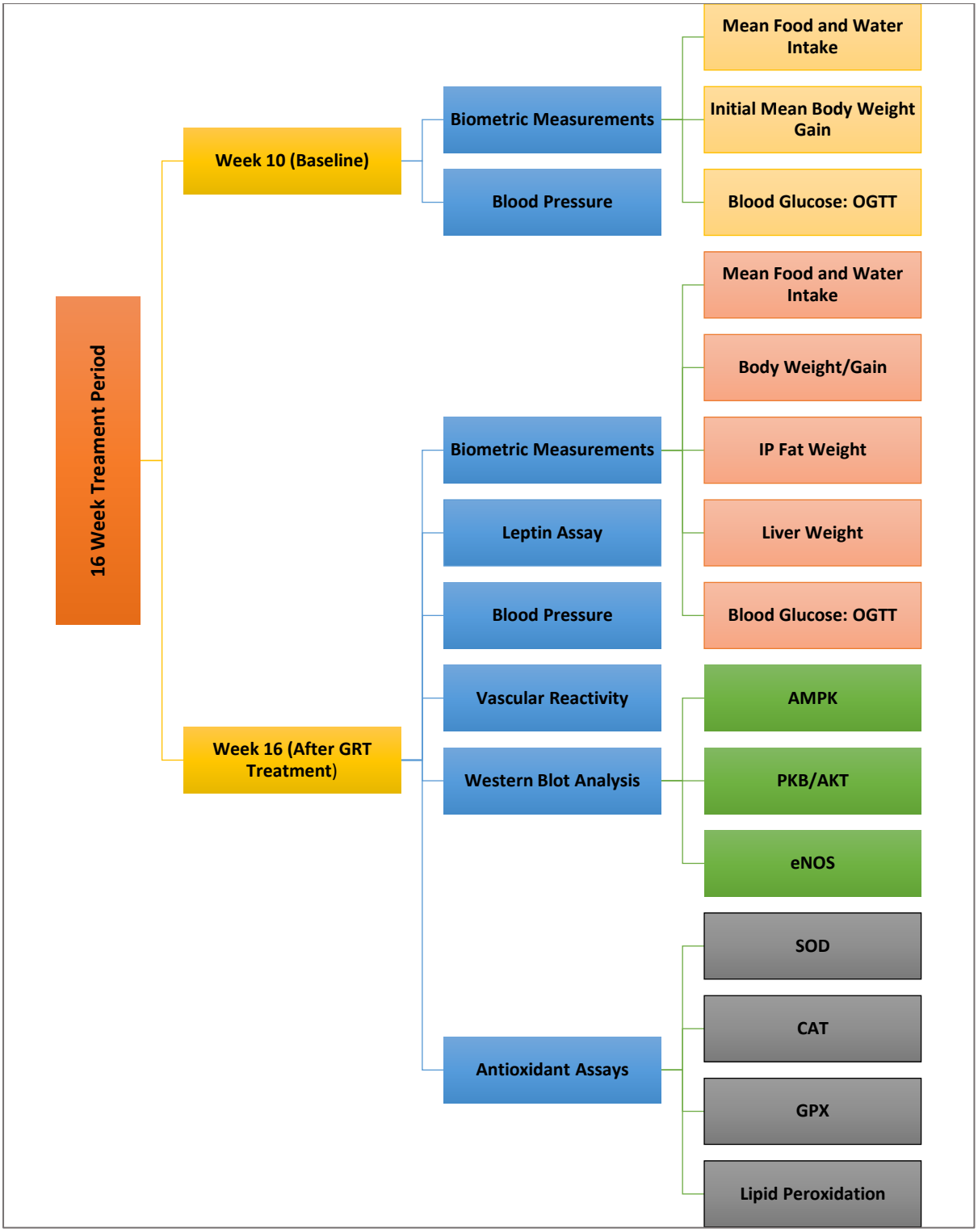

Figure 3.1 *Summary of the measurements performed throughout the study.*

3.2 Baseline Studies: Biometric and Blood Pressure Measurements

Below are the measurements at baseline (over 10 weeks) of the HFD vs Control group before treatment with the GRT extract.

Table 3.1 *Mean food and water intake per rat per day together with the mean body weight gain of the HFD vs Control group before treatment with the GRT extract.*

	Mean Food Intake	Mean Water Intake	Mean Body Weight
CONTROL	17.18 ± 0.272 g	20.48 ± 0.445 ml	246.00 ± 4.404 g
HFD	20.58 ± 0.429 g****	13.60 ± 0.229 ml****	274.10 ± 4.886 g***

All data is expressed as mean ± SEM, (**** $p < 0.0001$ HFD vs Control, *** $p < 0.001$ HFD vs Control), n = 20-28 per group.

3.2.1 Mean Food and Water Intake

The food and water intake were measured thrice a week over the 16-week period. The results below represent measurements over the 10 week period. The HFD group showed a significant increase in food intake when compared to the Control (20.58 ± 0.429 g vs 17.18 ± 0.272; $p < 0.0001$). Furthermore, the HFD group were presented with a significant decrease in the mean water intake (13.60 ± 0.229 ml vs 20.48 ± 0.447 ml; $p < 0.001$) relative to the Control group (***Fig 3.2*** and ***Fig 3.3***), respectively.

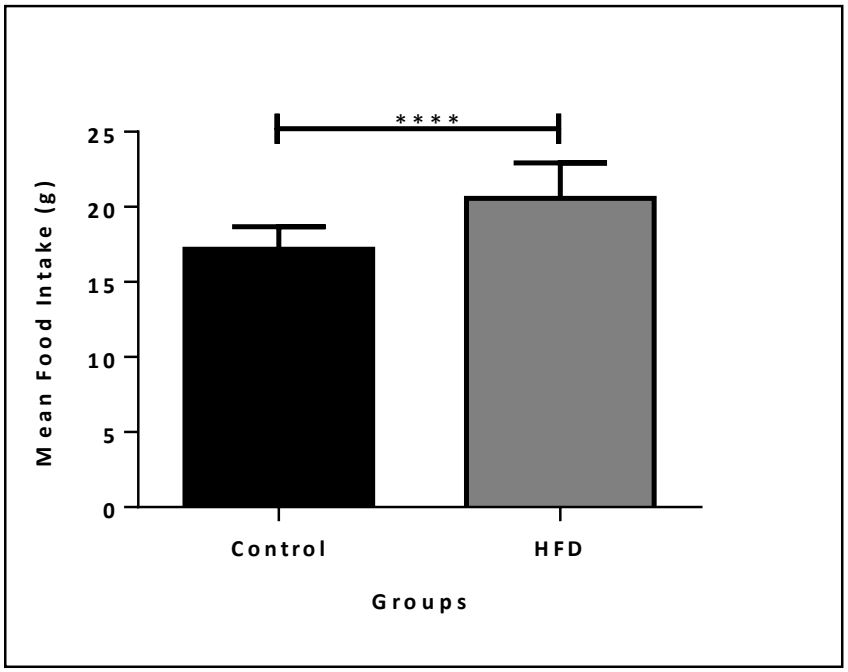

Figure 3.2 *Mean food intake of the HFD vs Control animals over 10 weeks, **** $p < 0.0001$ (n = 20-28 per group).*

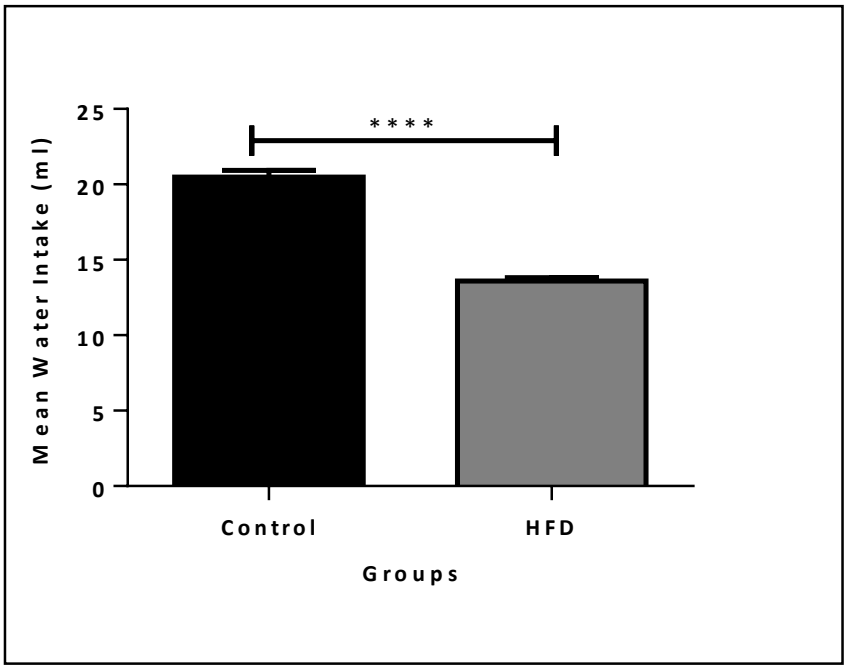

Figure 3.3 *Mean water intake of the HFD vs Control animals over 10 weeks, **** $p < 0.0001$ (n = 20-28 per group).*

3.2.2 Initial Mean Body Weight

Body weight was measured once a week over the 16-week treatment period. The HFD group showed a significant increase in the mean body weight at baseline (before the onset of GRT treatment) when compared to the Control group (274.10 ± 4.886 g vs 246.00 ± 4.404 g; $p < 0.001$).

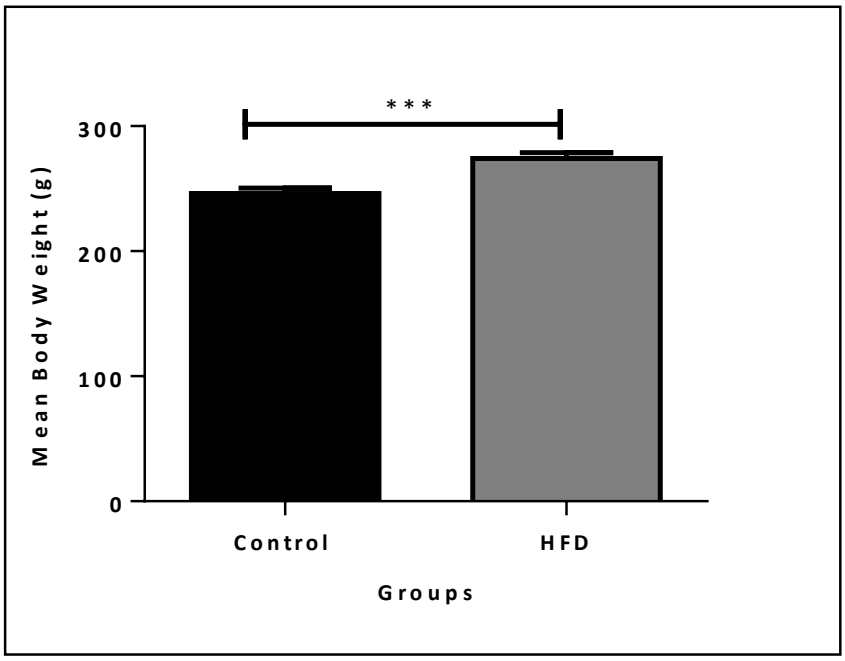

Figure 3.4 *Mean body weight of the HFD vs Control animals in week 10, *** $p < 0.001$ (n = 20-28 per group).*

3.2.3 Blood Glucose: Oral Glucose Tolerance Test (OGTT)

In week 10, quantitative blood glucose measurements were obtained in both the Control and HFD group after an overnight fasting period. After the baseline (0 min, fasting level) measurement, the animals were gavaged with 1g/kg of sucrose solution and the disappearance of plasma glucose levels was measured over 2 hrs at 3 min, 5 min, 15 min, 20 min, 25 min, 30 min, 45 min, 60 min, 90 min and 120 min.

At baseline, the HFD group showed a significant increase in plasma blood glucose levels when compared to the Control (5.56 ± 0.220 mmol/L vs 4.66 ± 0.113 mmol/L; $p < 0.01$). After the oral administration of the 50 % sucrose solution, the HFD group showed a significant increase in the plasma glucose levels after 25 min when compared to the Control group (7.04 ± 0.248 vs 6.31 ± 0.212; $p < 0.05$) (***Table 3.2*** *and* ***Fig 3.5A***). There were no significant differences between the Control and HFD group after 30 min to 120 min. Additionally, according to the

area under a curve (AUC, ***Fig 3.5B***) analysis, the HFD group was presented with a significantly increase in basal glucose levels when compared to the Control group (716 ± 15.4 vs 635 ± 31.2 AUC arbitrary units, * $p < 0.05$).

Table 3.2 *OGTT in HFD vs Control animals (n =7 - 8 per group).*

	CONTROL	**HFD**
Time (min)	Glucose levels (mmol/L)	
0	4.66 ± 0.113	5.56 ± 0.220**
3	4.84 ± 0.341	6.13 ± 0.219**
5	5.06 ± 0.229	6.59 ± 0.108****
10	5.89 ± 0.245	7.31 ± 0.437*
15	5.51 ± 0.362	7.63 ± 0.359**
20	6.40 ± 0.229	7.44 ± 0.270*
25	6.31 ± 0.212	7.04 ± 0.248*
30	6.41 ± 0.401	6.84 ± 0.179
45	5.94 ± 0.292	6.16 ± 0.196
60	5.34 ± 0.361	5.89 ± 0.250
90	5.16 ± 0.284	5.16 ± 0.150
120	4.80 ± 0.213	4.963 ± 0.131

All data is expressed as mean ± SEM, (* $p < 0.05$, ** $p < 0.01$, **** $p < 0.0001$ HFD vs Control.

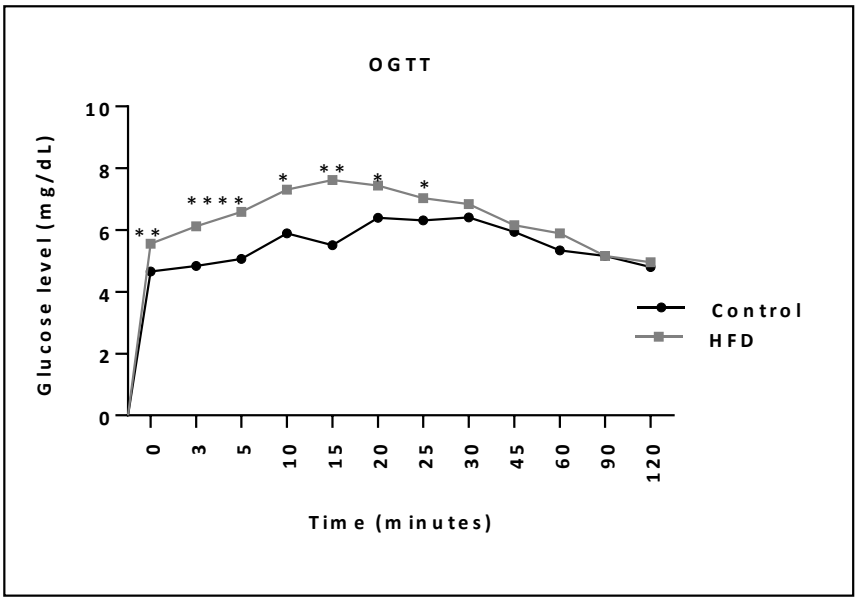

***Figure 3.5 A**) Glucose levels (mmol/L) and **B**) AUC representation of glucose tolerance in the HFD vs Control group. **A**) Blood glucose levels (mmol/L) of the HFD vs Control animals measured in week 10. * $p < 0.05$ HFD vs Control; ** $p < 0.01$ HFD vs Control; **** $p < 0.0001$ HFD vs Control), n = 7 - 8 per group.*

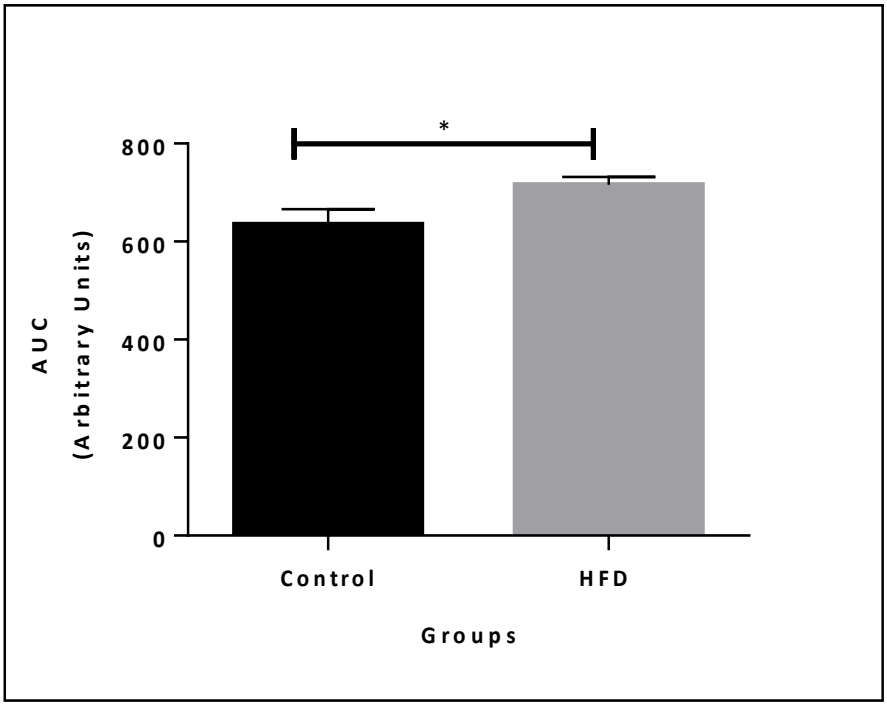

***B**) AUC representation of the effect of the diet in glucose tolerance of the HFD vs Control group. * $p < 0.05$, HFD vs Control group, n = 7-8 per group.*

3.3 Blood Pressure

The results below reflect baseline blood pressure measurements from week 8-9, before treatment with the GRT extract. The HFD group showed a significant increase in the mean systolic (***Fig 3.6***), mean diastolic (***Fig 3.7***) and mean arterial blood pressure (***Fig 3.8***) when compared to the Control group (***Table 3.3***). The mean arterial pressure was calculated as follows:

$$\text{Mean Diastolic Blood Pressure} + \frac{1}{3} \times \text{(Mean Systolic-Mean Diastolic Blood Pressure)}$$

Table 3.3 *Mean systolic, diastolic and arterial pressure of the Control vs HFD group.*

Groups	Mean Systolic Pressure (mmHg)	Mean Diastolic Pressure (mmHg)	Mean Arterial Pressure (mmHg)
CONTROL	125.00 ± 1.720	84.48 ± 1.171	99.94 ± 1.480
HFD	139.00± 2.460****	93.95 ± 1.226****	111.70 ± 2.240****

All data is expressed in mean ± SEM, (**** p < 0.001 HFD vs Control), n = 20-28 per group

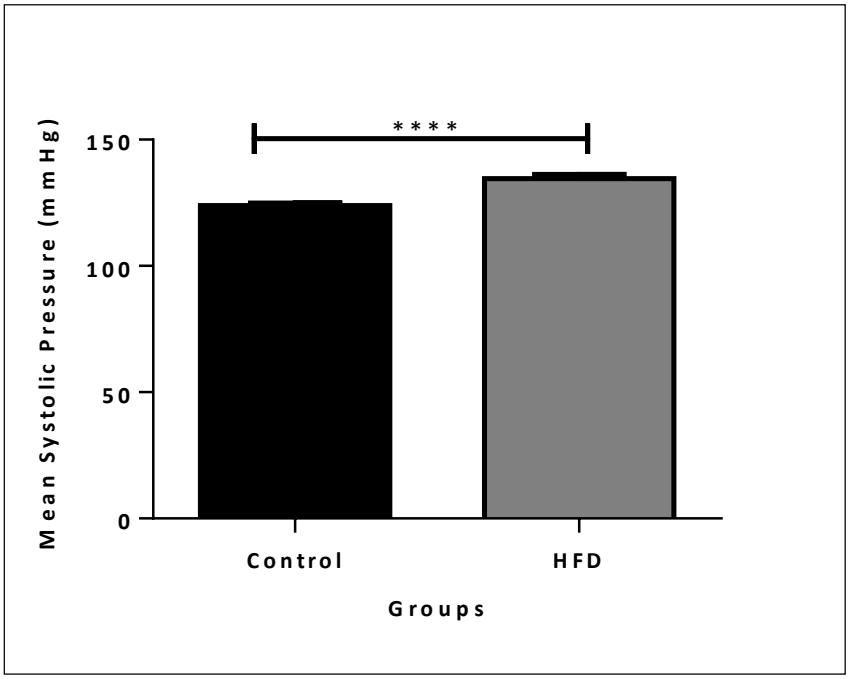

Figure 3.6 *Mean systolic blood pressure of the HFD vs Control group (**** p < 0.0001), measured from week 8-10, (n = 20-28 per group).*

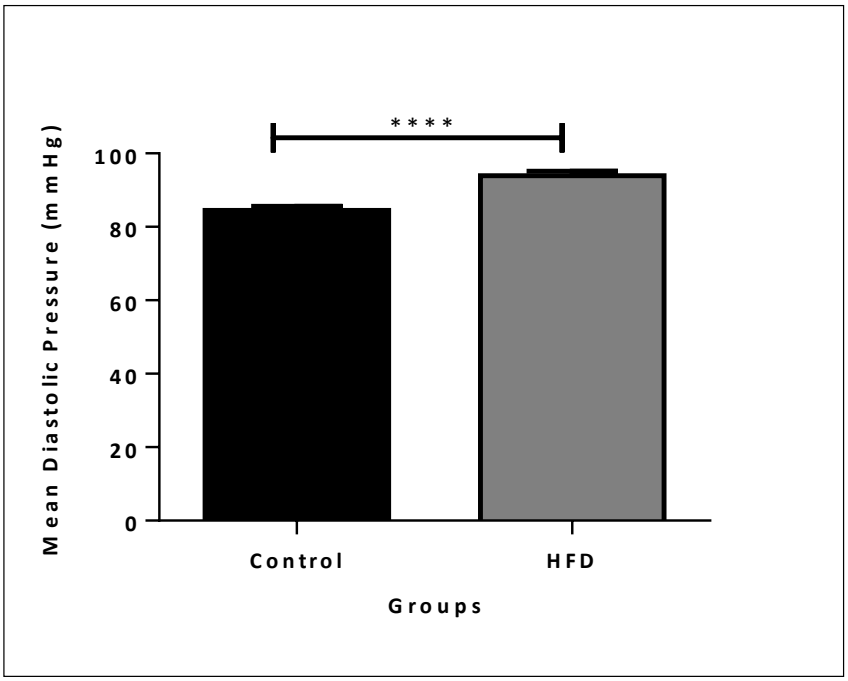

Figure 3.7 *Mean diastolic blood pressure of the HFD vs Control group (**** $p < 0.0001$), measured from week 8-10, (n = 20-28 per group).*

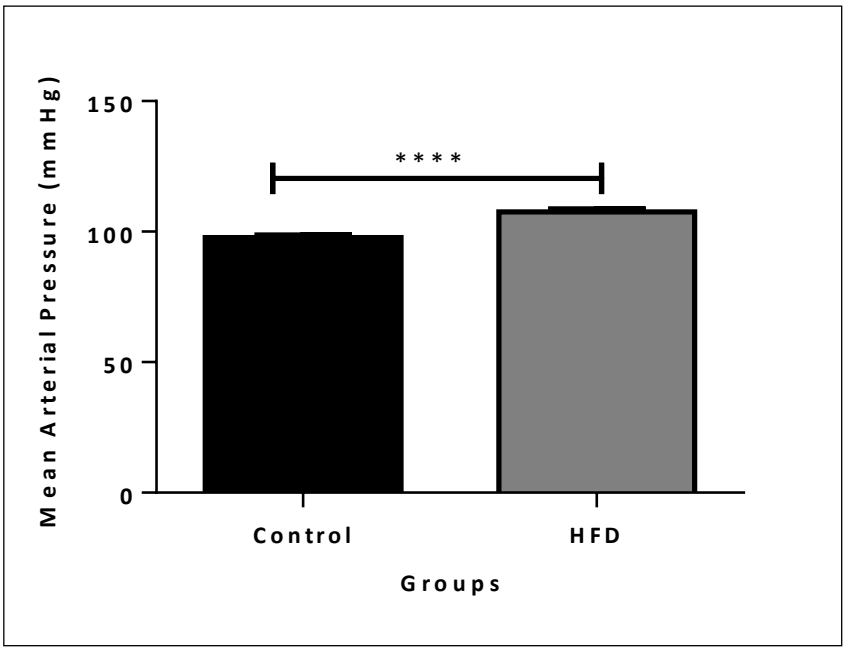

Figure 3.8 *Mean arterial pressure of the HFD vs Control group (**** $p < 0.000$), measured from week 8-10, (n = 10 per group).*

3.4 Results During and after the 16-Week Treatment Period

3.4.1 Biometric Measurements

The results below reflect biometric measurement (Mean food and water intake, body weight/ gain, IP fat weight and fasting blood glucose levels) analysis. All data is expressed as mean ± SEM.

Table 3.4 *Summary of the biometric measurements during and after the 16-week treatment period.*

Groups	Food Intake (g)	Water Intake (ml)	Body Weight (g)	IP fat weight (g)	Fasting blood glucose levels (mmol/L
CONTROL	17.11 ± 0.529	23.38 ± 0.442	339.50 ± 6.870	7.32 ± 0.995	5.23 ± 0.304
HFD	20.64 ± 0.631***	17.01 ± 0.647****	396.20 ± 13.660**	23.79 ± 3.481***	6.23 ± 0.190*
CONTROL + GRT	17.45 ± 0.468	26.66 ± 0.859$^{###}$	324.30 ± 7.460	8.27 ± 0.596	4.83 ± 0.128
HFD + GRT	21.11 ± 0.622	14.76 ± 1.324	344.50 ± 11.740$^{@}$	13.90 ± 1.315$^{@}$	5.69 ± 0.253

All data is expressed as mean ± SEM, (* $p < 0.05$, ** $p < 0.01$, *** $p < 0.001$, **** $p < 0.0001$ HFD vs Control; $^{###}$ $p < 0.001$ Control + GRT vs Control; $^{@}$ $p < 0.05$ HFD + GRT vs HFD).

3.4.2 Mean Food Intake

Food intake was monitored 3 times a week over the 16-week period. The HFD animals showed a significant increase in food intake when compared to the Control animals (20.64 ± 0.631 g vs 17.11 ± 0.529 g; $p < 0.001$). Treatment with the GRT extract showed no effect on the food intake.

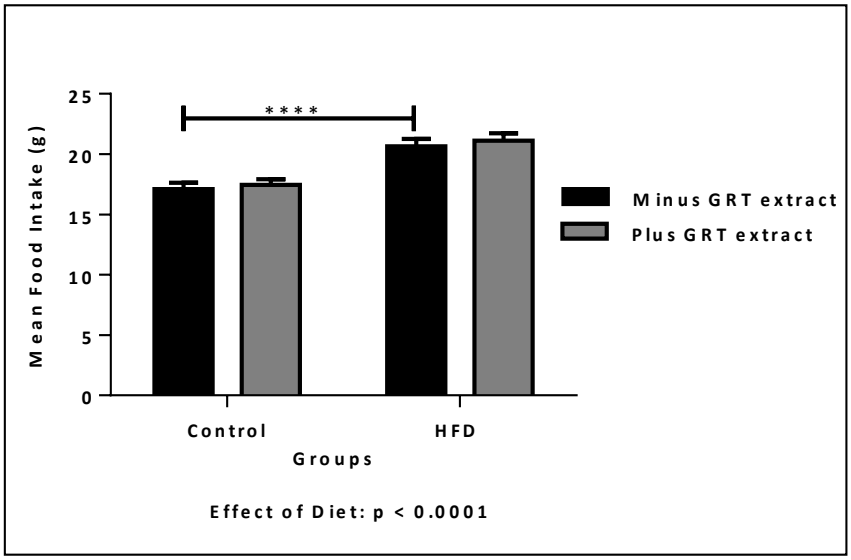

Figure 3.9 *Mean food intake of the HFD vs Control group (GRT treated and untreated), measured over 16 weeks. *** p < 0.001, HFD vs Control group. According to a two-way ANOVA, the HFD resulted in a significant increase (p < 0.0001) in food intake, n = 10 per group.*

3.4.3 Mean Water Intake

Water intake was monitored 3 times a week over the 16-week period. The HFD animals showed a significant decrease in the water intake when compared to the Control animals (17.01 ± 0.647 ml vs 23.38 ± 0.442 ml; $p < 0.0001$). Treatment with the GRT extract in the treated Control animals showed a significant increase in the water intake when compared to the untreated Control animals (26.66 ± 0.859 ml vs 23.38 ± 0.442 ml; $p < 0.01$).

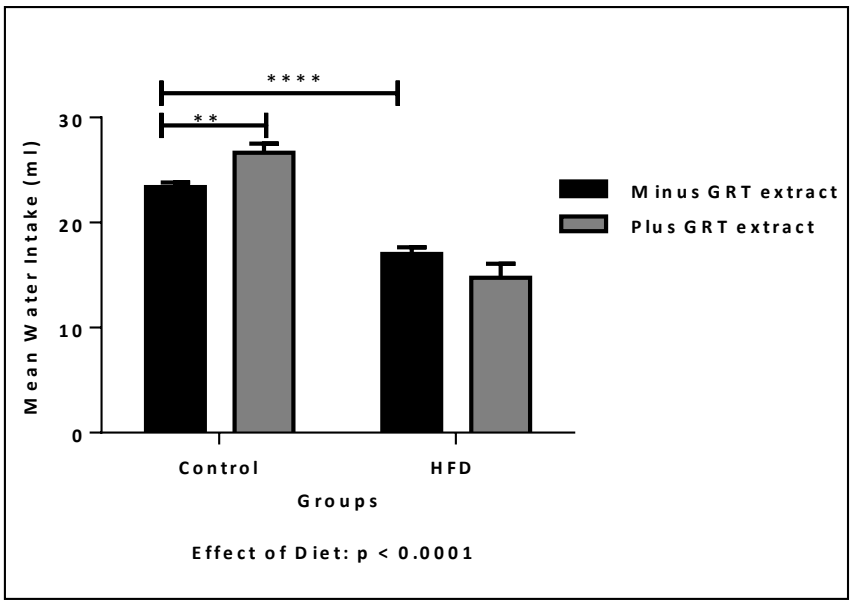

Figure 3.10 *Mean water intake of the HFD vs Control group (GRT treated and untreated), measured over 16 weeks. **** $p < 0.0001$ HFD vs Control group and ** $p < 0.01$ Control + GRT vs Control group. According to a two-way ANOVA, the HFD resulted in a significant decrease in water intake ($p < 0.0001$), $n = 10$ per group.*

3.4.4 Body Weight

The results indicate the absolute body weight of the animals measured in week 16. The HFD animals showed a significant increase in body weight when compared to the Control animals (396.20 ± 13.660g vs 339.50 ± 6.870 g; $p < 0.01$). Treatment with the GRT extract in the treated HFD animals significantly decreased the body weight when compared to the untreated HFD group (344.50 ± 11.740 g vs 396.20 ± 13.660 g; $p < 0.05$). Additionally, GRT treatment did not affect the body weight of the Control animals.

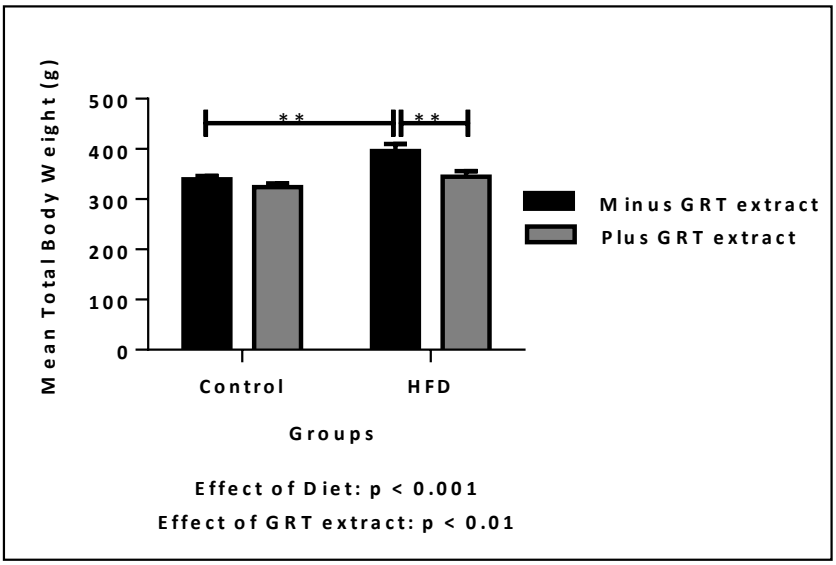

Figure 3.11 *Body weight measured in week 16 of the HFD vs Control group (GRT treated and untreated). ** p < 0.01 HFD vs Control group and * p < 0.05, HFD + GRT vs HFD group. According to a two-way ANOVA, the HFD significantly increased (p < 0.001) body weight whereas the GRT extract resulted in a significant decrease (p < 0.01) in body weight, n = 10 per group.*

3.4.5 Weekly Body Weight Gain

The graph below depicts the weekly body weight of the animals groups over the 16 week period. The HFD animals showed a significant increase in body weight gain when compared to the Control animals (55.71 ± 2.657g vs 36.66 ± 3.033g; $p < 0.001$). The GRT extract resulted in less weight gain in the treated HFD animals when compared to the untreated HFD animals (29.40 ± 6.781g vs 55.71 ± 2.657g; $p < 0.01$). Lastly, treatment with the GRT extract did not affect the weight of the treated Control animals.

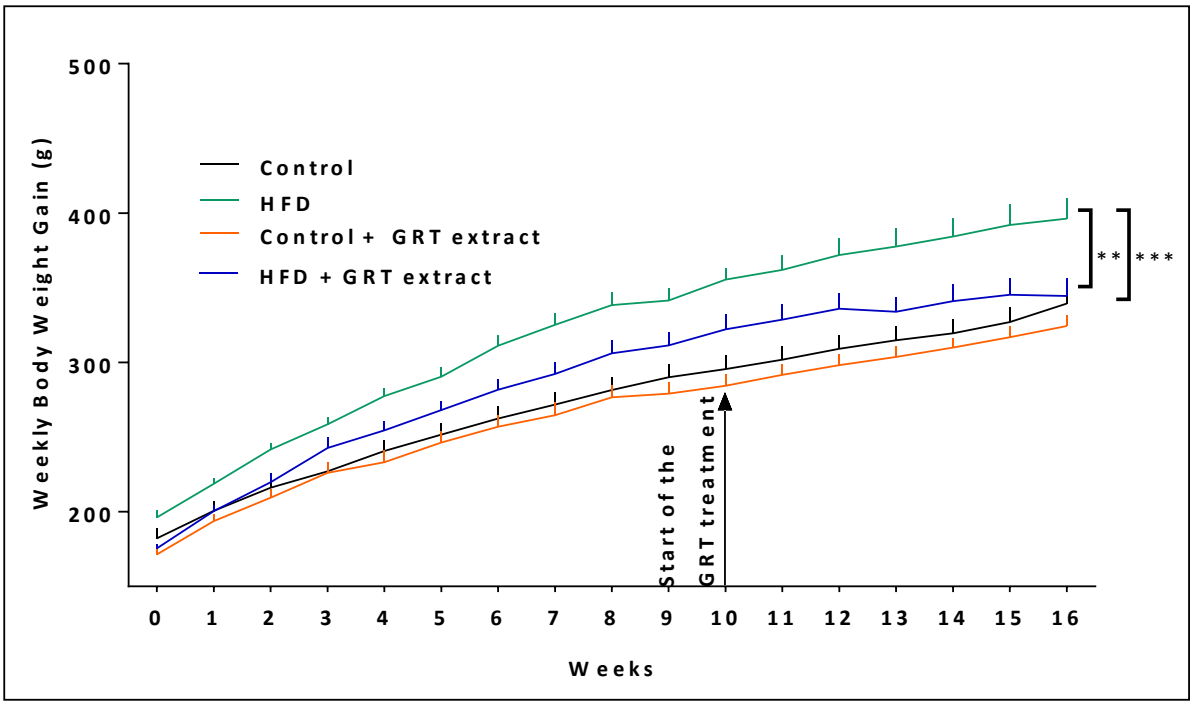

Figure 3.12 *Weekly body weight measured over the 16-week period. *** $p < 0.001$, HFD vs Control group and ** $p < 0.01$ HFD + GRT vs HFD group (n = 10 per group).*

3.4.6 IP Fat Weight

The HFD animals showed a significant increase in the IP fat weight when compared to the Control animals (23.79 ± 3.481 g vs 7.32 ± 0.995 g; $p < 0.001$). HFD animals treated with GRT extract were presented with a decreased IP fat weight when compared to the untreated HFD animals (13.90 ± 1.315 g vs 23.79 ± 3.481 g; $p < 0.05$). Additionally, treatment with the GRT extract did not affect the IP fat weight of the Control animals.

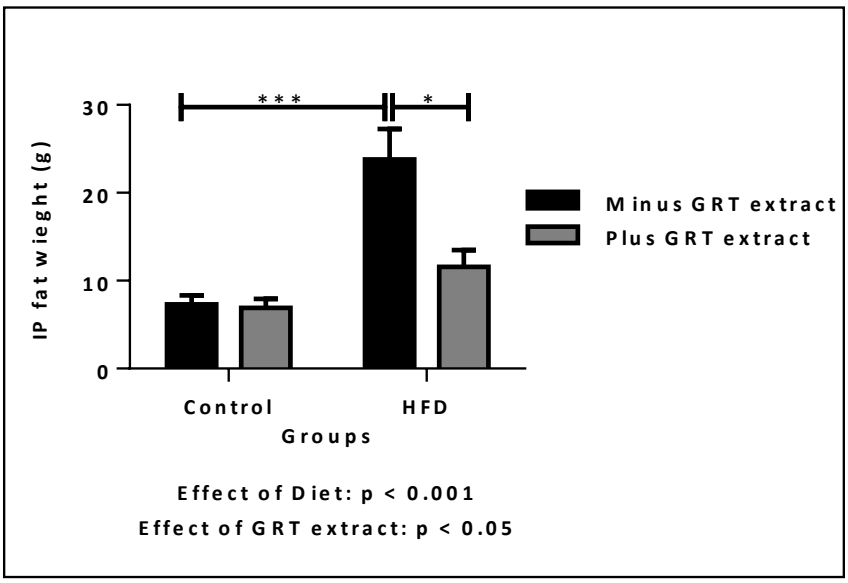

Figure 3.13 *IP fat weight of the HFD vs Control group (GRT treated and untreated) collected and weighted in week 16. *** p < 0.001, HFD vs Control and * p < 0.05, HFD + GRT vs HFD. According to a two-way ANOVA, the HFD resulted to a significant increase (p < 0.001) in IP fat weight, whereas the GRT extract resulted in a significant decrease (p < 0.05) in IP fat weight, n = 10 per group.*

3.4.7 Liver Weight

The HFD group had significantly increased liver weight when compared to the Control group (15.23 ± 0.8027 g vs 10.30 ± 0.3923 g; $p < 0.0001$). Treatment with the GRT extract in the HFD animals significantly decreased the liver weight when compared to the untreated HFD group (11.70 ± 0.5409 g vs 15.23 ± 0.8027 g; $p < 0.01$). Additionally, treatment with GRT extract did not affect the liver weight of the Control animals.

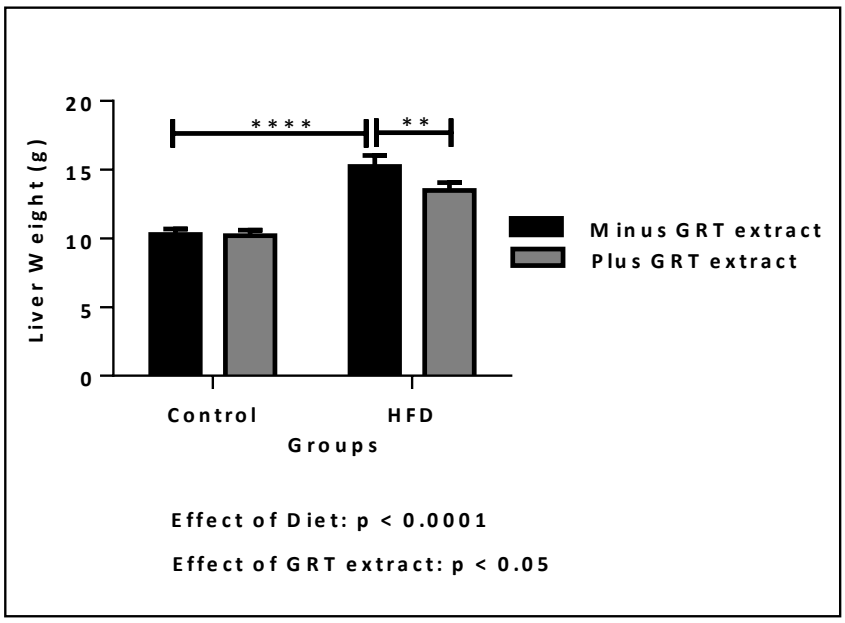

Figure 3.14 *Liver weight of the HFD vs Control (GRT treated and untreated). **** p < 0.0001, HFD vs Control and ** p < 0.01, HFD + GRT vs HFD group. According to a two-way ANOVA, the HFD resulted to a significant increase (p < 0.001) in liver weight, whereas the GRT extract resulted in a significant decrease (p < 0.05) in liver weight, n = 10 per group.*

3.4.8 Blood Glucose: OGTT

In week 15, the blood glucose levels (***Fig 3.15A***) of the HFD and Control (GRT treated and untreated) were determined as explained in section 3.2.3. According to the area under a curve (AUC, ***Fig 3.15B***) analysis, the HFD animals showed a significant increase in the blood glucose levels when compared to the Control animals (741.1 ± 16.20 vs 671.5 ± 23.93 AUC arbitrary units; $p < 0.05$). In addition, treatment with GRT extract significantly decreased blood glucose levels in the treated HFD animals when compared to the untreated HFD animals (657.2 ± 32.02 vs 741.1 ± 16.20 AUC arbitrary units; $p < 0.05$). Furthermore, treatment with GRT extract did not affect the glucose levels of the treated Control animals, relative to the untreated Control animals (555.9 ± 56.45 vs 671.5 ± 23.93 AUC arbitrary units).

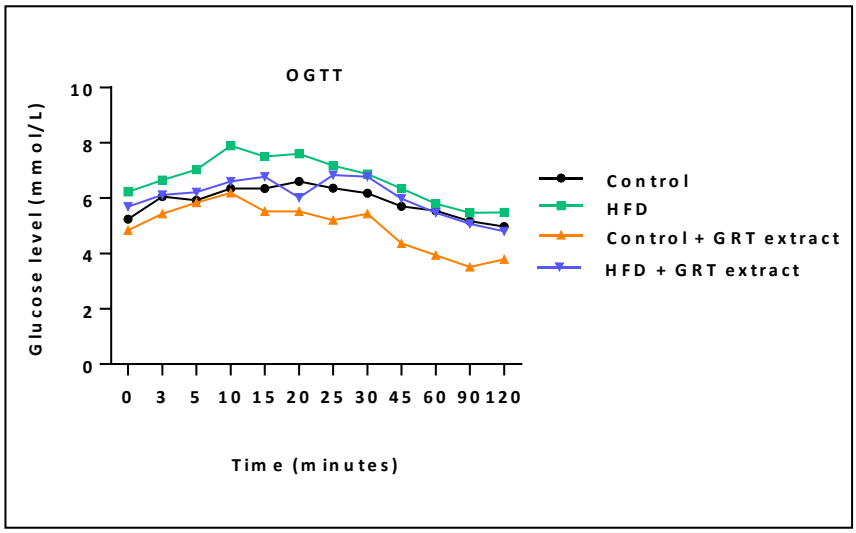

Figure 3.15 A) *Glucose tolerance (mmol/L) and* ***B****) AUC analysis for the HFD vs Control group (GRT treated and untreated).*

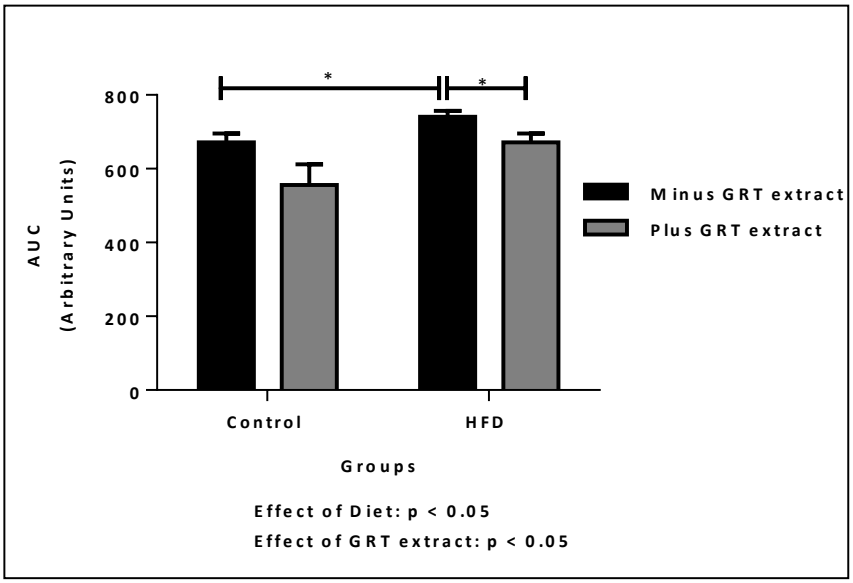

B*) AUC representation of the effect of diet and GRT extract in glucose tolerance of the HFD vs Control (GRT treated and untreated). * p < 0.05, HFD vs Control group; * p < 0.05, HFD + GRT vs HFD group, n = 6-8 per group. According to a two-way ANOVA, the HFD resulted in a significant (p < 0.05) increase in blood glucose levels in the HFD animals relative to the Control animals. Additionally, the GRT extract significantly (p < 0.05) attenuated the increase in glucose levels in both groups.*

3.5 Leptin Assay

Biochemical ELISA assays were performed using the serum from non-fasted animals collected in week 16. The HFD group showed a significant increase in the leptin levels (***Fig 3.16***) when compared to the Control group (5477 ± 791.50 pg/mL vs 2858 ± 210.80 pg/mL; $p < 0.05$). HFD animals treated with the GRT extract presented with significantly decreased leptin levels when compared to the untreated HFD group (2431 ± 608.70 pg/mL vs 5477 ± 791.50 pg/mL; $p < 0.01$). Additionally, treatment with GRT extract did not affect the leptin levels of the Control animals.

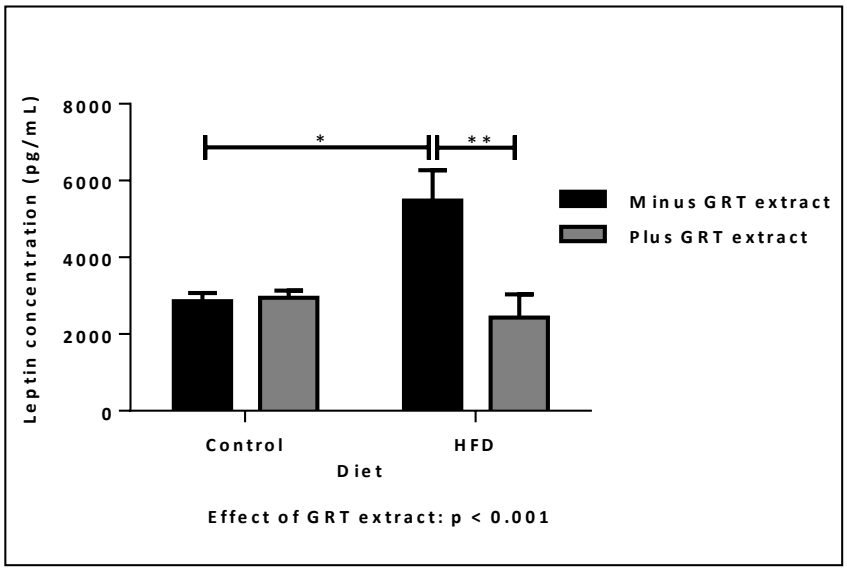

Figure 3.16 *Leptin levels of the HFD vs Control group (GRT treated and untreated). * $p < 0.05$, HFD vs Control group and ** $p < 0.01$, HFD + GRT vs HFD group. According to a two-way ANOVA, the GRT had a significant effect ($p < 0.001$), on the leptin levels, n = 5 per group.*

3.6 Blood Pressure

The data below reflect the blood pressure measurements over the last 6 weeks of the 16 week diet regime. The HFD group showed a significant increase in the mean systolic (***Fig 3.17***), diastolic (***Fig 3.18***) and arterial pressure (***Fig 3.19***) when compared to the Control group (***Table 3.6*)**. Treatment with the GRT extract significantly decreased the mean systolic (***Fig 3.17***) diastolic (***Fig 3.18***) and arterial pressure (***Fig 3.19***) in the HFD group when compared to the Control group (***Table 3.5***). Additionally, treatment with Captopril in the HFD animals also significantly decreased the mean systolic, diastolic and arterial pressure when compared to the untreated HFD group. Treatment with the GRT extract did not affect the blood pressure of the Control animals.

Table 3.5 *Mean systolic, diastolic and arterial pressure of the HFD vs Control group, GRT treated and untreated (n = 10 per group).*

Groups	Mean Systolic Pressure (mmHg)	Mean Diastolic Pressure (mmHg)	Mean Arterial Pressure (mmHg)
CONTROL	122.30 ± 1.317	81.270 ± 1.645	94.94 ± 1.417
HFD	134.00 ± 1.770 ***	91.64 ± 1.477****	105.80 ± 1.415****
CONTROL + GRT	119.90 ± 1.252	79.22 ± 1.428	92.80 ± 1.283
HFD + GRT	120.60 ± 1.531####	81.02 ± 1.482####	94.22 ± 1.431####
HFD + CAPTOPRIL	115.40 ± 1.381@@@@	78.96 ± 0.7391@@@@	91.09 ± 0.8435@@@@

All data is expressed as mean ± SEM, (*** $p < 0.001$; **** $p < 0.0001$ HFD vs Control, #### $p < 0.0001$ HFD + GRT vs HFD, @@@@ HFD + Captopril vs HFD).

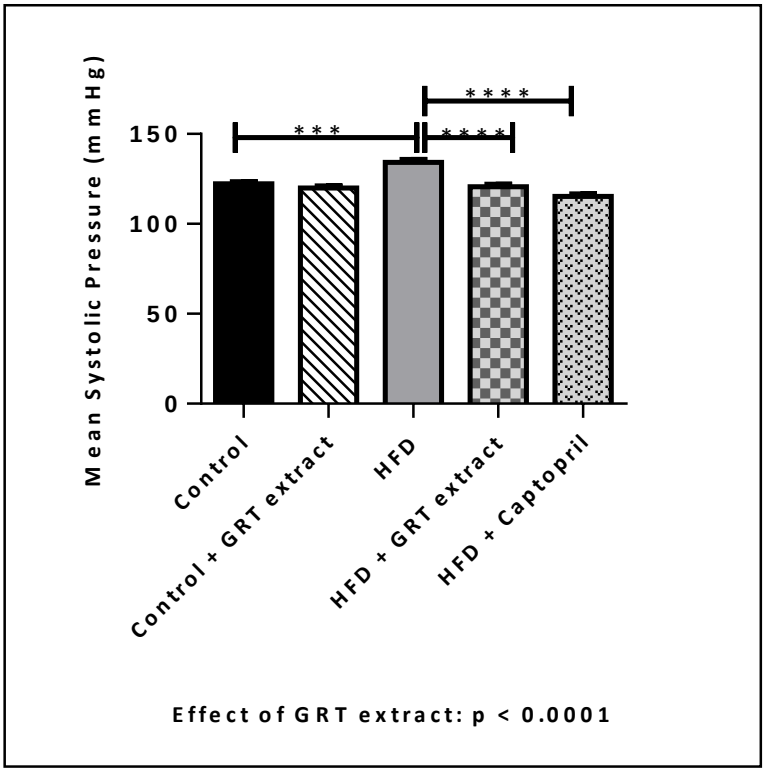

Figure 3.17 *Mean systolic blood pressure of the HFD vs Control group (GRT treated and untreated) and the HFD animals treated with Captopril. *** $p < 0.001$, HFD vs Control; **** $p < 0.0001$, HFD + GRT vs HFD and HFD + Captopril vs HFD. According to a two-way ANOVA, the GRT extract resulted in a significant decrease ($p < 0.0001$) in the systolic pressure, n = 10 per group.*

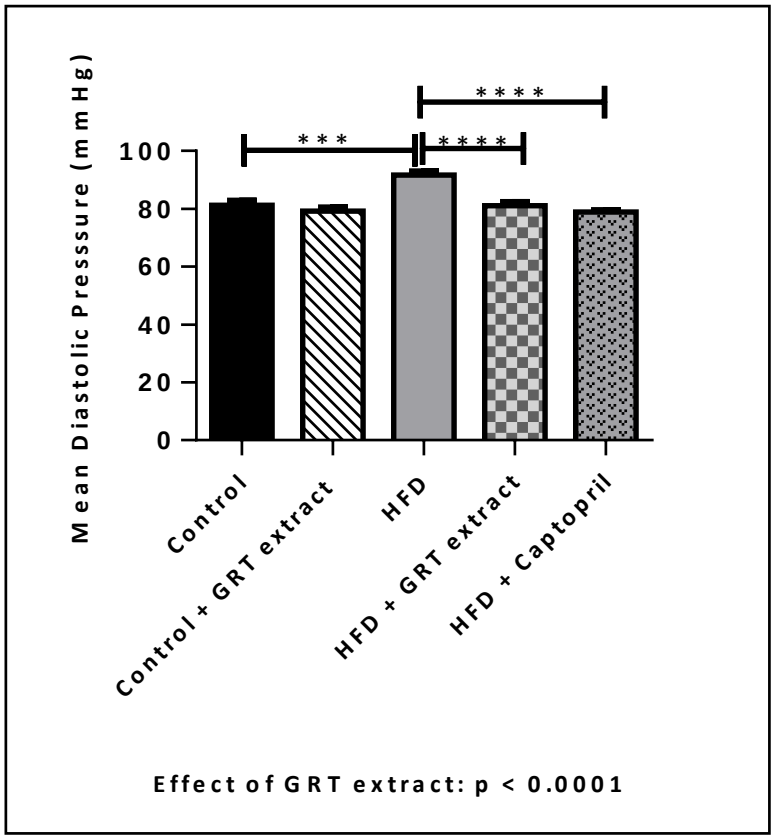

Figure 3.18 *Mean diastolic blood pressure of the HFD vs Control group (GRT treated and untreated) and the HFD animals treated with Captopril. *** p < 0.001, HFD vs Control; **** p < 0.0001, HFD + GRT vs HFD and HFD + Captopril vs HFD. According to a two-way ANOVA, the GRT extract resulted in a significant decrease in the diastolic pressure (p < 0.0001), n = 10 per group.*

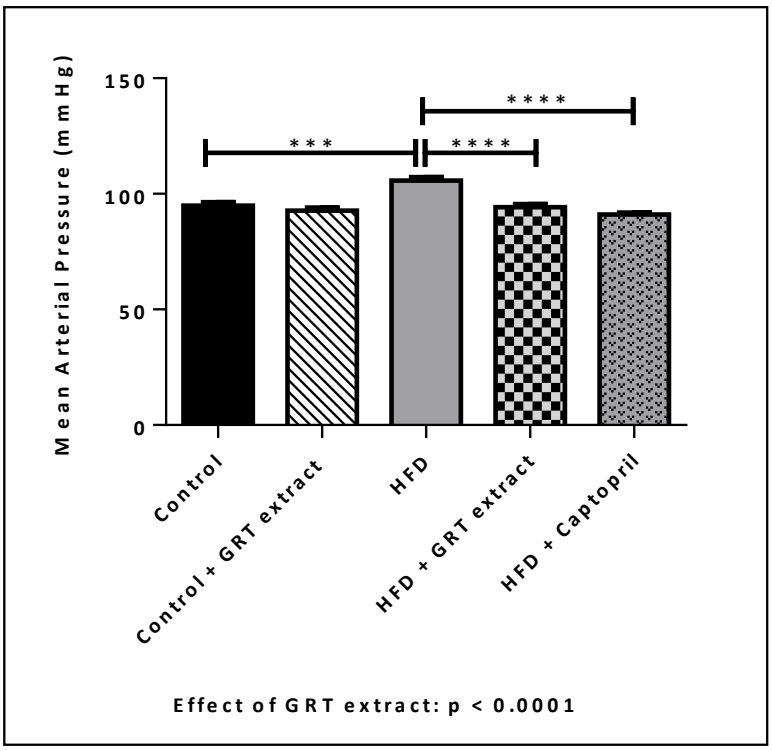

Figure 3.19 *Mean arterial blood pressure of the HFD vs Control group (GRT treated and untreated) and the HFD animals treated with Captopril. *** p < 0.001, HFD vs Control; **** p < 0.0001, HFD + GRT vs HFD and HFD + Captopril vs HFD. According to a two-way ANOVA , the GRT extract resulted in a significant decrease in the mean arterial pressure (p < 0.0001), n = 10 per group.*

3.7 Vascular Reactivity

Endothelial function of all the groups was assessed by means of isometric tension studies using a 3-4 mm section of the aortic ring with the perivascular (PVAT) fat intact. The aortic rings were exposed to phenylephrine induced cumulative vasocontraction (***Fig 3.20***) and acetylcholine-induced cumulative vasodilation (***Fig 3.21***).

3.7.1 Phenylephrine Induced Vascular Cumulative Contraction

HFD group showed a significant reduction in vascular contractility when compared to the Control group (p = 0.0011). Treatment with the GRT extract significantly decreased contraction in the HFD group when compared to the untreated HFD group (p =0.0107).

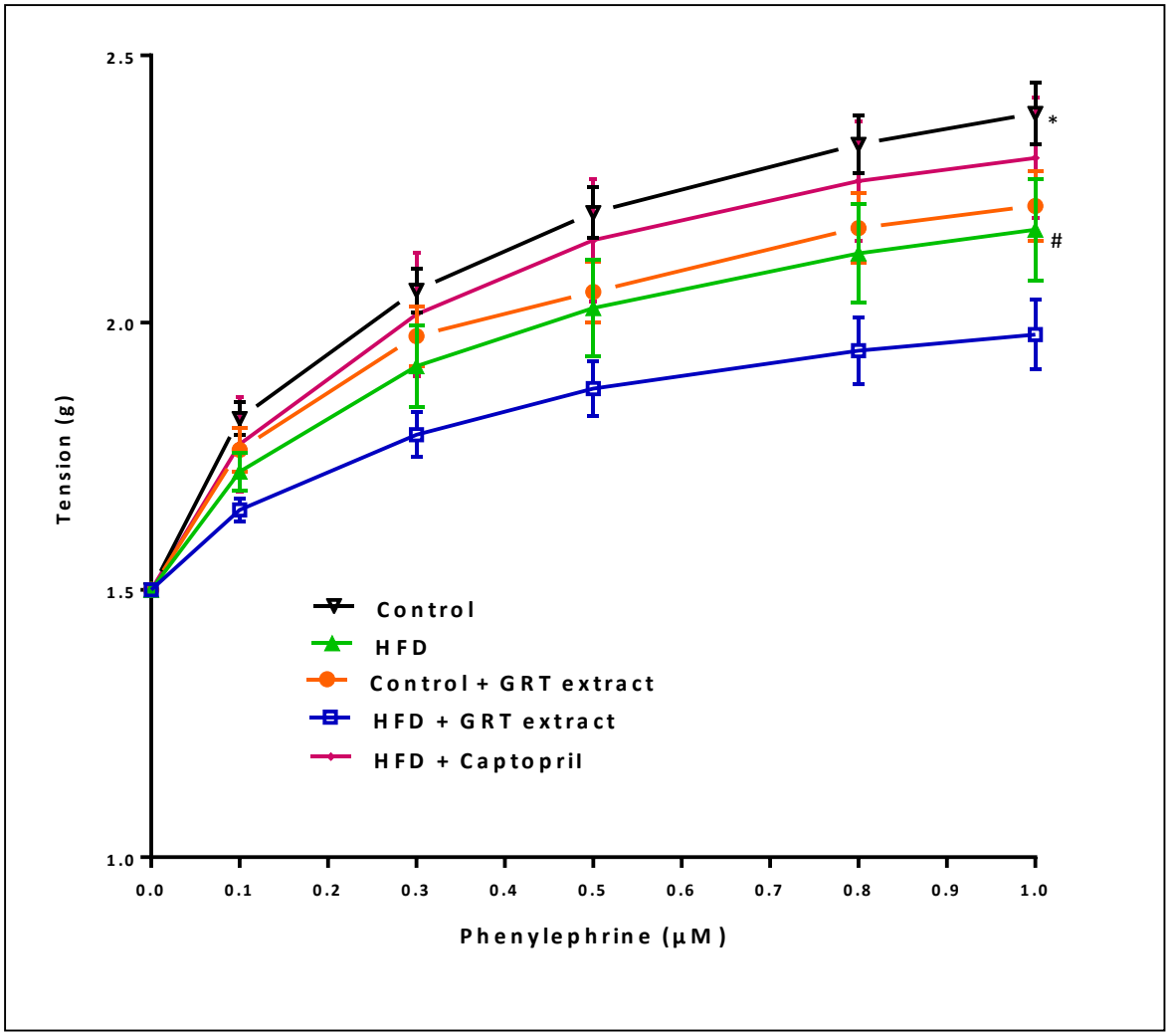

Figure 3.20 *Cumulative Phenylephrine induced vascular contraction of the HFD vs Control group (GRT treated and untreated), including the HFD + Captopril group. * $p < 0.001$, HFD vs Control and # $p < 0.05$, HFD + GRT vs HFD (n = 10-12 per group).*

3.7.2 Acetylcholine Induced Vascular Cumulative Relaxation

Treatment with the GRT extract significantly increased vascular relaxation in the HFD group when compared to the untreated HFD group (p = 0.0001). The same effect was observed in the HFD Captopril treated group when compared to the untreated HFD group (p = 0.0123).

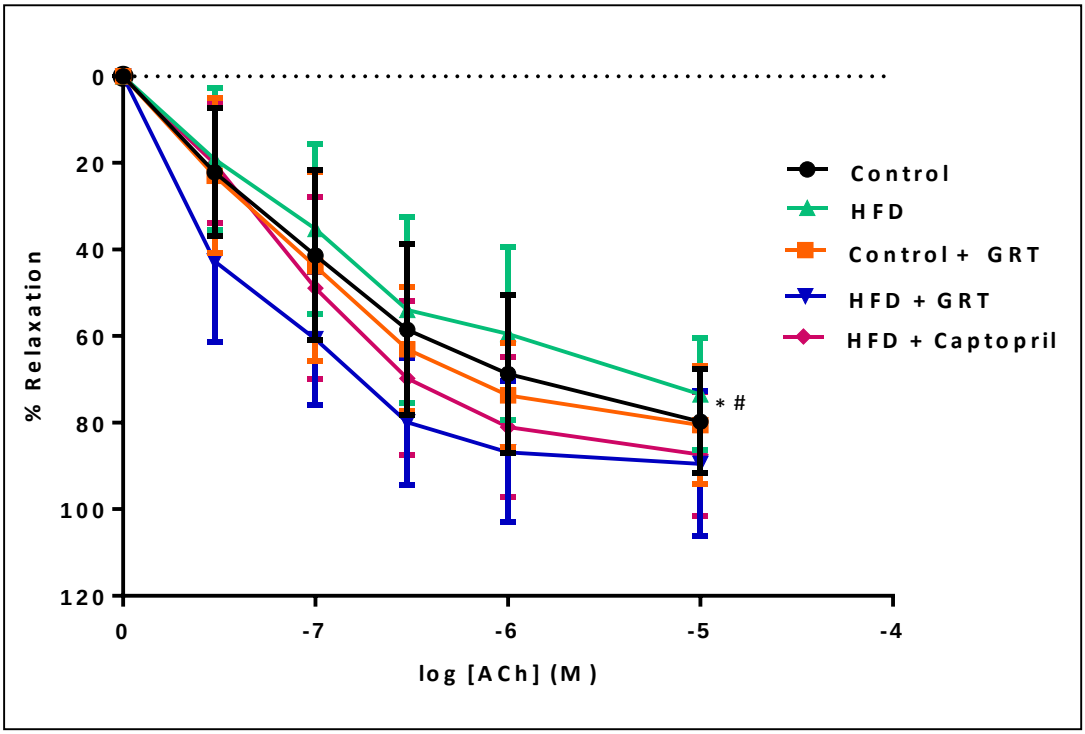

Figure 3.21 *Cumulative Acetylcholine induced vascular relaxation of the HFD vs Control group (GRT treated and untreated) including the HFD + Captopril group. * $p < 0.0001$, HFD + GRT vs HFD and # $p < 0.05$, HFD + Captopril vs HFD (n = 10-12 per group).*

3.8 Western Blot Analysis

Western blot analysis of all the groups was carried out in the aortic tissue, previously stored at -80°C using 26 well pre-cast gels. The signalling proteins involved in the endothelial health by stimulating NO production, analysed in this study were; AMPK (63kDa), PKB (56kDa) and eNOS (140kDa). The data below reflects the total (T) expression, phosphorylated (P) protein levels and the ratio (phosphorylation over total expression) of each protein.

3.8.1 Example of How the Western Blots Were Calculated

The gel gives a clear indication of the proteins separated (***Fig 3.22***), whereas the membrane gives a presentation of the full set of proteins transferred from the gel (***Fig 3.23***). The blot gives a clear presentation of the specific protein probed for, total AMPK in this example (***Fig 3.24***). The bands in the blot were normalised according to the full amount of proteins transferred to the membranes, to eliminate the need of a loading Control.

3.8.1.1 Example of the Gel

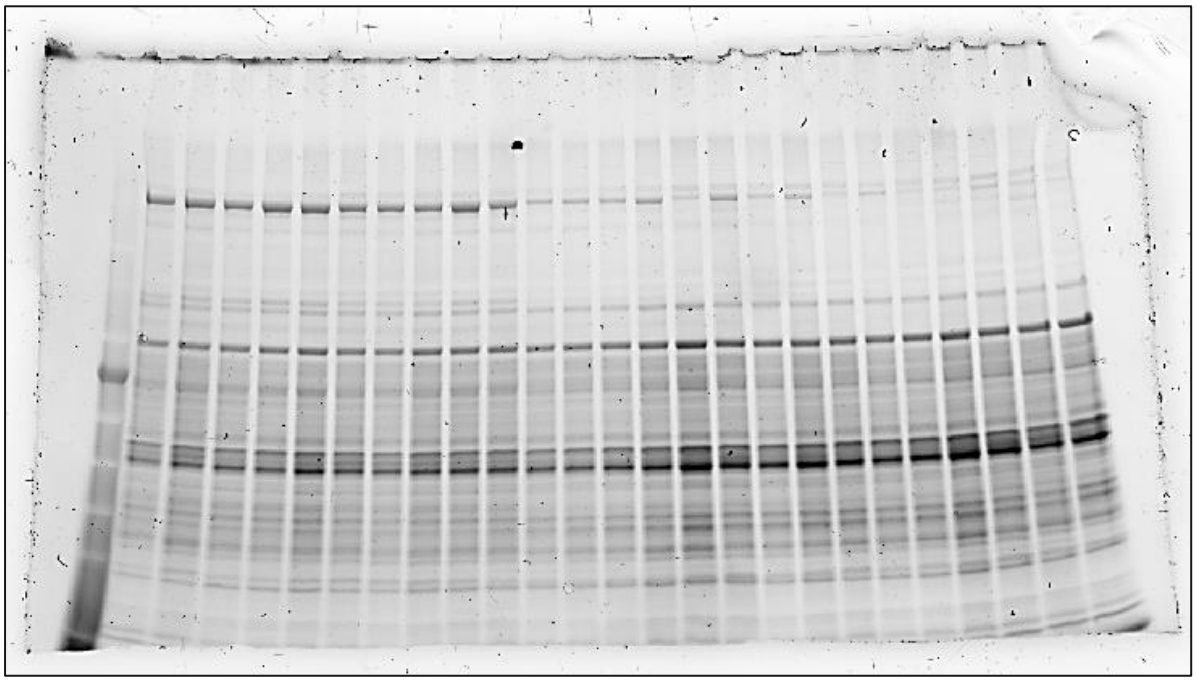

Figure 3.22: *A 26-well Pre-Cast gel depicting successful protein separation.*

3.8.1.2 Example of the Membrane

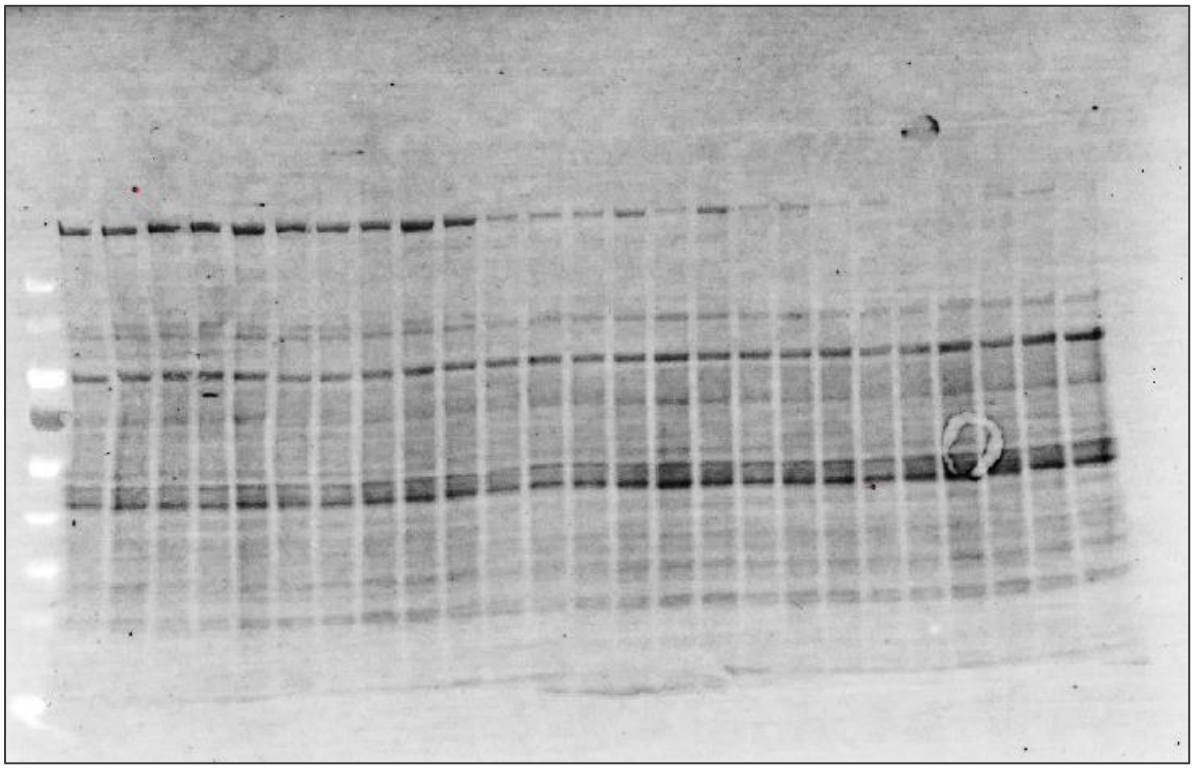

Figure 3.23: *Membrane picture depicting successful protein transfer from the 26-well pre-cast gel.*

3.8.1.3 Example of the Blot

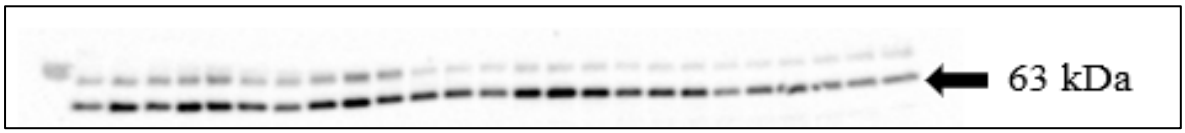

Figure 3.24: *Blot depicting bands of the specific protein probed for, total AMPK in this case with a size of 63 kDa.*

3.8.2 AMPK

The HFD group had significantly lower T-AMPK expression ($p < 0.0001$) and P-AMPK levels ($p < 0.0001$) when compared to the Control group (***Fig 3.25*** and ***Fig 3.26***), respectively. The Captopril increased the P-AMPK levels in the HFD animals treated with Captopril ($p < 0.05$) when compared to the HFD group (***Fig 3.26***). The GRT extract and Captopril significantly increased of the AMPK P:T ratio in the HFD + GRT extract/Captopril treated group ($p < 0.05$ and $p < 0.0001$, respectively) when compared to the HFD group (***Fig 3.27***).

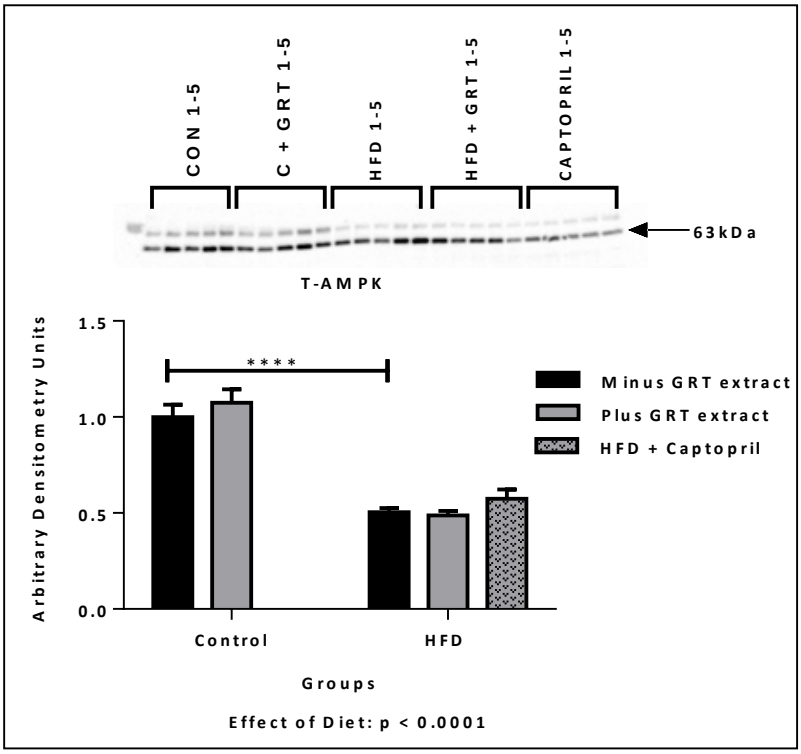

Figure 3.25 *T-AMPK expression in the aortic rings of the HFD vs Control group (GRT treated and untreated), including the HFD animals treated with Captopril. **** $p < 0.0001$, HFD vs Control group. According to a two-way ANOVA, the HFD had a significant effect ($p < 0.0001$) on the T-AMPK expression, n= 5 per group.*

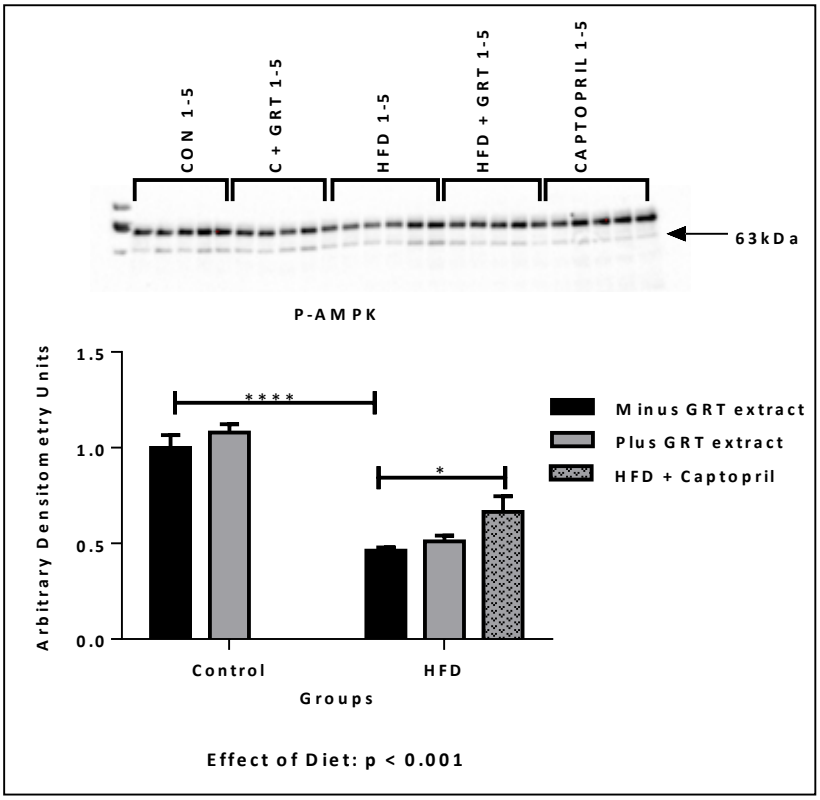

Figure 3.26 *P-AMPK levels in the aortic rings of the HFD vs Control group (GRT treated and untreated), including the HFD animals treated with Captopril. **** $p < 0.0001$, HFD vs Control group; * $p < 0.05$, HFD + Captopril vs HFD + GRT. According to a two-way ANOVA, the HFD had a significant effect ($p < 0.001$), on the P-AMPK levels n= 5 per group.*

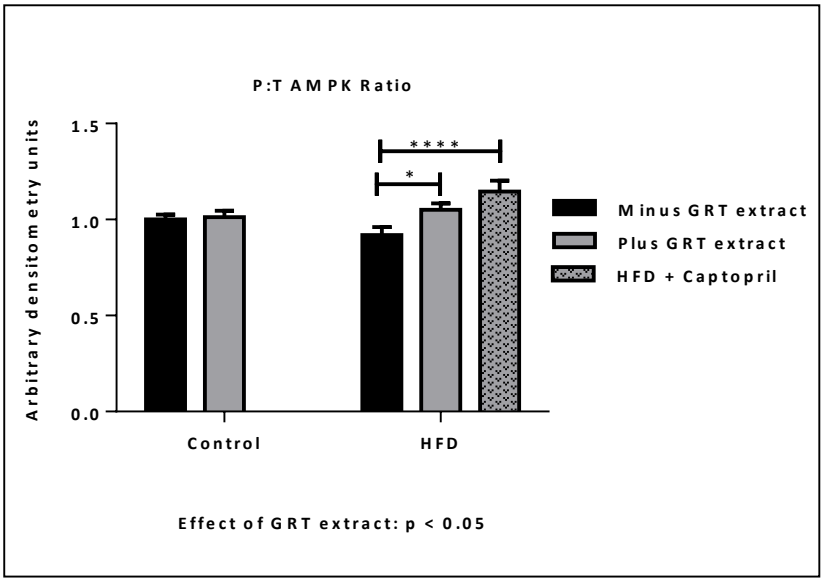

Figure 3.27 *AMPK P:T ratio in the aortic rings of the HFD vs Control group (GRT treated and untreated), including the HFD animals treated with Captopril. * p < 0.05, HFD + GRT vs HFD; **** p < HFD + Captopril vs HFD. According to the two-way ANOVA, the GRT extract had a significant effect (p < 0.05) on the P:T AMPK ratio, n = 5 per group.*

3.8.3 PKB

The HFD group ($p < 0.001$) showed a significant decrease in the total PKB expression and phosphorylated PKB levels when compared to the Control group (***Fig 3.28*** *and* ***Fig 3.29***). The Captopril in the HFD + Captopril group ($p < 0.001$) significantly increased PKB phosphorylation when compared to the HFD group **(*Fig 3.29***). No significant differences were observed in the PKB P:T ratio in all the groups assessed (***Fig 3.30***).

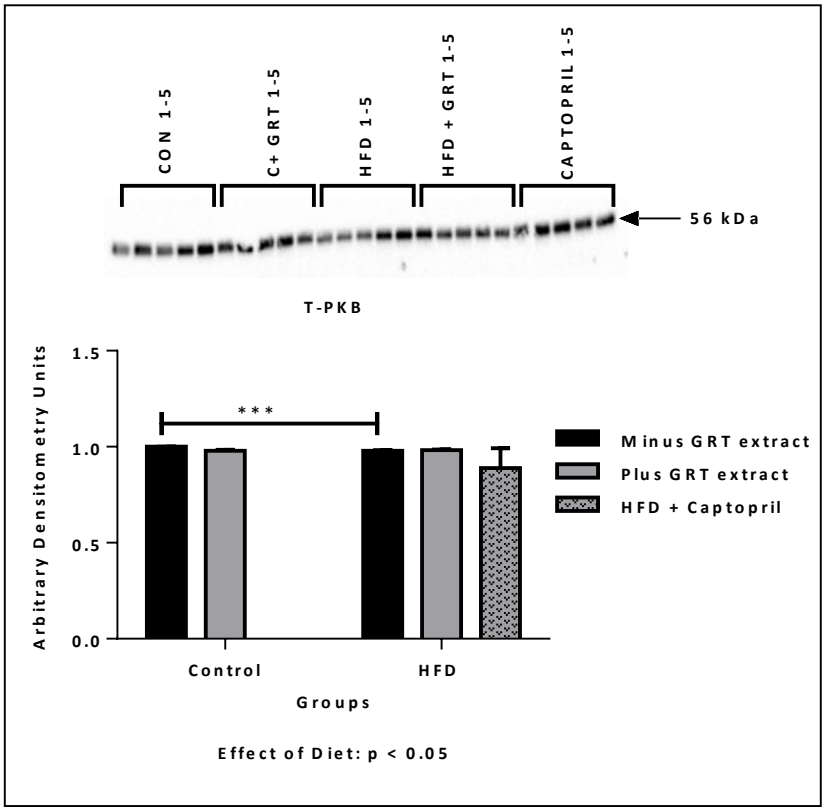

Figure 3.28 *T-PKB expression in the aortic rings of the HFD vs Control group (GRT treated and untreated), including the HFD animals treated with Captopril. *** $p < 0.001$, HFD vs Control, n =5 per group. According to a two-way ANOVA, the HFD had a significant effect ($p < 0.05$), on the T-PKB expression n= 5 per group.*

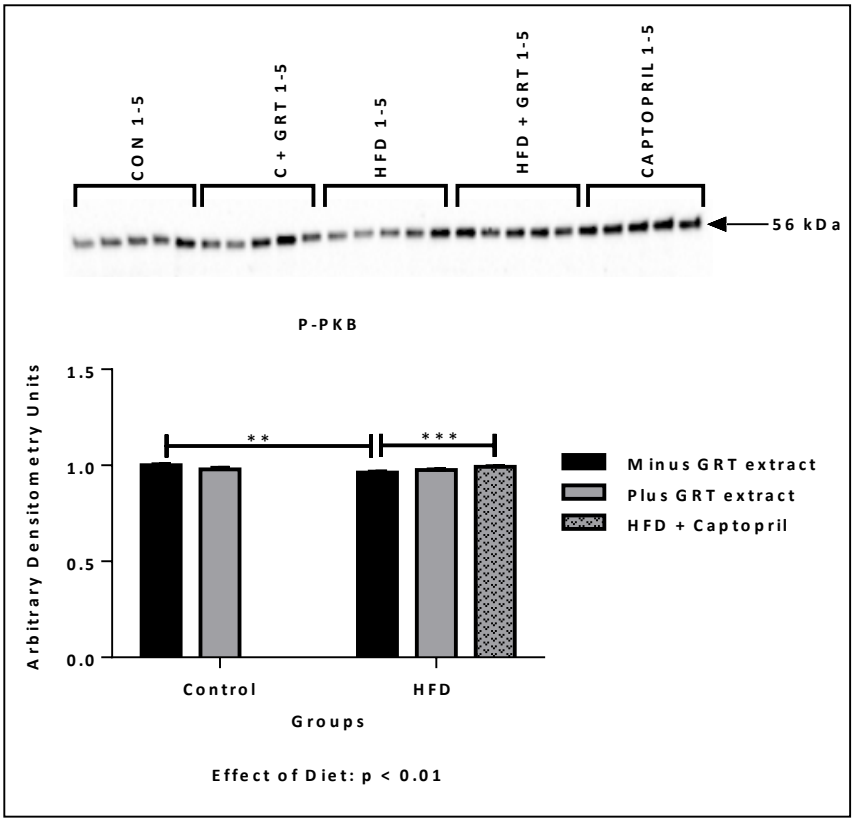

Figure 3.29 *P-PKB levels in the aortic rings of the HFD vs Control group (GRT treated and untreated), including the HFD animals treated with Captopril. ** p < 0.01, HFD vs Control group;*** p < 0.001, HFD + Captopril vs HFD group. According to a two-way ANOVA, the HFD had a significant effect (p < 0.01), on P-PKB levels n= 5 per group.*

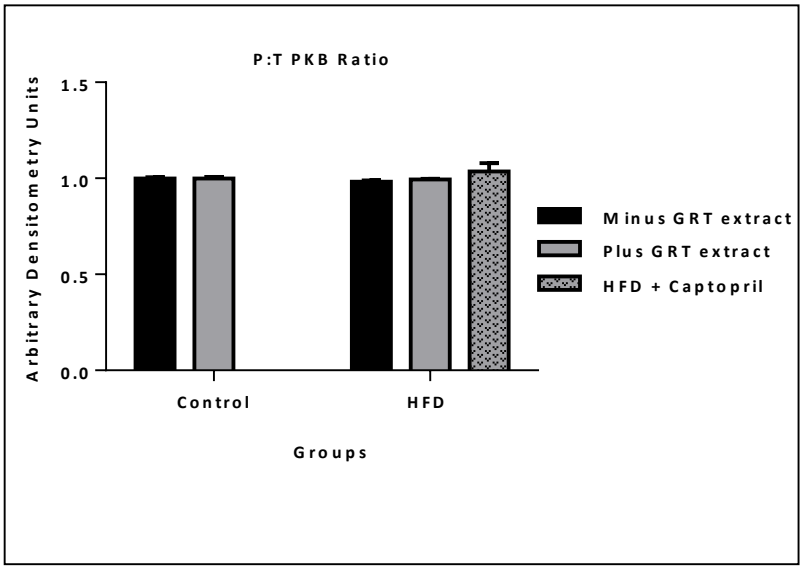

Figure 3.30 *P:T PKB ratio in the aortic rings of the HFD vs Control group (GRT treated and untreated), including the HFD animals treated with Captopril (n = 5 per group).*

3.8.4 eNOS

The GRT extract significantly increased the T-eNOS expression in the HFD + GRT treated group ($p < 0.01$) when compared to the HFD group (***Fig 3.31***). The HFD and HFD + Captopril treated groups ($p < 0.001$ and $p < 0.05$, respectively) had significantly increased P-eNOS levels when compared to the Control and HFD group (***Fig 3.32*).** The HFD and HFD + Captopril treated group ($p < 0.01$ and $p < 0.05$, respectively) had significantly increased P:T eNOS ratio in the Control and the HFD group (***Fig 3.33***).

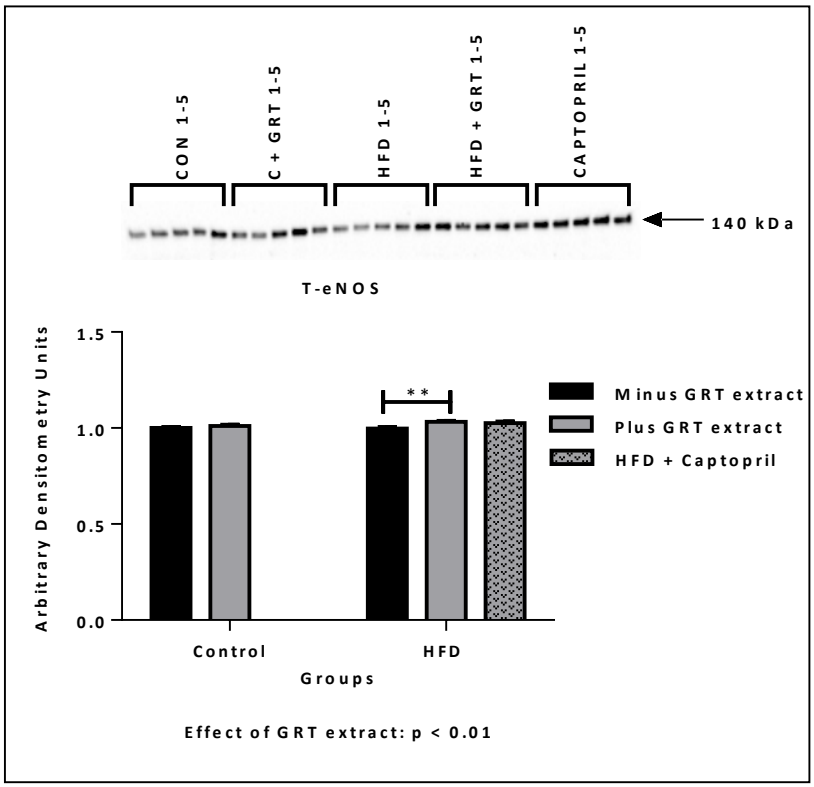

Figure 3.31 *T-eNOS expression in the aortic rings of the HFD vs Control group (GRT treated and untreated), including the HFD animals treated with Captopril. ** $p < 0.01$, HFD + GRT vs HFD. According to a two-way ANOVA, the GRT had a significant effect ($p < 0.01$) on the T-eNOS expression, n= 5 per group.*

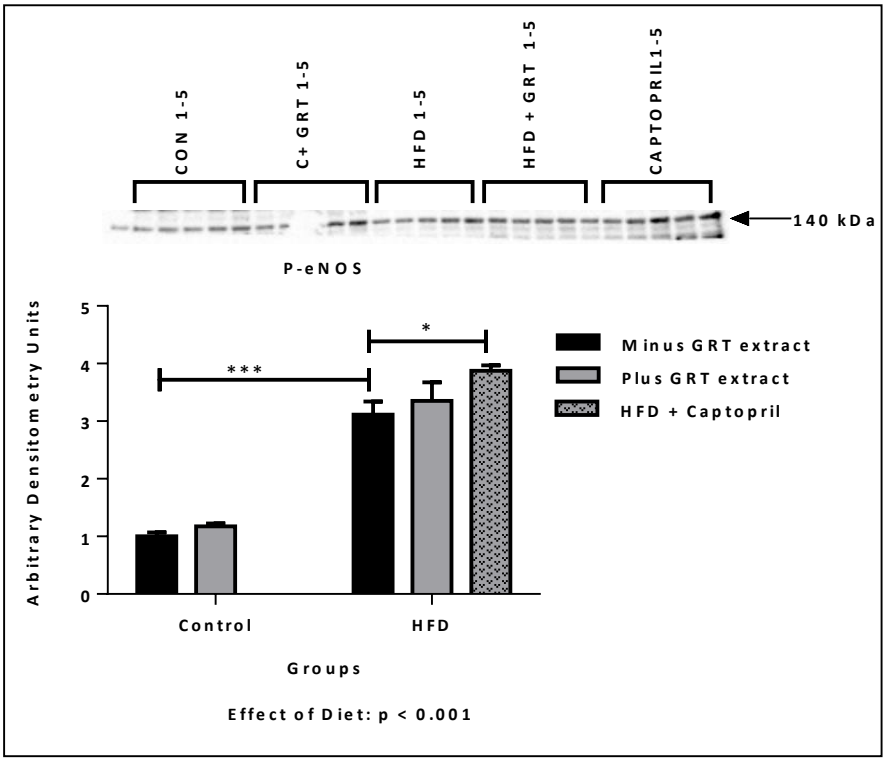

Figure 3.32 *P-eNOS expression in the aortic rings of the HFD vs Control group (GRT treated and untreated), including the HFD animals treated with Captopril. *** p < 0.001, HFD vs Control group; * p < 0.05, HFD + Captopril vs HFD group. According to a two-way ANOVA, the HFD had a significant effect (p < 0.001) on the P-eNOS levels, n= 5 per group.*

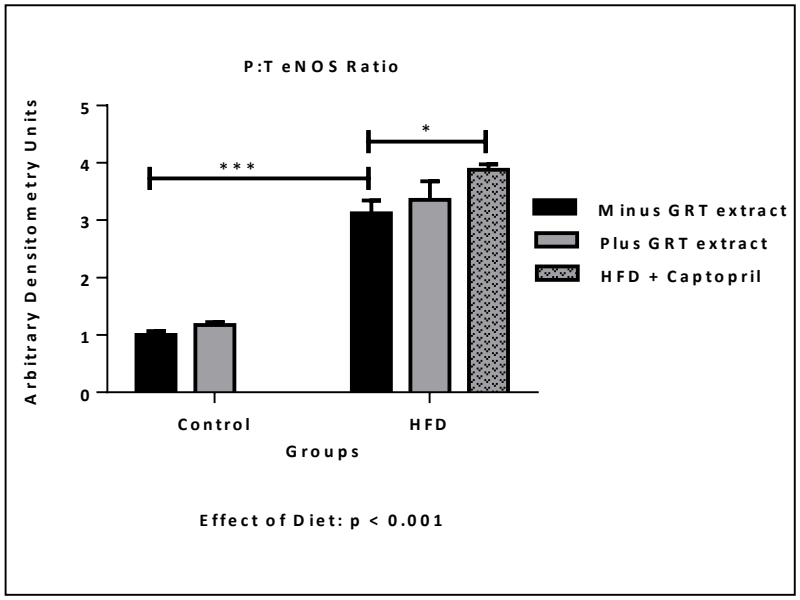

Figure 3.33 *P: T eNOS ratio in the aortic rings of the HFD vs Control group (GRT treated and untreated), including the HFD animals treated with Captopril. *** p < 0.001 HFD vs Control group; HFD + Captopril vs HFD group. According to a two-way ANOVA, the HFD had a significant effect (p < 0.001) on the P:T eNOS levels, n= 5 per group.*

3.9 Antioxidant status

The activities of the primary antioxidant enzymes were determined in the liver.

3.9.1 SOD

The HFD animals had significantly low SOD activity when compared to the Control animals (227.60 ± 5.631 vs 281.90 ± 10.640 Units/mg protein; $p < 0.001$). The GRT extract significantly increased SOD activity in the HFD treated animals when compared to the untreated HFD animals (335.60 ± 37.310 vs 227.60 ± 5.631 Units/mg protein; $p < 0.01$).

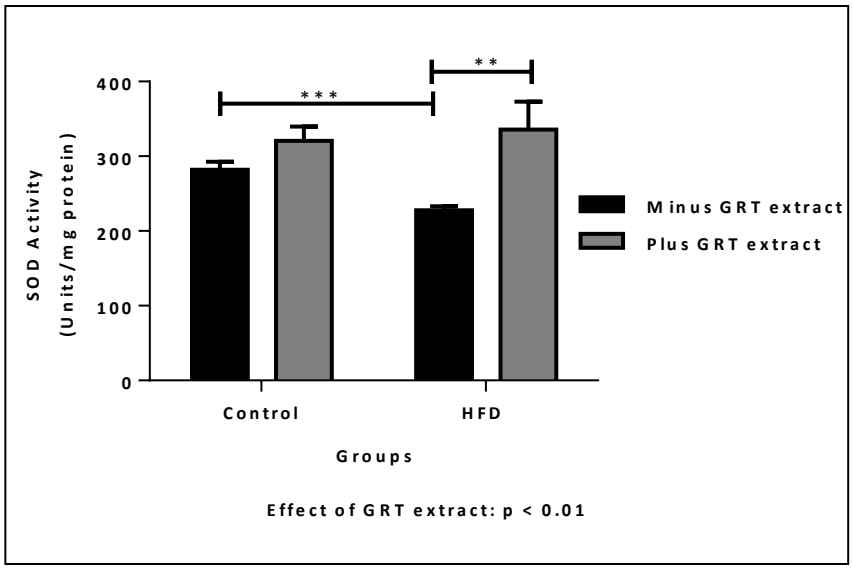

Figure 3.34 *SOD activity in the liver of the HFD vs Control group (GRT treated and untreated). *** p < 0.001, HFD vs Control group; ** p < 0.01, HFD + GRT vs HFD group. According to a two-way ANOVA, the GRT extract resulted in a significant increase in SOD activity (p < 0.01), n = 10 per group.*

3.9.2 CAT

The HFD animals had significantly low CAT activity when compared to the Control animals (63.59 ± 2.801 vs 91.88 ± 6.507 µmole/min/µg; $p < 0.001$). Treatment with the GRT extract in the treated HFD animals significantly increased catalase activity when compared to the untreated HFD animals (76.88 ± 3.900 vs 63.59 ± 2.801 µmole/min/µg; $p < 0.05$).

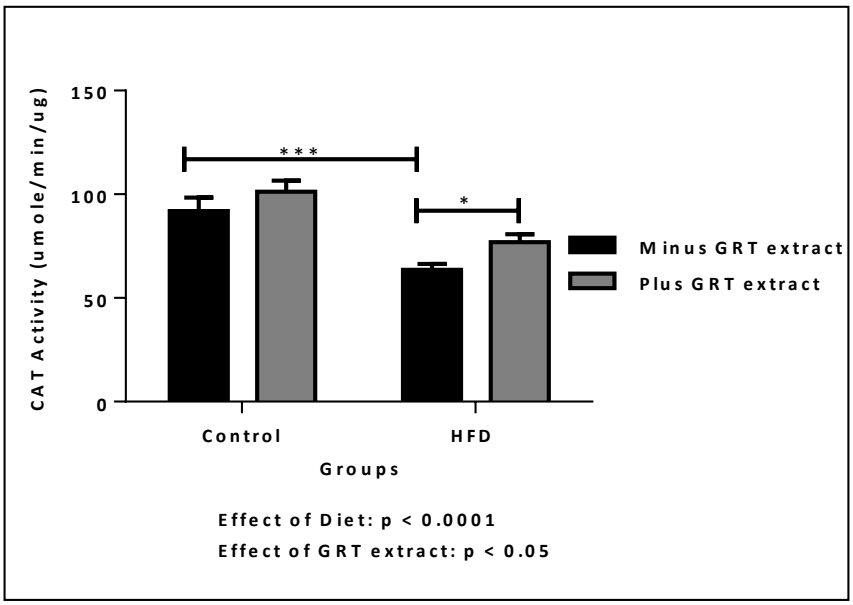

Figure 3.35 *Catalase activity in the liver of the HFD vs Control group (GRT treated and untreated). *** p < 0.001, HFD vs Control group;* p < 0.05, HFD + GRT vs HFD group. According to a two-way ANOVA, the HFD significantly decreased (p < 0.0001) catalase activity, whereas the GRT extract significantly increased (p < 0.05) catalase activity, n = 10 per group.*

3.9.3 GPx

The HFD animals had significantly lower GPx activity relative to the Control animals (0.003563 ± 0.000889 vs 0.01848 ± 0.001635 µmole/min); $p < 0.0001$. The GRT extract in the treated Control animals significantly increased the GPx activity when compared to the untreated Control animals (0.03535 ± 0.006116 vs 0.01848 ± 0.001635 µmole/min; $p < 0.05$).

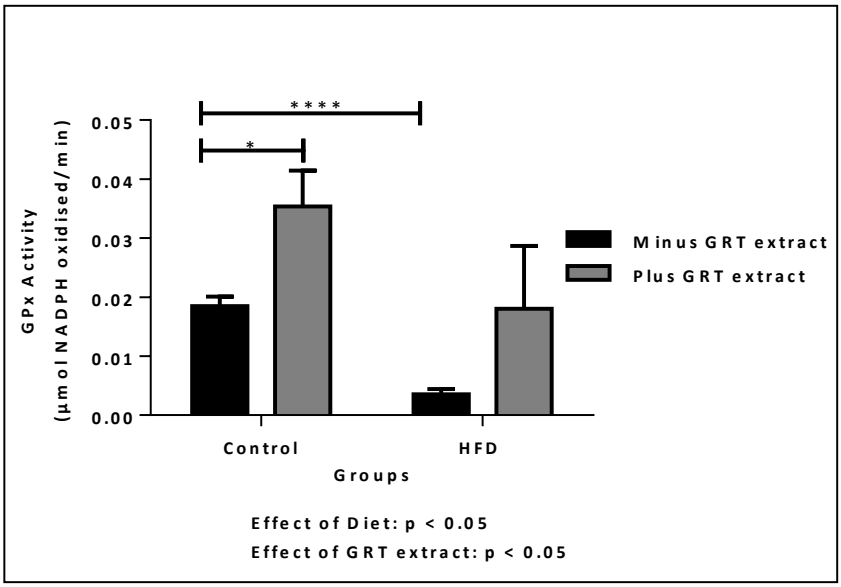

Figure 3.36 *GPx activity in the liver of the HFD vs Control group (GRT treated and untreated). **** p < 0.0001, HFD vs Control group,* p < 0.05, Control + GRT vs Control group, n = 10 per group. According to a two-way ANOVA, the HFD resulted in a significant decrease (p < 0.05) in GPx activity, whereas the GRT extract resulted in a significant increase in GPx activity,(p < 0.05), n = 10 per group.*

3.9.4 TBARS

The HFD animals had significantly increased MDA levels when compared to the Control animals (5.12 ± 0.347 vs 3.60 ± 0.276 µmol/mg protein; $p < 0.01$). Treatment with GRT extract in the treated Control significantly decreased the MDA levels when compared to the untreated Control group (2.51 ± 0.226 vs 3.60 ± 0.276 µmol/mg protein; $p < 0.01$). Furthermore, supplementation with GRT extract in the HFD animals significantly decreased MDA levels, relative to the untreated HFD animals (3.10 ± 0.2841 vs 5.12 ± 0.347 µmol/mg protein; $p < 0.01$).

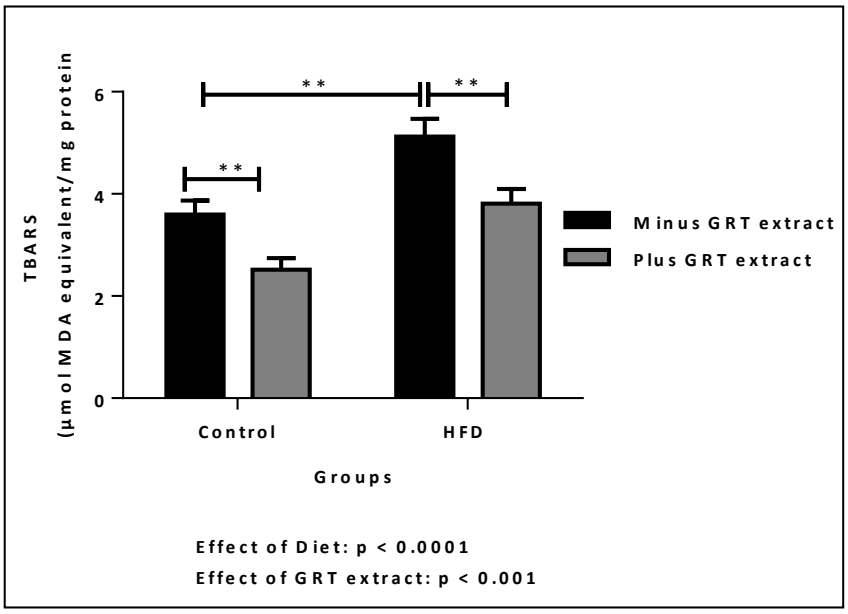

Figure 3.37 *TBARS levels in the liver of the HFD vs Control group (GRT treated and untreated. ** p < 0.01, HFD vs Control group; ** p < 0.01, HFD + GRT vs HFD group; ** p < 0.01, Control + GRT vs Control group, n = 10 per group. According to a two-way ANOVA, the HFD resulted in a significant increase (p < 0.0001) in TBARS levels, whereas the GRT extract resulted in a significant decrease (p < 0.001) in TBARS levels, n = 10 per group.*

Chapter 4. Discussion

4.1 Biometric Parameters

4.1.1 Food and Water Intake

In the present study, the HFD animals showed a significant increase in mean food intake before and after treatment with the GRT extract, when compared to the age matched Controls, ***Fig 3.2*** *and* ***Fig 3.9***, respectively. Seemingly, the HFD group enjoyed the HFD diet and this may be attributed to the moisture and sweetness of the food. These findings correspond with a previous study which showed that, excessive consumption of diets rich in sugar (fructose) content is driven by the pleasure in the sweet taste and that excess consumption of a sugar-rich diet subsequently results in obesity (Lenoir, Serre, Cantin & Ahmed, 2007). The HFD group drank significantly less water in comparison to the Control group, before (***Fig 3.3***) and after treatment with the GRT extract (***Fig 3.10***). The significantly lower water consumption observed in the HFD group, when compared to the Control group may be due to the food being moist as opposed to the dry standard rat chow (pellets) given to the Control group, which elicits more fluid intake. A study conducted in humans showed that there is an inverse correlation between increased water content and energy intake (Kant, Graubard & Atchison, 2009). That is, the higher the sugar content, the lower the fluid intake.

Treatment with the GRT extract had no significant effect on the mean food intake in both groups (***Fig 3.9***). However, it the significantly increased mean water intake in the treated Control group (***Fig 3.10****)* when compared to the untreated Control. This corresponds with a study that showed an increase in the daily fluid intake by rats drinking unfermented rooibos (Canda, Oguntibeju & Marnewick, 2014). This could also potentially be as a result of the dry pellets causing the Control animals to drink more water as GRT treatment did not increase the mean fluid intake in the HFD animals.

In summary: HFD animals had a significantly increased mean food intake when compared to the Control animals. Additionally, the HFD animals had a lower fluid intake relative to the Control animals. The animals fed HFD seemed to have enjoyed the diet as opposed to the standard rat chow due to the food being moist, with a pleasurable sweet taste as opposed the standard rat. This may also be the reason for the decreased mean fluid intake observed in the HFD animals, relative to the Control animals. The GRT extract increased water intake, and may be a result of the dry standard rat chow which they ingested compared to the HFD groups.

4.1.2 Body Weight/Gain

The HFD group showed a significantly increased body weight when compared to the Control group, before (***Fig 3.4***) and after treatment with the GRT extract (***Fig 3.11***). The animals in all the different groups assessed, presented a weekly increase in body weight gain (***Fig 3.12***). Therefore, the diet composition used in this study successfully induced obesity in the HFD group. These findings correspond with previous studies done in our laboratory that used the same diet (Huisamen, George, Dietrich & Genade, 2013; Salie, Huisamen & Lochner, 2014), including that of other investigators who used a diet of similar composition in order induce obesity (Srinivasan, Viswanad, Asrat, Kaul & Ramarao, 2005). Treatment with the GRT extract significantly reduced body weight in the treated HFD group when compared to the untreated HFD group (***Fig 3.11***). In addition, treatment with GRT extract did not affect the body weight of the Control animals. The above findings are also reflected in the weekly body weight gain, emphasising the effect of the diets on the body weight gain of the animals.

The anti-obesity properties of the GRT extract, specifically, have not been investigated. However, the anti-obesity effects of the individual polyphenolic compounds (aspalathin, rutin) found in the GRT extract (see Appendix A) have been investigated (Choi, Park, Choi & Lee, 2006; Sanderson, Mazibuko, Joubert, De Beer, Johnson, Pheiffer, Louw & Muller, 2014). These polyphenols may bring about the anti-obesity effects by inhibiting adipogenesis (the differentiation of preadipocytes to mature adipocytes) and downregulating the mRNA expression of the transcription factors responsible for adipocyte differentiation such as peroxisome proliferator-activated receptor-gamma (γ) (PPAR-γ) (Choi *et al.*, 2006). The mechanism behind the reduction in body weight/gain induced by the GRT extract observed in the present study, may be correlated with the anti-obesity findings from the previous studies mentioned above. Unfermented rooibos and GRE have been shown to have no effect on the body weight of the Control animals fed a standard rat chow (Canda, Oguntibeju & Marnewick, 2014; Van Der Merwe, De Beer, Joubert & Gelderblom, 2015). This corresponds with our findings, as the GRT extract did not affect the body weight of the Control animals.

In summary: Excess consumption of a high-fat, high-sugar diet is a contributing factor to obesity (Srinivasan, Viswanad, Asrat, Kaul & Ramarao, 2005) and obesity has been characterised by an increase in calorie intake vs low energy expenditure, which may impair health (Ratzan, 2009). Food intake is an important parameter to elucidate body weight gain and the increase in body weight/gain correlates with the increased mean food intake observed especially in the HFD group, as discussed in section 4.1.1. GRT extract may be a useful therapeutic agent against obesity and the metabolic disorders related to obesity.

4.1.3 IP Fat Weight

The IP fat weight was collected and recorded on the day of sacrifice. The HFD group showed a significant increase in the IP fat mass, relative to the age matched Controls (***Fig 3.13***). The GRT extract significantly decreased the IP fat weight in the treated HFD group. Additionally, treatment with GRT extract did not affect the IP fat weight of the Control animals.

An increase in IP fat, as a result of fat accumulation in the abdomen is elicited by excess consumption of a high-fat, high-sugar diet and sometimes obesity. In previous studies, rodents fed a HFD were presented with an increase in adipose tissue relative to Control animals fed a standard diet (Del Bas, Crescenti, Arola-Arnal, Oms-Oliu, Arola & Caimari, 2015; Milagro, Campión & Martíez, 2006).

Continuous consumption of Rooibos extracts have been shown to decrease the size and number of adipose tissue. The mechanism behind this finding, according to this study, was as a result of AMPK activation and restoration of the cell energy homeostasis (Beltrán-Debón, Rull, Rodríguez-Sanabria, Iswaldi, Herranz-López, Aragonès, Camps, Alonso-Villaverde, Menéndez, Micol, Segura-Carretero & Joven, 2011).

In summary: The HFD animals had increased IP fat mass when compared to the Control animals. Treatment with GRT extract significantly decreased IP fat weight in the treated HFD animals but did not affect the IP fat weight of the Control animals. These findings correlate with the increase in body weight and food intake observed in the HFD group as described in section 4.1.2. Dysfunction of the adipose tissue due to fat accumulation result in the dysregulation of adipose tissue. It has been shown that enlarged adipose tissue elicit impaired glucose tolerance, and insulin resistance in diet-induced rat models (D'Alessandro, Selenscig, Illesca, Chicco & Lombardo, 2015; Rader, 2007). A decrease in the IP fat weight can reverse the dysregulation in glucose and lipid homeostasis thus improving insulin resistance. Therefore, treatment with GRT extract may be a potential agent used against adverse metabolic disorders induced by the enlarged adipose tissue, as a result of obesity, in this case.

4.1.4 Liver Weight

The HFD group had significantly increased liver weight, when compared to the Controls (***Fig 3.14***). The GRT extract significantly decreased the liver weight in the HFD treated group when compared to the untreated HFD group.

These findings are consistent with a study done by Milagro *et al* (2006), that showed an increase in liver weight in the animals fed a HFD compared to the animals fed a standard diet. In obese subjects, the rate of FFA release from the adipose tissue to the liver and the skeletal muscle is increased. As a result, the fat accumulation inside the liver might result in the increased liver weight. Obese patients

are often characterised by severe liver disease, NAFLD, when compared to the lean patients with NALFD. Fatty liver and the persistent increase in aminotransferase is the cause of liver disease. Increase in serum alanine transferase activity is furthermore positively associated with visceral obesity, insulin resistance, increase leptin and insulin levels (Fabbrini, Sullivan & Klein, 2010; Ruhl & Everharty, 2003). Insulin resistance has been proven to be an independent cause for the development of NAFLD (Choudhary, Duseja, Kalra, Das, Dhiman & Chawla, 2012; Farrell & Larter, 2006; Kumar & Mohan, 2017). When the liver is fatty, it becomes insulin resistant. In this state, insulin fails to counteract the increase in glucose levels and hyperglycaemia results. The elevated glucose in the liver subsequently is released to the systematic circulation, in the plasma. In the liver, insulin resistance increases lipolysis in the adipose tissue and FFA uptake is upregulated (Fabbrini *et al.*, 2010).

Lifestyle changes can also reverse the early stages of NAFLD to the irreversible stage of liver fibrosis. Unfermented rooibos, GRE and pure aspalathin extract have been shown to have ameliorative effects reversing the dysregulation in lipid homeostasis, glucose homeostasis, lipoprotein metabolism and insulin resistance (Kamakura, Son, de Beer, Joubert, Miura & Yagasaki, 2015; Mazibuko, Joubert, Johnson, Louw, Opoku & Muller, 2015; Muller, Joubert, De Beer, Sanderson, Malherbe, Fey & Louw, 2012). That way it is able to counteract or reverse the NAFLD.

In summary: The increased liver weight observed in the HFD animals may be attributed to the increase FFA release from the enlarged adipose tissue and reduced lipolysis inside the liver. Excessive accumulation of triglycerides inside the liver is associated with dysregulation in the lipid and glucose homeostasis thus resulting in the development of NALFD amongst pathological conditions such as insulin resistance, inflammation and dyslipidaemia and T2D. Increasing prevalence of obesity is the initial regulator of the development these pathological conditions. Rooibos extracts have been shown to have ameliorative effects against the progression of NALFD to irreversible liver damage by regulating glucose, lipid homeostasis including insulin resistance. The effect of the GRT extract in reducing liver weight therefore supports these findings, however further investigation into the mechanism is needed.

4.1.5 Blood Glucose

The HFD group had significantly increased glucose levels when compared to the Control group, before (***Fig 3.5A***) and after treatment with the GRT extract (***Fig 3.15B***). The GRT extract significantly decreased glucose levels in the treated HFD group when compared to the untreated HFD group (***Fig 3.15B***). According to our findings, the HFD reduced glucose metabolism in the HFD animals and this corresponds with the previous studies that used the same diet (Salie, Huisamen &

Lochner, 2014; Srinivasan, Viswanad, Asrat, Kaul & Ramarao, 2005). Previous studies have documented that animals fed the HFD have decreased glucose metabolism (Huisamen, George, Dietrich & Genade, 2013). Obesity is strongly associated with the a decrease in glucose metabolism, increased fasting blood glucose levels and impaired glucose tolerance and these metabolic changes were evident in the HFD-fed animals used in this study. Leptin directly affects insulin levels by controlling the pancreatic islets. This implies that, when the leptin levels are high, hyperinsulinemia results (Kennedy, Askelund, Premkumar, Phillips, Murphy, Windsor & Petrov, 2016; Wozniak, Gee, Wachtel & Frezza, 2009). This subsequently results in hyperglycaemia and this is often seen in obese people.

The GRT extract improved glucose metabolism in the HFD fed animals. GRE extract has been shown to suppress the increase in plasma glucose levels in an *in vivo* study (Mikami, Tsujimura, Sato, Narasada, Shigeta, Kato, Hata & Hitomi, 2015). Furthermore, the GRE extract and aspalathin have been shown to improve glucose uptake and lipid metabolism *in vivo* (Mazibuko, Joubert, Johnson, Louw, Opoku & Muller, 2015). The major active compound, in the GRE extract, aspalathin, has been shown to increase glucose uptake in muscle cells and insulin secretion by the pancreatic-β cells *in vitro* (Kawano, Nakamura, Hata, Minakawa, Miura & Yagasaki, 2009). In the same study, aspalathin decreased fasting blood glucose and improved glucose intolerance in the diabetic rat model, confirming the effects of aspalathin on glucose homeostasis (Kawano *et al.*, 2009).

Anti-diabetic effects of GRE, aspalathin and an unfermented rooibos extract in cultured cells and type 2 diabetic mice have been documented (Kamakura, Son, de Beer, Joubert, Miura & Yagasaki, 2015; Muller, Joubert, De Beer, Sanderson, Malherbe, Fey & Louw, 2012). To elaborate, the GRE extract enhanced glucose uptake via the phosphorylation of AMPK and PKB signalling proteins which resulted in translocation of the insulin-regulated GLUT4 in the plasma membrane (Kamakura *et al.*, 2015; Muller *et al.*, 2012), Interestingly, in this study, the GRT extract showed no significant effect on the phosphorylation of PKB and AMPK (***Fig 3.29*** and ***Fig 3.26***), respectively. However, according to the P:T AMPK ratio, GRT extract increased the AMPK phosphorylation in the treated HFD group (***Fig 3.27***). This could mean that GRT extract may have induced the upregulation of glucose uptake in the tissues via the AMPK pathway.

In summary: Obesity, especially abdominal obesity, is strongly associated with impaired glucose metabolism (D'Alessandro, Selenscig, Illesca, Chicco & Lombardo, 2015) and this results in hyperglycaemia. The HFD animals were presented with a reduction in glucose metabolism when compared to the Control animals. It has been shown that hyperglycaemia and increased plasma FFA leads to ROS generation. This, consequently results in oxidative stress, which then impairs insulin signalling thus resulting in insulin resistance (D'Alessandro, Selenscig, Illesca, Chicco & Lombardo,

2015; Jung & Choi, 2014). The GRT extract however, increased glucose metabolism in the treated HFD animals. This could be as a result of the AMPK phosphorylation according to the upregulated P:T AMPK levels.

4.2 Leptin levels

The HFD group had significantly increased leptin levels when compared to the control group and the GRT extract significantly decreased leptin levels in the treated HFD group when compared to the untreated HFD group (***Fig 3.14***).

Experimental studies done in rats have shown an increase in leptin levels in the obese rat-rodents fed a HFD diet when compared to the rats fed a standard diet (Lozano, Van der Werf, Bietiger, Seyfritz, Peronet, Pinget, Jeandidier, Maillard, Marchioni, Sigrist & Dal, 2016; Shapiro, Mu, Roncal, Cheng, Johnson & Scarpace, 2008). Obesity has been associated with increased leptin levels (Shapiro, Mu, Roncal, Cheng, Johnson & Scarpace, 2008) and it has been reported that elevated leptin levels in an obese state are due to the obese (ob) gene mutation (adipocyte-specific) that encodes for leptin, resulting in leptin resistance (Considine, Sinha, Heiman, Kriauciunas, Stephens, Nyce, Ohannesian, Marco, McKee & Bauer, 1996). It has been shown that the insulin-dependent PI3K pathway plays a significant role in leptin resistance, as shown by artificial inhibition of the pathway in a mice model (Oswal & Yeo, 2010). The PI3K pathway is also involved in energy homeostasis with leptin and insulin acting together to elicit this balance (Oswal & Yeo, 2010).

In obese humans, there appears to be a reduction in leptin transport from the plasma/peripheral tissues to the blood brain barrier in obese individuals, low leptin levels in the cerebrospinal fluid, compared to the plasma (Caro, Kolaczynski, Nyce, Ohannesian, Opentanova, Goldman, Lynn, Zhang, Sinha & Considine, 1996; Considine, Sinha, Heiman, Kriauciunas, Stephens, Nyce, Ohannesian, Marco, McKee & Bauer, 1996).

Increased levels of triglycerides interferes with and impairs the transport of leptin across the blood brain barrier (Veyrat-Durebex, Poher, Caillon, Somm, Vallet, Charnay & Rohner-Jeanrenaud, 2013). In rodents fed a high-fat and high-fructose diet, the increased triglycerides levels elicited insulin and leptin resistance (Veyrat-Durebex *et al.*, 2013).

Leptin is a hormone that regulates weight loss. Rooibos treatment has been shown to decrease leptin levels in differentiating 3T3-L1 adipocytes (Sanderson, Mazibuko, Joubert, De Beer, Johnson, Pheiffer, Louw & Muller, 2014). According to these findings, one way that GRT extract could have induced less weight gain in the animals is by acting on the hypothalamus improving leptin transportation across the blood brain barrier thus reducing the leptin levels in the plasma. Further

mechanisms need to be explored for example, the inhibitory effects of the pancreatic lipase by the GRT extract *in vivo* and *in vitro*.

In summary: According to our findings, it can be concluded that the HFD-fed animals may have been leptin resistant, with the failure to reduce or control hunger which subsequently resulted to increased food intake (Wang, Obici, Morgan, Barzilai, Feng & Rossetti, 2001). One effective way of reversing the pathophysiological conditions induced by obesity is by losing weight or decreasing the consumption of energy dense foods with a diet low in energy. GRT extract has exhibited a therapeutic potential to be used as an agent against leptin resistance, although further investigations are needed.

4.3 Blood Pressure

The HFD group showed a significant increase in the mean systolic, diastolic and arterial pressure when compared to the Control, before (***Fig 3.6, Fig 3.7*** *and* ***Fig 3.8***) and after the GRT treatment (***Fig 3.17, Fig 3.18*** *and* ***Fig 3.19***). According to the above findings, the HFD composition used in this study resulted in hypertensive effects as measured in weeks 8-9, before treatment with GRT. These findings are consistent with a previous study done in our laboratory (Huisamen, George, Dietrich & Genade, 2013).

Obesity has been strongly associated with the development of hypertension and renal injury via various mechanisms, including renal sodium reabsorption, impaired pressure natriuresis, defined as the relationship between excretion of sodium and mean arterial pressure, and by eliciting volume expansion via the activation of RAAS and sympathetic nervous system (SNS). Additionally, increased visceral adiposity results in elevated blood pressure via the physical compression of the kidneys, due to accumulation of fat inside and around the kidneys (Hall, Do Carmo, Da Silva, Wang & Hall, 2015).

Another mechanism is via increased leptin levels resulting in the stimulation of the SNS (Machleidt, Simon, Krapalis, Hallschmid, Lehnert & Sayk, 2013). Experimental studies performed in rodents and humans have shown a correlation between increased leptin levels and the development of hypertension-induced obesity (Haynes, Morgan, Walsh, Mark & Sivitz, 1997; Machleidt *et al.*, 2013). These experimental studies are in accordance with our findings, such that the HFD animals were presented with increased leptin levels (***Fig 3.16***) and an increase in IP fat mass (***Fig 3.13***) when compared to the Control animals. This could be potentially be another mechanism that elicited high blood pressure. An impairment in the vasodilatory response is as result of the reduction in NO production, a characteristic of ED and ED is strongly associated with hypertension (Hall, do Carmo, da Silva, Juncos, Wang & Hall, 2014; Lobato, Filgueira, Akamine, Tostes, Carvalho & Fortes, 2012).

This therefore, could be another potential mechanism behind the elevated blood pressure as observed in the HFD animals.

Furthermore, Ang II plays a major role in mediating hypertension by stimulating sodium reabsorption (Noblet, Owen, Goodwill, Sassoon & Tune, 2015). Previous studies performed in diet-induced obese animals have shown an attenuated response in increased blood pressure and sodium retention when ACE is inhibited (Boustany, 2005). In addition, inhibition of the RAAS system may serve as potential therapeutic strategy for hypertension, dyslipidaemia and impaired glucose homeostasis (Putnam, Shoemaker, Yiannikouris & Cassis, 2012). However, due to limiting factors, the expression of Ang II was not investigated in this study, as this could have been another way of elucidating the mechanism behind the raised blood pressure, including the inhibitory effects of GRT extract.

The GRT extract significantly decreased the mean systolic (***Fig 3.17***), diastolic (***Fig 3.18***) and arterial pressure (***Fig 3.19***), however, it did not affect the blood pressure of the Control animals as measured in the last 6 weeks of the 16 week diet regime. The HFD presented with pre-hypertensive blood pressure however, as measured over the same time period. Previous experimental studies have only shown the anti-hypertensive effects of unfermented rooibos *in vitro* and *in vivo* (Persson, Josefsson & Andersson, 2006; Persson, Persson, Hägg & Andersson, 2010; Persson, 2012). To date, no experimental studies have been conducted, investigating the blood pressure lowering effects of the Afriplex GRT™ extract, in an obese Wistar rat model. A reduction in leptin levels may be an effective strategy to lower blood pressure, by reducing visceral fat. As shown in ***Fig 3.13*** and ***Fig 3.16***, the GRT extract significantly decreased the IP fat mass and leptin levels, respectively, in the HFD animals treated with GRT extract. This could be one of the mechanisms that potentially contributed to the reduction in blood pressure, as observed in the HFD animals treated with the GRT extract. Additionally, the GRT extract improved the vasodilation of the treated HFD animals, suggesting an increased NO production. Due to time and financial constraints, the effects of the GRT extract in NO production in aortic endothelial cell was not investigated, as this could have made further contribution in elucidating the mechanism behind these findings.

In summary: Obesity has been strongly associated with elevated blood pressure and studies performed in humans have shown a positive correlation between visceral, renal adiposity and hypertension (Chandra, Neeland, Berry, Ayers, Rohatgi, Das, Khera, McGuire, De Lemos & Turer, 2014; Chughtai, Morgan, Rocco, Stacey, Brinkley, Ding, Nicklas, Hamilton & Hundley, 2010). The HFD animals presented with increased blood pressures when compared to the Control animals. This could potentially be as a result of the increased leptin levels, visceral fat, impaired vasodilation and fluid retention in the HFD animals. However, the GRT extract showed ameliorative effects on increased

leptin levels, visceral fat, and improved vasodilation in the treated HFD animals. This implies that the GRT extract may be used a therapeutic agent against increased blood pressure and ED.

4.4 Vascular Function/Reactivity

At the end of the 16 week feeding period, the aortic rings of all the different groups were isolated and immediately used for isometric tension studies. The aortic rings of the HFD animals showed a significantly lower contractile response to the administration of Phe when compared to the Control animals (***Fig 3.20)***. The GRT extract decreased contraction in the treated HFD animals and further increased the relaxation of the aortic rings isolated from the treated HFD animals in response to the administration of ACh relative to the untreated HFD group (***Fig 3.21***). Additionally, the Captopril significantly increased the relaxation of the aortic rings isolated from the treated HFD group in response to the administration of ACh relative to the untreated HFD group (***Fig 3.21***).

Impaired vasodilation is a result of a reduction in NO production, this consequently leads to ED, a risk factor for hypertension. Obesity has been shown as the major contributing factor to the reduction in NO production (Bernatova, 2014) and increase in body weight has been shown to be an independent risk factor for the development of ED (Naderali, Pickavance, Wilding & Williams, 2001). This is evident in obese individuals, presented with blunted vasodilatory function (Cardillo, Campia, Iantorno & Panza, 2004; Naderali *et al.*, 2001). Impairment in NO production is a result of eNOS uncoupling, increased activation of nuclear factor kappa beta (NF-κβ), increased expression of endothelium-derived contracting factors (EDCF), such as Ang II and ET-1. eNOS uncoupling occurs when eNOS produces superoxide instead of NO. This is a result of decreased antioxidant enzymes, especially SOD enzyme (Lobato, Filgueira, Akamine, Tostes, Carvalho & Fortes, 2012), also found in the present study.

In a lean state, PVAT produces active molecules that regulates vascular tone, by releasing endothelium derived relaxing factors (EDRF), such as NO and adiponectin (Aghamohammadzadeh, Unwin, Greenstein & Heagerty, 2016), however experimental studies performed in obese rodents and humans showed that the vasodilatory effects of PVAT are attenuated as a result of dysfunction in visceral adipose tissue function (Bussey, Withers, Aldous, Edwards & Heagerty, 2016; Gao, Zeng, Teoh, Sharma, Abouzahr, Cybulsky, Lamy, Semelhago & Lee, 2005; Lu, Su, Lee & Gao, 2010; Virdis, Duranti, Rossi, Dell'Agnello, Santini, Anselmino, Chiarugi, Taddei & Solini, 2015; Xia, Weisenburger, Koch, Burkart, Reifenberg, Förstermann & Li, 2017).

Dysfunction in the visceral adiposity and PVAT are involved in the imbalance between NO production and EDCF by stimulating chronic inflammation. Furthermore, metabolic disorders stimulated by adipose dysfunction are strongly associated with ED, such as insulin resistance (Lobato,

Filgueira, Akamine, Tostes, Carvalho & Fortes, 2012). Insulin regulates vascular homeostasis by stimulating NO production via the PI3K pathway resulting thus promoting an increase in blood flow and glucose uptake by the skeletal muscle and also regulates the production of ET-1. In an insulin resistant state, NO production via the PI3K pathway is impaired and ET-1 production is enhanced, resulting in ED (Pessin & Saltiel, 2000).

In accordance to the above mechanism, the potential mechanisms behind the impaired vasodilation observed in the HFD animals in our study, could be as a result of the loss of the PVAT vasodilatory effects due to a reduction in the release of the EDRF such as NO. Although the production of NO was not measured in the present study, measuring its production would have contributed in further elucidating the mechanism behind the impaired vasodilation. Additionally, other mechanisms may be as a result of increased IP fat mass, an indication of visceral adipose dysfunction, insulin resistance, hyperleptinemia and oxidative stress. Under normal physiological conditions, leptin induces NO production via AMPK and PKB pathway, which in turn phosphorylates eNOS. However, in obesity, the leptin-NO mediated vasodilatory function is impaired as a result of chronic hyperlipidaemia, which leads to the activation of different mechanisms (Bełtowski, 2012). The HFD animals in this study have been presented with decrease in insulin sensitivity, increased leptin levels and a decrease in the antioxidant enzymes (discussed in section 4.6).

The aspalathin-rich rooibos has been shown to possess anti-hypertensive effects by inhibiting ACE and enhancing NO production (Persson, Josefsson & Andersson, 2006; Persson, Persson, Hägg & Andersson, 2010). This is attributed to its polyphenolic content, especially aspalathin, the major active flavonoid compound. According to the previous studies on the effects of rooibos polyphenols in improving ED, mechanistic ways by which GRT extract induced vasorelaxation could be via NO production and through improving in insulin sensitivity, as insulin plays a role in NO production via PI3K pathway. Additionally, by upregulating the expression of the antioxidant enzyme, particularly SOD to scavenge $O_2^{\bullet-}$ and by improving the function of vasodilatory function of the PVAT. The Captopril, an ACE inhibitor, yielded the expected results, as it is an anti-hypertensive drug that inhibits the conversion of Ang I to Ang II (Rizos, 2014).

In summary: The HFD animals were presented with a low contractile response when compared to the Control animals. However, there were no observed vasodilatory effects between the HFD animals vs Control animals. The GRT extract improved vasorelaxation in the treated HFD animals relative to their respective Controls and reduced vasocontraction in the treated Control animals when compared to the untreated Controls group. A variety of disorders induced or stimulated by obesity are the resultant cause of the impaired endothelial function in the HFD animals. Therefore, the GRT extract

with a high aspalathin content can be used as a therapeutic agent in reversing the CVD risk factors, such as ED and hypertension.

4.5 Western Blot Analysis

The HFD group were presented with significantly lower T-AMPK expression (***Fig 3.25***) and P-AMPK (***Fig 3.26***) levels when compared to the Control group. The GRT extract significantly increased the P:T AMPK ratio (***Fig 3.27***) in the treated HFD group when compared to the untreated HFD group. Furthermore, Captopril significantly increased P-AMPK levels in the treated HFD group when compared to the untreated HFD group (***Fig 3.26***). The HFD group showed significantly lower T-PKB expression (***Fig 3.28***) and P-PKB levels (***Fig 3.29***) when compared to the Control group. The GRT extract had no significant effect on the T-PKB expression and P-PKB levels in the HFD and Control animals. However, the Captopril significantly increased the P-PKB levels (***Fig 3.29***) in the treated HFD group, relative to the untreated HFD group. No significant differences were observed in the P:T PKB ratio (***Fig 3.30***). The HFD group showed a significantly increased P-eNOS levels (***Fig 3.32***) when compared to the Control group. The GRT extract significantly increased T-eNOS in the treated HFD animals when compared to the untreated HFD animals (***Fig 3.31***). Additionally, the Captopril significantly increased P-eNOS in the treated HFD group, relative to the untreated HFD group. The P:T eNOS ratio (***Fig 3.33***) in the HFD group was significantly increased when compared to the Control group and was further significantly increased by Captopril in the treated HFD animals, when compared to the untreated HFD group.

AMPK is an insulin-independent signalling protein that is activated in stress conditions, such as low glucose and ischemic conditions. When activated it stimulates glucose uptake, fatty acid oxidation and switches off fatty acid synthesis, triglycerides and glucose through the gluconeogenesis (Hardie, 2004, 2008). Furthermore, it also stimulates the production of NO via eNOS phosphorylation (Fleming, Schulz, Fichtischerer, Kemp, Fisslthaler & Busse, 2003). AMPK is inhibited by elevated glucose levels. It has been observed that AMPK activity in obesity is altered, subsequently resulting in increased glucose levels, fatty acid synthesis, triglycerides and impaired NO production.

The HFD animals in this study were presented with impaired vasodilatory function (discussed in section 4.4). This may be as a result of the significantly low AMPK and PKB activity observed in the western blot analysis of the aortic rings isolated form HFD animals, relative to the Control animals. PKB is an insulin dependent pathway. When activated by insulin, it stimulates the production of NO via eNOS phosphorylation (Fleming *et al.*, 2003). The HFD animals in the present study were presented with an increase in glucose levels as a result of a decrease in insulin sensitivity. This finding

potentially explains the low PKB activation, decreased NO and impaired vasodilation observed in the HFD animals in this study.

Interestingly, eNOS expression, which includes total and phosphorylated eNOS levels in the HFD animals was increased. As a result of the impaired vasodilation observed in the HFD animals, one would expect a downregulation in the eNOS expression in the HFD animals to further elucidate the reason behind the impaired vasodilatory function. However, this may be as a result of eNOS uncoupling. In this study, the HFD animals were predisposed to oxidative stress as seen in the liver potentially explaining the pathophysiological status in the whole organism, hence the conclusion that the HFD animals were predisposed to oxidative stress. The increase in the eNOS expression, signifying an increase in NO production, when it is coupled with an increase in $O_2^{\bullet-}$ free radical this leads to the production of a highly reactive free radical, peroxynitrite. This is a result of the increase in NO production that binds with $O_2^{\bullet-}$ free radical, due to increase ROS generation (Yang, Huang, Kaley & Sun, 2009).

The GRT extract significantly increased the phosphorylation of AMPK according to the upregulation of the P:T AMPK ratio and T-eNOS. This implies that the GRT extract might have improved the production of NO in the treated HFD group via the AMPK pathway. Treatment with rooibos and aspalathin has been shown to activate AMPK in *in vivo* studies (Johnson, Shabalala, Louw, Kappo & Muller, 2017; Sanderson, Mazibuko, Joubert, De Beer, Johnson, Pheiffer, Louw & Muller, 2014). However, further investigation needs to be done on the effects of GRT extract on the phosphorylation of AMPK, PKB and eNOS, as the effects were not observed in this study. This will further elucidate the mechanisms of the GRT extract behind some of the findings observed in this study, such as the improvement of insulin sensitivity, vasodilation and reduced blood pressure observed in the treated HFD animals.

The Captopril significantly increased P-AMPK, P:T AMPK, P-PKB and P-eNOS in the treated HFD animals, when compared to the untreated HFD animals. These findings are in accordance with the blood pressure and vascular reactivity results (discussed in section 4.3 and 4.4, respectively). Captopril is a known anti-hypertensive drug that exhibits vasodilatory effects (Huisamen, George, Dietrich & Genade, 2013; Rizos, 2014). According to these findings, it upregulated the production of NO by activating the signalling pathways responsible for eNOS phosphorylation.

In summary: The HFD animals were presented with a significant decrease in the T-AMPK, P-AMPK, T-PKB and P-PKB when compared to the Control animals. In addition, the HFD animals had increased P-eNOS relative to the Control animals. The GRT extract increased the P:T AMPK and T-eNOS in the HFD treated animals when compared to the untreated HFD.

4.6 Antioxidant Status

The activity of the endogenous antioxidant enzymes was measured in the liver. CAT, GPx and SOD activity was analysed, including determination of lipid peroxidation. Due to time constraints, the activity of the above mentioned enzymes in the kidney, pancreas and aortic tissue was not assessed as proposed, to further elucidate the mechanisms behind some of the findings observed in this study.

In the liver, the HFD group showed a significantly low SOD, CAT and GPx activity, respectively when compared to the Control group (***Fig 3.34, Fig3.35*** *and* ***Fig 3.36***). The GRT extract in the HFD treated group, significantly increased SOD and CAT activity when compared to the untreated HFD group. Furthermore, the GRT extract did not show a significant effect in the GPx activity in the HFD treated group when compared to the untreated HFD group. We speculate that this may be due to the large standard error in the HFD treated group which could possibly be attributed to some differences observed in these lysates for the assay. The GRT extract also significantly increased the GPx activity in the Control treated group when compared to the untreated Control group. According to a two-way ANOVA, the diet and the GRT extract showed an overall significant effect in SOD, CAT and GPX activity in both diet groups. The HFD group showed a significant increase in the MDA levels when compared to the Control group (***Fig 3.37***), indicating increased lipid peroxidation which is an indication of oxidative stress. Furthermore, the GRT extract significantly decreased the MDA levels in both the Control and the HFD treated group when compared to their counterparts (***Fig 3.37***). According to a two-way ANOVA, the diet and the GRT extract had an overall significant effect in the MDA levels in both groups. According to the above findings, these animals were predisposed to oxidative stress as a result of the reduction in these innate antioxidant enzymes (CAT, GPx and SOD). This is further confirmed by the increased levels of MDA, signifying the presence of lipid peroxidation in the liver of these animals. A number of studies have shown a positive correlation between prevalence of obesity and a reduction in the innate antioxidant enzymes, subsequently resulting in oxidative stress (Tran, Oliver, Rosa & Galassetti, 2012). SOD enzyme catalyses the conversion of O_2•- into a less reactive product, H_2O_2 which is further decomposed into H_2O and O_2 by the CAT enzyme, and by GPx in a glutathione coupled reaction. It has been observed that in obese people, the innate antioxidant enzyme defence system is altered (Gutierrez-Lopez, Garcia-Sanchez, Rincon-Viquez, Lara-Padilla, Sierra-Vargas & Olivares-Corichi, 2012; Nikolaidis, Kyparos, Spanou, Paschalis, Theodorou & Vrabas, 2012). CAT, SOD, GPx activity in both obese adults and children has been found to be downregulated, coupled with increased MDA levels (Mittal & Kant, 2009; Viroonudomphol, Pongpaew, Tungtrongchitr, Phonrat, Supawan, Vudhivai & Schelp, 2000). Therefore, there exists a positive correlation between increasing BMI and oxidative stress.

The liver is a very dynamic organ responsible for various physiological and biochemical functions to ensure metabolic homeostasis. Additionally, it is also highly reactive against xenobiotics and therefore also susceptible to toxic effects. As a result, when the biochemical functions are disrupted, liver damage may result. Obesity has been rendered the major contributor to liver disease, such as NAFLD, primarily as a result of the adipocytokines secreted by the enlarged adipose tissue, triggering subsequent pathophysiological conditions, such as hyperglycaemia, hyperlipidaemia, diabetes and hypertension (Polimeni, Del Ben, Baratta, Perri, Albanese, Pastori, Violi & Angelico, 2015; Reccia, Kumar, Akladios, Virdis, Pai, Habib & Spalding, 2017).

NAFLD is characterised by mitochondrial dysfunction as a result of ROS overproduction by the adipocytes. ROS production is induced by hyperglycaemia and overnutrition which overwhelms the mitochondria resulting in insulin resistance. Oxidative stress in the liver results in lipid peroxidation, inflammation and consequently the pathogenesis of NAFLD (Koroglu, Canbakan, Atay, Hatemi, Tuncer, Dobrucali, Sonsuz, Gultepe & Senturk, 2016). A study done in patients with and without insulin resistance, showed patients with insulin resistance had increased MDA levels and presented with a reduction in SOD activity (Koroglu *et al.*, 2016). Increased leptin levels also contributes to the development of oxidative stress by increasing peroxisomal fatty acid and mitochondrial oxidation (Bełtowski, 2012; Ceci, Sabatini, Duranti, Savini, Avigliano & Rossi, 2007). The HFD-fed animals in this study presented with increased leptin levels.

Numerous studies have shown that dietary antioxidant supplementation can improve liver function and oxidative balance (Murer, Aeberli, Braegger, Gittermann, Hersberger, Leonard, Taylor, Traber & Zimmermann, 2014). Plant polyphenols, including those from rooibos, have been shown to have ameliorative effects on the antioxidant status (Canda, Oguntibeju & Marnewick, 2014). Unfermented rooibos and aspalthin-enriched rich green rooibos extract, in particular, modulates the MDA levels (Cullere, Hoffman & Zotte, 2013; Villaño, Pecorari, Testa, Raguzzini, Stalmach, Crozier, Tubili & Serafini, 2010). These products improve the redox antioxidant status by enhancing the activity of SOD, GPX and CAT enzymes (Villaño *et al.*, 2010). A study done in a rat model has shown that rooibos may ameliorates oxidative stress by preventing inflammation via its anti-oxidative activity (Baba, Ohtsuka, Haruna, Lee, Nagata, Maeda, Yamashiro & Shimizu, 2009). This is attributed to its polyphenolic components, especially aspalathin and nothofagin.

Other strategies to reduce oxidative stress include physical activity, weight loss and a well-balanced diet, rich in antioxidants (Savini, Catani, Evangelista, Gasperi & Avigliano, 2013). A reduction in weight loss has been shown to reduce colorectal inflammation as a result of the increase in pro-inflammatory markers, such as adiponectin and significantly reducing TNF- α and IL-6 (Savini, Catani, Evangelista, Gasperi & Avigliano, 2013). An increase in GPx activity has also been observed

after weight loss in obese women (Bougoulia, Triantos & Koliakos, 2006). Therefore, a decrease in visceral adipose tissue is another important mechanistic way of combating oxidative stress. It has been shown that total antioxidant capacity has an inverse effect on visceral adiposity and the GRT extract reduced the IP fat mass, which could potentially contribute to the increase expression of the innate antioxidant enzymes (Hermsdorff, Puchau, Volp, Barbosa, Bressan, Zulet & Martínez, 2011; Del Rio, Agnoli, Pellegrini, Krogh, Brighenti, Mazzeo, Masala, Bendinelli, Berrino, Sieri, Tumino, Rollo, Gallo, Sacerdote, Mattiello, Chiodini & Panico, 2011).

In summary: Obese individuals are presented with an alteration in the antioxidant defence system, thus predisposing them to oxidative stress and chronic inflammation. The HFD animals presented with a reduction in the activity of the innate primary antioxidant enzymes, such as SOD, CAT and GPx when compared to the Control animals. Moreover, these animals had increased MDA levels relative to their counterparts, which indicates oxidative stress. However, the GRT extract increased the activity of the SOD, CAT and GPx activity and decreased lipid peroxidation in the HFD treated animals when compared to the untreated HFD animals.

4.7 Summary of the Main Findings

Obesity, especially visceral obesity is strongly associated with the pathogenesis of CVD risk factors, such as, impaired glucose homeostasis, dyslipidaemia, hypertension, oxidative stress and ED. The HFD used in this study, successfully induced obesity in the Wistar rat model, as to the proposed objectives. This is supported by an increase in leptin, in body weight, IP fat mass and liver mass. Furthermore, the HFD impaired glucose metabolism, induced hypertension, ED and oxidative stress, which was validated by an increase in lipid peroxidation and the downregulation of CAT, GPx and SOD activity in the liver. The HFD also downregulated the expression of AMPK and PKB. This could potentially be the result of the observed decrease in glucose metabolism, impaired vascular function, and increased blood pressure. However, the observed phosphorylation of eNOS, impaired ED and increased blood pressure may also be associated with oxidative stress.

Our aim was to investigate the ameliorative effects of the GRT extract, on hypertension, vascular dysfunction, and oxidative stress in diet-induced obese Wistar rats. Treatment with the GRT extract decreased leptin levels, resulted in less weight gain, decreased IP fat mass, liver mass and increased glucose metabolism, observed in the treated HFD animals. It also improved vascular function, reduced blood pressure and reversed oxidative stress by upregulating the activity of the innate antioxidant enzymes, CAT, GPx and SOD, including lipid peroxidation. A decrease in leptin levels has been associated with a decrease in blood pressure and improved vascular function. This may be part of the mechanism by which GRT exerted these effects in this study, and includes the upregulation

of AMPK expression, and a decrease in visceral adiposity. However, the exact mechanism needs to be further explored.

Chapter 5. Conclusion

5.1 Final Conclusion

Obesity is strongly associated with impaired glucose homeostasis, increased blood pressure, ED, dyslipidaemia and oxidative stress, synergistically increasing cardiovascular risk. Considering the study research question: “Does ingestion of GRT extract alleviate hypertension, vascular dysfunction and oxidative stress in diet-induced obese Wistar rats?” the present study has successfully addressed the research question and met the proposed aim. The mechanisms behind the effects of GRT extract were elucidated, however, further investigations need to be done. Therefore, GRT extract may be a potential therapeutic agent against obesity-related vascular dysfunction, impaired glucose homeostasis, elevated blood pressure, oxidative stress, leptin resistance and weight gain.

5.2 Study Limitations

- Major limitations were financial and time constraints as we could not measure some of the parameters mentioned under future directions that would have further elucidated the mechanisms behind our findings.

5.3 Future Directions

- Evaluation of the serum and liver lipid profile, LDL, High density lipoprotein (HDL), very low-density lipoprotein (VLDL), total cholesterol, triglycerides.
- Measurement of pro-inflammatory cytokine (IL-6, TNF-α) and anti-inflammatory cytokines (adiponectin release) in the serum.
- Measurement of homeostatic model assessment (HOMA) index to determine insulin levels in the fasted and non-fasted serum, using an insulin ELISA assay kit.
- Measurement of ET-1 and aldosterone expression in the serum to elucidate the effect of GRT extract on decreased blood pressure.
- Investigate the effects of GRT extract on NO production in cultured endothelial cells, including Ang II, to further elucidate the vasodilatory effects observed in the treated HFD animals.
- Determination of the ACE inhibitory effects of the GRT extract.
- Determination of the primary antioxidant enzymes and the assessment of oxidative stress in in the pancreas, kidney and aorta.

- Determine the effect of GRT extract on pancreatic lipases and its anti-obesity mechanism.
- Determine the effect of GRT extract on adipose tissue to elucidate the mechanism behind decreased IP fat weight.
- Determination of the mechanism behind decreased liver weight by performing liver histopathology.

Appendix A: HPLC Analysis of GRT extract

***Table A.1**: HPLC analysis of the GRT extract used in the study (Beelders, 2012).*

[compound] (g compound/ 100 g Soluble Solids)	
Phenylpyruvic acid-2-Oglucoside (PPAG)	0.423265
Aspalathin	12.78348
Nothofagin	1.974419
Isoorientin	1.427281
Orientin	1.255839
Ferulic acid	nq
Vitexin	0.338513
Isovitexin	0.298022
Quercetin-3- robinobioside	1.040565
Hyperoside	0.398773
Rutin	0.496034
Isoquercitin	0.572251852

Abbreviations: nq (not quantifiable)

Appendix B: Preparation of the strawberry jelly/gelatine blocks for the animals

A. **Jelly/gelatine block protocol (Normal Batch-25ml)**
   - 4 grams red jelly
   - 4 grams gelatine
   - In 25 ml of **BOILED** water

B. **GRT extract dose concentration was 60 mg/kg/day, and 50 mg/kg/day for Captopril, administered according to body weight.(measured once a week)**
   - When adding the drug dosage to the jelly/gelatine mixture the following was considered;
   - Determine the average body weight of the rat.
   - For example: If the rat weighed **300g,** this was multiplied with the extract dosage (e.g. **60 mg/kg/day)** and divided by **1000** (to cancel out the kg) then multiplied by the total volume required for the week in **ml**.

C. **Calculated example:**

$$\frac{300\ g\ X\ 60\ mg\ /kg}{1000} X\ 25\ ml$$

The end unit value will be mg per ml.

Chapter 6. Bibliography (Stellenbosch Harvard Referencing style)

Abcam. 2013. *Instructions for Use For the quantitative measurement of rat Leptin in serum, plasma and cell culture supernatants. ab100773 – Leptin Rat ELISA Kit*. [Online], Available: http://www.abcam.com/ps/products/100/ab100773/documents/ab100773-Leptin Rat ELISA Kit v4 (website).pdf [2017, November 06].

Adams, L.A., Lymp, J.F., St. Sauver, J., Sanderson, S.O., Lindor, K.D., Feldstein, A. & Angulo, P. 2005. The natural history of nonalcoholic fatty liver disease: A population-based cohort study. *Gastroenterology*. 129(1):113–121.

Aghamohammadzadeh, R., Greenstein, A.S., Yadav, R., Jeziorska, M., Hama, S., Soltani, F., Pemberton, P.W., Ammori, B., et al. 2013. Effects of bariatric surgery on human small artery function: Evidence for reduction in perivascular adipocyte inflammation, and the restoration of normal anticontractile activity despite persistent obesity. *Journal of the American College of Cardiology*. 62(2):128–135.

Aghamohammadzadeh, R., Unwin, R.D., Greenstein, A.S. & Heagerty, A.M. 2016. Effects of Obesity on Perivascular Adipose Tissue Vasorelaxant Function: Nitric Oxide, Inflammation and Elevated Systemic Blood Pressure. *Journal of Vascular Research*. 52(5):299–305.

Ahn, J., Lee, H., Kim, S., Park, J. & Ha, T. 2008. The anti-obesity effect of quercetin is mediated by the AMPK and MAPK signaling pathways. *Biochemical and Biophysical Research Communications*. 373(4):545–549.

Ajuwon, O., Marnewick, J.L. & Davids, L.M. 2015. Rooibos (*Aspalathus linearis*) and its Major Flavonoids — Potential Against Oxidative Stress-Induced Conditions. In S.J.T. Gowder (ed.). InTech *Basic Principles and Clinical Significance of Oxidative Stress*. 172–195.

Ajuwon, O.R., Katengua-Thamahane, E., Van Rooyen, J., Oguntibeju, O.O. & Marnewick, J.L. 2013. Protective effects of rooibos (*Aspalathus linearis*) and/or red palm oil (elaeis guineensis) supplementation on tert -butyl hydroperoxide-induced oxidative hepatotoxicity in wistar rats. *Evidence-based Complementary and Alternative Medicine*. 2013:1–12.

Ajuwon, O.R., Oguntibeju, O.O. & Marnewick, J.L. 2014. Amelioration of lipopolysaccharide-induced liver injury by aqueous rooibos (*Aspalathus linearis*) extract via inhibition of pro-inflammatory cytokines and oxidative stress. *BMC complementary and alternative medicine*. 14(1):392.

Al-Mawali, A. 2015. Non-communicable diseases: Shining a light on cardiovascular disease, Oman???s biggest killer. *Oman Medical Journal*. 30(4):227–228.

Asferg, C.L., Nielsen, S.J., Andersen, U.B., Linneberg, A., Møller, D. V., Hedley, P.L., Christiansen, M.,

Goetze, J.P., et al. 2013. Relative atrial natriuretic peptide deficiency and inadequate renin and angiotensin II suppression in obese hypertensive men. *Hypertension*. 62(1):147–153.

Awoniyi, D.O., Aboua, Y.G., Marnewick, J. & Brooks, N. 2012. The effects of rooibos (*Aspalathus linearis*), green te (Camelli sinensis) and commercial rooibos and green te supplements on epididymal sperm in oxidative stress-induced rats. *Phytotherapy Research*. 26(8):1231–1239.

Baba, H., Ohtsuka, Y., Haruna, H., Lee, T., Nagata, S., Maeda, M., Yamashiro, Y. & Shimizu, T. 2009. Studies of anti-inflammatory effects of Rooibos tea in rats. *Pediatrics International*. 51(5):700–704.

Bae, S.W., Kim, H.S., Cha, Y.N., Park, Y.S., Jo, S.A. & Jo, I. 2003. Rapid increase in endothelial nitric oxide production by bradykinin is mediated by protein kinase A signaling pathway. *Biochemical and Biophysical Research Communications*. 306(4):981–987.

Bakker, W., Eringa, E.C., Sipkema, P. & van Hinsbergh, V.W.M. 2009. Endothelial dysfunction and diabetes: roles of hyperglycemia, impaired insulin signaling and obesity. *Cell and tissue research*. 335(1):165–189.

Baleta, A. & Mitchell, F. 2014. Country in Focus: Diabetes and obesity in South Africa. *The lancet.Diabetes & endocrinology*. 2(9):687–688.

Del Bas, J.M., Crescenti, A., Arola-Arnal, A., Oms-Oliu, G., Arola, L. & Caimari, A. 2015. Grape seed procyanidin supplementation to rats fed a high-fat diet during pregnancy and lactation increases the body fat content and modulates the inflammatory response and the adipose tissue metabolism of the male offspring in youth. *International Journal of Obesity*. 39(1):7–15.

Beelders, T. 2012. kinetic optimisation of the reversed phase liquid... - Google Scholar. *Journal of Chromatography A*. [Online], Available: https://scholar.google.co.za/scholar?q=kinetic+optimisation+of+the+reversed+phase+liquid+chromatographic+separation+of+rooibos+tea&hl=en&as_sdt=0&as_vis=1&oi=scholart&sa=X&ved=0ahUKEwj5peSF0YzXAhUFxxQKHeAxBPkQgQMIJzAA [2017, October 25].

Bełtowski, J. 2012. Leptin and the regulation of endothelial function in physiological and pathological conditions. *Clinical and Experimental Pharmacology and Physiology*. 39(2):168–178.

Beltrán-Debón, R., Rull, A., Rodríguez-Sanabria, F., Iswaldi, I., Herranz-López, M., Aragonès, G., Camps, J., Alonso-Villaverde, C., et al. 2011. Continuous administration of polyphenols from aqueous rooibos (*Aspalathus linearis*) extract ameliorates dietary-induced metabolic disturbances in hyperlipidemic mice. *Phytomedicine*. 18(5):414–424.

Bernatova, I. 2014. Endothelial Dysfunction in Experimental Models of Arterial Hypertension: Cause or Consequence? *BioMed Research International*. 2014:1–14.

Böhm, F. & Pernow, J. 2007. The importance of endothelin-1 for vascular dysfunction in cardiovascular disease. *Cardiovascular Research*. 76(1):8–18.

Boo, Y.C. & Jo, H. 2003. Flow-dependent regulation of endothelial nitric oxide synthase: role of protein kinases. *American journal of physiology. Cell physiology*. 285(3):499–508.

Boo, Y.C., Sorescu, G., Boyd, N., Shiojima, I., Walsh, K., Du, J. & Jo, H. 2002. Shear stress stimulates phosphorylation of endothelial nitric-oxide synthase at Ser1179 by Akt-independent mechanisms: role of protein kinase A. *The Journal of biological chemistry*. 277(5):3388–96.

Bougoulia, M., Triantos, A. & Koliakos, G. 2006. Plasma interleukin-6 levels, glutathione peroxidase and isoprostane in obese women before and after weight loss. Association with cardiovascular risk factors 1605. *Hormones.(Athens.)*. 5(1109–3099):192–199.

Boustany, C.M. 2005. AT1-receptor antagonism reverses the blood pressure elevation associated with diet-induced obesity. *AJP: Regulatory, Integrative and Comparative Physiology*. 289(1):R181–R186.

Bradford, M.M. 1976. A rapid and sensitive method for the quantitation of microgram quantities of protein utilizing the principle of protein-dye binding. *Analytical Biochemistry*. 72(1–2):248–254.

Bramati, L., Minoggio, M., Gardana, C., Simonetti, P., Mauri, P. & Pietta, P. 2002. Quantitative characterization of flavonoid compounds in Rooibos tea (*Aspalathus linearis*) by LC-UV/DAD. *Journal of Agricultural and Food Chemistry*. 50(20):5513–5519.

Brigelius-Flohe, R. & Traber, M.G. 1999. Vitamin E: function and metabolism. *FASEB journal : official publication of the Federation of American Societies for Experimental Biology*. 13(10):1145–1155.

Bussey, C.E., Withers, S.B., Aldous, R.G., Edwards, G. & Heagerty, A.M. 2016. Obesity-Related Perivascular Adipose Tissue Damage Is Reversed by Sustained Weight Loss in the Rat. *Arteriosclerosis, Thrombosis, and Vascular Biology*. 36(7):1377–1385.

Caballero, A.E. 2003. Endothelial dysfunction in obesity and insulin resistance: a road to diabetes and heart disease. *Obesity research*. 11(11):1278–1289.

Canda, B.D., Oguntibeju, O.O. & Marnewick, J.L. 2014. Effects of consumption of rooibos (*Aspalathus linearis*) and a rooibos-derived commercial supplement on hepatic tissue injury by tert -butyl hydroperoxide in wistar rats. *Oxidative Medicine and Cellular Longevity*. 2014.

Cardillo, C., Campia, U., Iantorno, M. & Panza, J.A. 2004. Enhanced Vascular Activity of Endogenous Endothelin-1 in Obese Hypertensive Patients. *Hypertension*. 43(1):36–40.

Caro, J.F., Kolaczynski, J.W., Nyce, M.R., Ohannesian, J.P., Opentanova, I., Goldman, W.H., Lynn, R.B., Zhang, P.L., et al. 1996. Decreased cerebrospinal-fluid/serum leptin ratio in obesity: A possible mechanism for leptin resistance. *Lancet*. 348(9021):159–161.

Caymen, C. 2016. Glutathione Peroxidase Assay Kit. (703102):1–13.

Caymen, C. 2014. TBARS Assay Kit. 38 (1993):9–10.

Ceci, R., Sabatini, S., Duranti, G., Savini, I., Avigliano, L. & Rossi, A. 2007. Acute, but not chronic, leptin

treatment induces acyl-CoA oxidase in C2C12 myotubes. *European Journal of Nutrition*. 46(6):364–368.

Chandra, A., Neeland, I.J., Berry, J.D., Ayers, C.R., Rohatgi, A., Das, S.R., Khera, A., McGuire, D.K., et al. 2014. The relationship of body mass and fat distribution with incident hypertension: Observations from the dallas heart study. *Journal of the American College of Cardiology*. 64(10):997–1002.

Chen, W., Sudji, I.R., Wang, E., Joubert, E., Van Wyk, B.E. & Wink, M. 2013. Ameliorative effect of aspalathin from rooibos (*Aspalathus linearis*) on acute oxidative stress in Caenorhabditis elegans. *Phytomedicine*.

Choi, I., Park, Y., Choi, H. & Lee, E.H. 2006. Anti-adipogenic activity of rutin in 3T3-L1 cells and mice fed with high-fat diet. *BioFactors (Oxford, England)*. 26(4):273–281.

Choudhary, N., Duseja, A., Kalra, N., Das, A., Dhiman, R. & Chawla, Y. 2012. Correlation of adipose tissue with liver histology in Asian Indian patients with nonalcoholic fatty liver disease (NAFLD). *Annals of Hepatology*. 11(4):478–486.

Chughtai, H.L., Morgan, T.M., Rocco, M., Stacey, B., Brinkley, T.E., Ding, J., Nicklas, B., Hamilton, C., et al. 2010. Renal sinus fat and poor blood pressure control in middle-aged and elderly individuals at risk for cardiovascular events. *Hypertension*. 56(5):901–906.

Considine, R. V, Sinha, M.K., Heiman, M.L., Kriauciunas, A., Stephens, T.W., Nyce, M.R., Ohannesian, J.P., Marco, C.C., et al. 1996. Serum immunoreactive-leptin concentrations in normal-weight and obese humans. *The New England journal of medicine*. 334(5):292–5.

Cullere, M., Hoffman, L.C. & Zotte, A.D. 2013. First evaluation of unfermented and fermented rooibos (*Aspalathus linearis*) in preventing lipid oxidation in meat products. *Meat Science*. 95(1):72–77.

D'Alessandro, M.E., Selenscig, D., Illesca, P., Chicco, A. & Lombardo, Y.B. 2015. Time course of adipose tissue dysfunction associated with antioxidant defense, inflammatory cytokines and oxidative stress in dyslipemic insulin resistant rats. *Food Funct.* 6(4):1299–1309.

Dalle-Donne, I., Rossi, R., Colombo, R., Giustarini, D. & Milzani, A. 2006. Biomarkers of oxidative damage in human disease. *Clinical chemistry*. 52(4):601–23.

Després, J.-P. & Lemieux, I. 2006. Abdominal obesity and metabolic syndrome. *American Journal of Clinical Nutrition*. 79(5):727–747.

Dhawan, V. 2014. Reactive Oxygen and Nitrogen Species: General Considerations. In N.K. Ganguly, S.K. Jindal, S. Biswal, P.J. Barnes, & R. Pawankar (eds.). (Oxidative Stress in Applied Basic Research and Clinical Practice). New York, NY: Springer New York *Studies on Respiratory Disorders*. 27–47.

Dröge, W., Granner, D.K. & Boveris, A. 2002. Free radicals in the physiological control of cell function. *Physiological reviews*. 82(1):47–95.

Ellerby, L.M. & Bredesen, D.E. 2000. Measurement of Cellular Oxidation, Reactive Oxygen Species, and

Antioxidant Enzymes during Apoptosis. *Methods in Enzymology*. 322:413–421.

Engeli, S. 2005. Is there a pathophysiological role for perivascular adipocytes? *American Journal of Physiology - Heart and Circulatory Physiology*. 289(5):H1794-5.

Engeli, S., Schling, P., Gorzelniak, K., Boschmann, M., Janke, J., Ailhaud, G., Teboul, M., Massiéra, F., et al. 2003. The adipose-tissue renin–angiotensin–aldosterone system: role in the metabolic syndrome? *The International Journal of Biochemistry & Cell Biology*. 35(6):807–825.

Eringa, E.C., Bakker, W. & van Hinsbergh, V.W.M. 2012. Paracrine regulation of vascular tone, inflammation and insulin sensitivity by perivascular adipose tissue. *Vascular Pharmacology*. 56(5–6):204–209.

Esterbauer, H. & Cheeseman, K.H. 1990. Determination of aldehydic lipid peroxidation products: Malonaldehyde and 4-hydroxynonenal. *Methods in Enzymology*. 186:407–421.

Fabbrini, E., Sullivan, S. & Klein, S. 2010. Obesity and nonalcoholic fatty liver disease: Biochemical, metabolic, and clinical implications. *Hepatology*. 51(2):679–689.

Fanglian, H. 2011. *Laemmli SDS PAGE*. [Online], Available: http://www.bio-protocol.org/e80 [2017, November 06].

Farrell, G.C. & Larter, C.Z. 2006. Nonalcoholic fatty liver disease: From steatosis to cirrhosis. *Hepatology*. 43(2 SUPPL. 1):18–24.

Fleming, I., Schulz, C., Fichtischerer, B., Kemp, B.E., Fisslthaler & Busse, R. 2003. AMP-activated protein kinase (AMPK) regulates the insulin-induced activation of the nitric oxide sythase in human platelets. *Thromb Haemost*. 90(5):863–871.

Franzini, L., Ardigò, D., Valtueña, S., Pellegrini, N., Del Rio, D., Bianchi, M.A., Scazzina, F., Piatti, P.M., et al. 2012. Food selection based on high total antioxidant capacity improves endothelial function in a low cardiovascular risk population. *Nutrition, Metabolism and Cardiovascular Diseases*. 22(1):50–57.

Gao, Y.J., Zeng, Z.H., Teoh, K., Sharma, A.M., Abouzahr, L., Cybulsky, I., Lamy, A., Semelhago, L., et al. 2005. Perivascular adipose tissue modulates vascular function in the human internal thoracic artery. *J Thorac Cardiovasc Surg*. 130(4):1130–1136.

Gelderblom, W.C.A., Joubert, E., Gamieldien, K., Sissing, L., Malherbe, C.J. & Maritz, G. 2017. Rooibos *(Aspalathus linearis*), honeybush (Cyclopia intermedia) and cancer bush (Sutherlandia frutescens subsp. microphylla) protect against tobacco-specific mutagenesis *in vitro*. *South African Journal of Botany*. 110:194–200.

Gillespie, E.L., White, C.M., Kardas, M., Lindberg, M. & Coleman, C.I. 2005. The impact of ACE inhibitors or angiotensin II type 1 receptor blockers on the development of new-onset type 2 diabetes. *Diabetes care*. 28(9):2261–2266.

Grundy, S.M. 2004. Obesity, Metabolic Syndrome, and Cardiovascular Disease. *The Journal of Clinical Endocrinology & Metabolism*. 89(6):2595–2600.

Gutierrez-Lopez, L., Garcia-Sanchez, J.R., Rincon-Viquez, M. de J., Lara-Padilla, E., Sierra-Vargas, M.P. & Olivares-Corichi, I.M. 2012. Hypocaloric diet and regular moderate aerobic exercise is an effective strategy to reduce anthropometric parameters and oxidative stress in obese patients. *Obesity Facts*. 5(1):12–22.

Hall, J.E., Da Silva, A.A., Do Carmo, J.M., Dubinion, J., Hamza, S., Munusamy, S., Smith, G. & Stec, D.E. 2010. Obesity-induced hypertension: Role of sympathetic nervous system, leptin, and melanocortins. *Journal of Biological Chemistry*. 285(23):17271–17276.

Hall, J.E., Do Carmo, J.M., Da Silva, A.A., Wang, Z. & Hall, M.E. 2015. Obesity-Induced Hypertension: Interaction of Neurohumoral and Renal Mechanisms. *Circulation Research*. 116(6):991–1006.

Hall, M.E., do Carmo, J.M., da Silva, A.A., Juncos, L.A., Wang, Z. & Hall, J.E. 2014. Obesity, hypertension, and chronic kidney disease. *International Journal of Nephrology and Renovascular Disease*. 7:75–88.

Hardie, D.G. 2004. AMP-activated protein kinase: a master switch in glucose and lipid metabolism. *Reviews in endocrine & metabolic disorders*. 5(2):119–25.

Hardie, D.G. 2008. AMPK: a key regulator of energy balance in the single cell and the whole organism. *International Journal of Obesity*. 32(S4):S7–S12.

Haynes, W.G., Morgan, D.A., Walsh, S.A., Mark, A.L. & Sivitz, W.I. 1997. Receptor-mediated regional sympathetic nerve activation by leptin. *Journal of Clinical Investigation*. 100(2):270–278.

Hermsdorff, H.H.M., Puchau, B., Volp, A.C.P., Barbosa, K.B., Bressan, J., Zulet, M.Á. & Martínez, J.A. 2011. Dietary total antioxidant capacity is inversely related to central adiposity as well as to metabolic and oxidative stress markers in healthy young adults. *Nutrition & Metabolism*. 8(1):59.

Huisamen, B., George, C., Dietrich, D. & Genade, S. 2013. Cardioprotective and anti-hypertensive effects of Prosopis glandulosa in rat models of pre-diabetes : cardiovascular topics. *Cardiovascular Journal Of Africa*. 24(2):10–16.

Iaccarino, G., Ciccarelli, M., Sorriento, D., Cipolletta, E., Cerullo, V., Iovino, G.L., Paudice, A., Elia, A., et al. 2004. AKT participates in endothelial dysfunction in hypertension. *Circulation*. 109(21):2587–2593.

Jo, J., Gavrilova, O., Pack, S., Jou, W., Mullen, S., Sumner, A.E., Cushman, S.W. & Periwal, V. 2009. Hypertrophy and/or Hyperplasia: Dynamics of Adipose Tissue Growth. *PLoS Comput Biol*. 5(3).

Johnson, R., Shabalala, S., Louw, J., Kappo, A.P. & Muller, C.J.F. 2017. Aspalathin reverts doxorubicin-induced cardiotoxicity through increased autophagy and decreased expression of p53/mTOR/p62 signaling. *Molecules*. 22(10):863–871.

Jomova, K., Jenisova, Z., Feszterova, M., Baros, S., Liska, J., Hudecova, D., Rhodes, C.J. & Valko, M. 2011.

Joubert, E. & de Beer, D. 2012. Phenolic content and antioxidant activity of rooibos food ingredient extracts. *Journal of Food Composition and Analysis*. 27(1):45–51.

Jung, U. & Choi, M.-S. 2014. Obesity and Its Metabolic Complications: The Role of Adipokines and the Relationship between Obesity, Inflammation, Insulin Resistance, Dyslipidemia and Nonalcoholic Fatty Liver Disease. *International Journal of Molecular Sciences*. 15(4):6184–6223.

Kamakura, R., Son, M.J., de Beer, D., Joubert, E., Miura, Y. & Yagasaki, K. 2015. Antidiabetic effect of green rooibos (*Aspalathus linearis*) extract in cultured cells and type 2 diabetic model KK-Ay mice. *Cytotechnology*. 67(4):699–710.

Kant, A.K., Graubard, B.I. & Atchison, E.A. 2009. Intakes of plain water, moisture in foods and beverages, and total water in the adult US population-nutritional, meal pattern, and body weight correlates: National Health and Nutrition Examination Surveys 1999-2006. *American Journal of Clinical Nutrition*. 90(3):655–663.

Katagiri, H., Yamada, T. & Oka, Y. 2007. Adiposity and cardiovascular disorders: Disturbance of the regulatory system consisting of humoral and neuronal signals. *Circulation Research*. 101(1):27–39.

Kawano, A., Nakamura, H., Hata, S. ichi, Minakawa, M., Miura, Y. & Yagasaki, K. 2009. Hypoglycemic effect of aspalathin, a rooibos tea component from *Aspalathus linearis*, in type 2 diabetic model db/db mice. *Phytomedicine*. 16(5):437–443.

Kennedy, J.I.C., Askelund, K.J., Premkumar, R., Phillips, A.R.J., Murphy, R., Windsor, J.A. & Petrov, M.S. 2016. Leptin Is Associated With Persistence of Hyperglycemia in Acute Pancreatitis: A Prospective Clinical Study. *Medicine*. 95(6):e2382.

Kim, W.-J. 2015. Is 5´-AMP-Activated Protein Kinase Both Jekyll and Hyde in Bladder Cancer? *International Neurourology Journal*. 19(2):55–66.

Kim, E.J., Jung, S.-N., Son, K.H., Kim, S.R., Ha, T.Y., Park, M.G., Jo, I.G., Park, J.G., et al. 2007. Antidiabetes and antiobesity effect of cryptotanshinone via activation of AMP-activated protein kinase. *Molecular pharmacology*. 72(1):62–72.

Kim, J., Yang, G., Kim, Y., Kim, J. & Ha, J. 2016. AMPK activators: mechanisms of action and physiological activities. *Experimental & Molecular Medicine*. 48(4):e224.

Kim, S.H., Després, J.-P. & Koh, K.K. 2016. Obesity and cardiovascular disease: friend or foe? *European Heart Journal*. 37(48):3560–3568.

Kobayasi, R., Akamine, E.H., Davel, A.P., Rodrigues, M.A., Carvalho, C.R. & Rossoni, L. V. 2010. Oxidative stress and inflammatory mediators contribute to endothelial dysfunction in high-fat diet-induced obesity in mice. *Journal of Hypertension*. 28(10):2111–2119.

Koroglu, E., Canbakan, B., Atay, K., Hatemi, I., Tuncer, M., Dobrucali, A., Sonsuz, A., Gultepe, I., et al. 2016. Role of oxidative stress and insulin resistance in disease severity of non-alcoholic fatty liver disease. *The Turkish Journal of Gastroenterology*. 27(4):361–366.

Kouidhi, S., Jarboui, S., Clerget Froidevaux, M.-S., Abid, H., Demeneix, B., Zaouche, A., Benammar Elgaaied,

A. & Guissouma, H. 2010. Relationship between subcutaneous adipose tissue expression of leptin and obesity in Tunisian patients. *La Tunisie medicale*. 88(8):569–72.

Ku, S.K., Kwak, S., Kim, Y. & Bae, J.S. 2014. Aspalathin and Nothofagin from Rooibos (*Aspalathus linearis*) Inhibits High Glucose-Induced Inflammation *In Vitro* and *In Vivo*. *Inflammation*. 38(1):445–455.

Kumar, R. & Mohan, S. 2017. Non-alcoholic Fatty Liver Disease in Lean Subjects: Characteristics and Implications. *Journal of clinical and translational hepatology*. 5(3):216–223.

Landmesser, U., Harrison, D.G. & Drexler, H. 2006. Oxidant stress - A major cause of reduced endothelial nitric oxide availability in cardiovascular disease. In Vol. 62 *European Journal of Clinical Pharmacology*. 13–19.

Lenoir, M., Serre, F., Cantin, L. & Ahmed, S.H. 2007. Intense sweetness surpasses cocaine reward. *PLoS ONE*. 2(8).

Li, H. & Förstermann, U. 2013. Uncoupling of endothelial NO synthase in atherosclerosis and vascular disease. *Current Opinion in Pharmacology*. 13(2):161–167.

Li, E.C., Heran, B.S. & Wright, J.M. 2014. Angiotensin converting enzyme (ACE) inhibitors versus angiotensin receptor blockers for primary hypertension. *Cochrane Database Syst Rev*. 8.

Li, H., Horke, S. & Förstermann, U. 2013. Oxidative stress in vascular disease and its pharmacological prevention. *Trends in Pharmacological Sciences*. 34(6):313–319.

Li, H., Horke, S. & Förstermann, U. 2014. Vascular oxidative stress, nitric oxide and atherosclerosis. *Atherosclerosis*. 237(1):208–219.

Liu, R.H. 2003. Health benefits of fruit and vegetables are from additive and synergistic combinations of phytochemicals. In Vol. 78. American Society for Nutrition *American Journal of Clinical Nutrition*. 517S–520S.

Lobato, N.S., Filgueira, F.P., Akamine, E.H., Tostes, R.C., Carvalho, M.H.C. & Fortes, Z.B. 2012. Mechanisms of endothelial dysfunction in obesity-associated hypertension. *Brazilian Journal of Medical and Biological Research*. 45(5):392–400.

Lozano, I., Van der Werf, R., Bietiger, W., Seyfritz, E., Peronet, C., Pinget, M., Jeandidier, N., Maillard, E., et al. 2016. High-fructose and high-fat diet-induced disorders in rats: impact on diabetes risk, hepatic and vascular complications. *Nutrition & Metabolism*. 13(1):15.

Lteif, A.A., Han, K. & Mather, K.J. 2005. Obesity, insulin resistance, and the metabolic syndrome: determinants of endothelial dysfunction in whites and blacks. *Circulation*. 112(1):32–38.

Lu, C., Su, L.Y., Lee, R.M.K.W. & Gao, Y.J. 2010. Mechanisms for perivascular adipose tissue-mediated potentiation of vascular contraction to perivascular neuronal stimulation: The role of adipocyte-derived angiotensin II. *European Journal of Pharmacology*. 634(1–3):107–112.

Machleidt, F., Simon, P., Krapalis, A.F., Hallschmid, M., Lehnert, H. & Sayk, F. 2013. Experimental hyperleptinemia acutely increases vasoconstrictory sympathetic nerve activity in healthy humans. *Journal of Clinical Endocrinology and Metabolism*. 98(3):491–496.

Marklund, S. 1980. Distribution of CuZn superoxide dismutase and Mn superoxide dismutase in human tissues and extracellular fluids. *Acta physiologica Scandinavica. Supplementum*. 492:19–23.

Marnewick, J.L., Rautenbach, F., Venter, I., Neethling, H., Blackhurst, D.M., Wolmarans, P. & Macharia, M. 2011. Effects of rooibos (*Aspalathus linearis*) on oxidative stress and biochemical parameters in adults at risk for cardiovascular disease. *Journal of ethnopharmacology*. 133(1):46–52.

Marroquí, L., Gonzalez, A., Ñeco, P., Caballero-Garrido, E., Vieira, E., Ripoll, C., Nadal, A. & Quesada, I. 2012. Role of leptin in the pancreatic β-cell: effects and signaling pathways. *Journal of molecular endocrinology*. 49(1):R9-17.

Mazibuko, S.E., Joubert, E., Johnson, R., Louw, J., Opoku, A.R. & Muller, C.J.F. 2015. Aspalathin improves glucose and lipid metabolism in 3T3-L1 adipocytes exposed to palmitate. *Molecular Nutrition and Food Research*. 59(11):2199–2208.

Mendis, S., Puska, P. & Norrving, B. 2011. Global Atlas on cardiovascular disease prevention and control. *World Health Organization*. 164.

Van Der Merwe, J.D., De Beer, D., Joubert, E. & Gelderblom, W.C.A. 2015. Short-term and sub-chronic dietary exposure to aspalathin-enriched green rooibos (*Aspalathus linearis*) extract affects rat liver function and antioxidant status. *Molecules*. 20(12):22674–22690.

Mikami, N., Tsujimura, J., Sato, A., Narasada, A., Shigeta, M., Kato, M., Hata, S. & Hitomi, E. 2015. Green Rooibos Extract from *Aspalathus linearis*, and its Component, Aspalathin, Suppress Elevation of Blood Glucose Levels in Mice and Inhibit α-amylase and α-glucosidase Activities *in vitro*. *Food Science and Technology Research*. 21(2):231–240.

Milagro, F.I., Campión, J. & Martíez, J.A. 2006. Weight gain induced by high-fat feeding involves increased liver oxidative stress. *Obesity*. 14(7):1118–1123.

Mittal, P.C. & Kant, R. 2009. Correlation of increased oxidative stress to body weight in disease-free post menopausal women. *Clinical Biochemistry*. 42(10–11):1007–1011.

Mittendorfer, B., Magkos, F., Fabbrini, E., Mohammed, B.S. & Klein, S. 2009. Relationship between body fat mass and free fatty acid kinetics in men and women. *Obesity (Silver Spring, Md.)*. 17(10):1872–7.

Mollentze, W.F. 2006. Obesity in South Africa : A call for action. *Jemdsa*. 11(2):44–45.

Mudau, M., Genis, A., Lochner, A. & Strijdom, H. 2012. Endothelial dysfunction: the early predictor of atherosclerosis. *Cardiovascular journal of Africa*. 23(4):222–31.

Muller, C.J.F., Joubert, E., De Beer, D., Sanderson, M., Malherbe, C.J., Fey, S.J. & Louw, J. 2012. Acute assessment of an aspalathin-enriched green rooibos (*Aspalathus linearis*) extract with hypoglycemic

potential. *Phytomedicine*. 20(1):32–39.

Muniyappa, R. & Sowers, J.R. 2013. Role of insulin resistance in endothelial dysfunction. *Reviews in Endocrine and Metabolic Disorders*. 14(1):5–12.

Murer, S.B., Aeberli, I., Braegger, C.P., Gittermann, M., Hersberger, M., Leonard, S.W., Taylor, A.W., Traber, M.G., et al. 2014. Antioxidant Supplements Reduced Oxidative Stress and Stabilized Liver Function Tests but Did Not Reduce Inflammation in a Randomized Controlled Trial in Obese Children and Adolescents. *Journal of Nutrition*. 144(2):193–201.

Naderali, E.K., Pickavance, L.C., Wilding, J.P. & Williams, G. 2001. Diet-induced endothelial dysfunction in the rat is independent of the degree of increase in total body weight. *Clinical science (London, England : 1979)*. 100(6):635–41.

Naruse, K., Rask-Madsen, C., Takahara, N., Ha, S.W., Suzuma, K., Way, K.J., Jacobs, J.R., Clermont, A.C., et al. 2006. Activation of vascular protein kinase C-beta inhibits Akt-dependent endothelial nitric oxide synthase function in obesity-associated insulin resistance. *Diabetes*. 55(3):691–698.

Nikolaidis, M.G., Kyparos, A., Spanou, C., Paschalis, V., Theodorou, A.A. & Vrabas, I.S. 2012. Redox biology of exercise: an integrative and comparative consideration of some overlooked issues. *Journal of Experimental Biology*. 215(10):1615–1625.

Noblet, J.N., Owen, M.K., Goodwill, A.G., Sassoon, D.J. & Tune, J.D. 2015. Lean and Obese Coronary Perivascular Adipose Tissue Impairs Vasodilation via Differential Inhibition of Vascular Smooth Muscle K+ Channels. *Arteriosclerosis, thrombosis, and vascular biology*. 35(6):1393–400.

Oswal, A. & Yeo, G. 2010. Leptin and the Control of Body Weight: A Review of Its Diverse Central Targets, Signaling Mechanisms, and Role in the Pathogenesis of Obesity. *Obesity*. 18(2):221–229.

Pamplona, R. & Costantini, D. 2011. Molecular and structural antioxidant defenses against oxidative stress in animals. *AJP: Regulatory, Integrative and Comparative Physiology*. 301(4):R843–R863.

Pennathur, S. & Heinecke, J.W. 2007. Oxidative stress and endothelial dysfunction in vascular disease. *Current Diabetes Reports*. 7(4):257–264.

Persson, I.A.L. 2012. The pharmacological mechanism of angiotensin-converting enzyme inhibition by green tea, Rooibos and enalaprilat - A study on enzyme kinetics. *Phytotherapy Research*. 26(4):517–521.

Persson, I.A.-L., Josefsson, M. & Andersson, R.G.G. 2006. Tea flavanols inhibit angiotensin-converting enzyme activity and increase nitric oxide production in human endothelial cells. *Journal of Pharmacy and Pharmacology*. 58(8):1139–1144.

Persson, I.A.L., Persson, K., Hägg, S. & Andersson, R.G.G. 2010. Effects of green tea, black tea and Rooibos tea on angiotensin-converting enzyme and nitric oxide in healthy volunteers. *Public health nutrition*. 13(5):730–737.

Pessin, J.E. & Saltiel, A.R. 2000. Signaling pathways in insulin action: Molecular targets of insulin resistance.

Journal of Clinical Investigation. 106(2):165–169.

Pober, J.S. & Sessa, W.C. 2007. Evolving functions of endothelial cells in inflammation. *Nature Reviews Immunology*. 7(10):803–815.

Polimeni, L., Del Ben, M., Baratta, F., Perri, L., Albanese, F., Pastori, D., Violi, F. & Angelico, F. 2015. Oxidative stress: New insights on the association of non-alcoholic fatty liver disease and atherosclerosis. *World journal of hepatology*. 7(10):1325–36.

Pourova, J., Kottova, M., Voprsalova, M. & Pour, M. 2010. Reactive oxygen and nitrogen species in normal physiological processes. *Acta Physiologica*. 198(1):15–35.

Prieto, D., Contreras, C. & Sánchez, A. 2014. Endothelial dysfunction, obesity and insulin resistance. *Current vascular pharmacology*. 12(3):412–26.

Putnam, K., Shoemaker, R., Yiannikouris, F. & Cassis, L.A. 2012. The renin-angiotensin system: a target of and contributor to dyslipidemias, altered glucose homeostasis, and hypertension of the metabolic syndrome. *AJP: Heart and Circulatory Physiology*. 302(6):H1219–H1230.

Rader, D.J. 2007. Effect of Insulin Resistance, Dyslipidemia, and Intra-abdominal Adiposity on the Development of Cardiovascular Disease and Diabetes Mellitus. *American Journal of Medicine*. 120(3 SUPPL. 1):12–18.

Rajendran, P., Rengarajan, T., Thangavel, J., Nishigaki, Y., Sakthisekaran, D., Sethi, G. & Nishigaki, I. 2013. The vascular endothelium and human diseases. *International Journal of Biological Sciences*. 9(10):1057–1069.

Ratzan, S.C. 2009. Editorial: Obesity-The facts are now in-Now what to do. *Journal of Health Communication*. 14(7):609–611.

Reccia, I., Kumar, J., Akladios, C., Virdis, F., Pai, M., Habib, N. & Spalding, D. 2017. Non-alcoholic fatty liver disease: A sign of systemic disease. *Metabolism: clinical and experimental*. 72:94–108.

Del Rio, D., Agnoli, C., Pellegrini, N., Krogh, V., Brighenti, F., Mazzeo, T., Masala, G., Bendinelli, B., et al. 2011. Total antioxidant capacity of the diet is associated with lower risk of ischemic stroke in a large Italian cohort. *J Nutr*. 141(1):118–123.

Ritchie, S.A. & Connell, J.M.C. 2007. The link between abdominal obesity, metabolic syndrome and cardiovascular disease. *Nutrition, Metabolism and Cardiovascular Diseases*. 17(4):319–326.

Rizos, C. V. 2014. Antihypertensive drugs and glucose metabolism. *World Journal of Cardiology*. 6(7):517.

Ruhl, C.E. & Everharty, J.E. 2003. Determinants of the association of overweight with elevated serum alanine aminotransferase activity in the United States. *Gastroenterology*. 124(1):71–79.

Salie, R., Huisamen, B. & Lochner, A. 2014. High carbohydrate and high fat diets protect the heart against ischaemia/reperfusion injury. *Cardiovascular Diabetology*. 13(1):109.

Sanderson, M., Mazibuko, S.E., Joubert, E., De Beer, D., Johnson, R., Pheiffer, C., Louw, J. & Muller, C.J.F. 2014. Effects of fermented rooibos (*Aspalathus linearis*) on adipocyte differentiation. *Phytomedicine*. 21(2):109–117.

Sandoo, A., van Zanten, J.J.C.S.V., Metsios, G.S., Carroll, D. & Kitas, G.D. 2010. The endothelium and its role in regulating vascular tone. *The open cardiovascular medicine journal*. 4:302–12.

Savini, I., Catani, M.V., Evangelista, D., Gasperi, V. & Avigliano, L. 2013. Obesity-associated oxidative stress: Strategies finalized to improve redox state. *International Journal of Molecular Sciences*. 14(5):10497–10538.

Scherz-Shouval, R. & Elazar, Z. 2011. Regulation of autophagy by ROS: Physiology and pathology. *Trends in Biochemical Sciences*. 36(1):30–38.

Schulz, H., Joubert, E. & Schütze, W. 2003. Quantification of quality parameters for reliable evaluation of green rooibos (*Aspalathus linearis*). *European Food Research and Technology*. 216(6):539–543.

Seidell, J.C. & Flegal^, K.M. 1997. Assessing obesity: classification and epidemiology. *Britiih Council Britijh M.dical Bulletin*. 53(2):23–252.

Sena, C.M., Pereira, A.M. & Seiça, R. 2013. Endothelial dysfunction - A major mediator of diabetic vascular disease. *Biochimica et Biophysica Acta - Molecular Basis of Disease*. 1832(12):2216–2231.

Shapiro, A., Mu, W., Roncal, C., Cheng, K.-Y., Johnson, R.J. & Scarpace, P.J. 2008. Fructose-induced leptin resistance exacerbates weight gain in response to subsequent high-fat feeding. *AJP: Regulatory, Integrative and Comparative Physiology*. 295(5):R1370–R1375.

Skurk, T., Alberti-Huber, C., Herder, C. & Hauner, H. 2007. Relationship between adipocyte size and adipokine expression and secretion. *Journal of Clinical Endocrinology and Metabolism*. 92(3):1023–1033.

Snijman, P.W., Swanevelder, S., Joubert, E., Green, I.R. & Gelderblom, W.C.A. 2007. The antimutagenic activity of the major flavonoids of rooibos (*Aspalathus linearis*): Some dose-response effects on mutagen activation-flavonoid interactions. *Mutation Research - Genetic Toxicology and Environmental Mutagenesis*. 631(2):111–123.

Son, M.J., Minakawa, M., Miura, Y. & Yagasaki, K. 2013. Aspalathin improves hyperglycemia and glucose intolerance in obese diabetic ob/ob mice. *European journal of nutrition*. 52(6):1607–1619.

Srinivasan, K., Viswanad, B., Asrat, L., Kaul, C.L. & Ramarao, P. 2005. Combination of high-fat diet-fed and low-dose streptozotocin-treated rat: A model for type 2 diabetes and pharmacological screening. *Pharmacological Research*. 52(4):313–320.

Stern, M.P., Williams, K. & Haffner, S.M. 2002. Identification of persons at high risk for type 2 diabetes mellitus: Do we need the oral glucose tolerance test? *Annals of Internal Medicine*. 136(8):575–581.

Steyn, K. & Fourie, J.M. 2007. The Heart and Stroke Foundation South Africa Heart Disease in South Africa

Compiled by Department of Medicine , University of Cape Town & Chronic Diseases of Lifestyle Unit , at the Medical Research Council Edited by Chronic Diseases of Lifestyle Unit , M. *The Lancet*. (July).

Steyn, K., Gaziano, T.A., Bradshaw, D., Laubscher, R. & Fourie, J. 2001. Hypertension in South African adults: results from the Demographic and Health Survey, 1998. *Journal of hypertension*. 19(10):1717–25.

Strijdom, H. & Lochner, A. 2009. Cardiac endothelium : More than just a barrier. *SAHeart*. 6:174–185.

Strijdom, H., Chamane, N. & Lochner, A. 2009. Nitric oxide in the cardiovascular system: a simple molecule with complex actions. *Cardiovascular journal of Africa*. 20(5):303–10.

Sud, N. & Black, S.M. 2009. Endothelin-1 Impairs Nitric Oxide Signaling in Endothelial Cells Through a Protein Kinase Cδ-Dependent Activation of STAT3 and Decreased Endothelial Nitric Oxide Synthase Expression. *DNA and Cell Biology*. 28(11):543–553.

Tang, E.H.C. & Vanhoutte, P.M. 2010. Endothelial dysfunction: A strategic target in the treatment of hypertension? *Pflugers Archiv European Journal of Physiology*. 459(6):995–1004.

Taniguchi, C.M., Emanuelli, B. & Kahn, C.R. 2006. Critical nodes in signalling pathways: insights into insulin action. *Nature Reviews Molecular Cell Biology*. 7(2):85–96.

Thethi, T., Kamiyama, M. & Kobori, H. 2012. The link between the renin-angiotensin-aldosterone system and renal injury in obesity and the metabolic syndrome. *Current hypertension reports*. 14(2):160–169.

Todorovic, M. & Mellick, G.D. 2015. TOP 1% Selection of our books indexed in the Book Citation Index in Web of Science™ Core Collection (BKCI) Chapter from the book A Master Regulator of Oxidative Stress -The Transcription Factor Nrf2 Nrf2 and Parkinson's Disease Nrf2 and Parkinson's Diseas. 3. [Online], Available: http://www.intechopen.com/books/basic-principles-and-clinical-significance-of-oxidative-stress [2017, November 09].

Tran, B., Oliver, S., Rosa, J. & Galassetti, P. 2012. Aspects of inflammation and oxidative stress in pediatric obesity and type 1 diabetes: An overview of ten years of studies. *Experimental Diabetes Research*. 2012:1–7.

Turner, N. 2013. Mitochondrial Metabolism and Insulin Action. In InTech *Type 2 Diabetes*. 71–114.

Valko, M., Rhodes, C.J., Moncol, J., Izakovic, M. & Mazur, M. 2006. Free radicals, metals and antioxidants in oxidative stress-induced cancer. *Chemico-Biological Interactions*. 160(1):1–40.

Valko, M., Leibfritz, D., Moncol, J., Cronin, M.T.D., Mazur, M. & Telser, J. 2007. Free radicals and antioxidants in normal physiological functions and human disease. *The International Journal of Biochemistry & Cell Biology*. 39(1):44–84.

Vanhoutte, P.M., Shimokawa, H., Tang, E.H.C. & Feletou, M. 2009. Endothelial dysfunction and vascular disease. *Acta Physiologica*. 196(2):193–222.

Veyrat-Durebex, C., Poher, A.L., Caillon, A., Somm, E., Vallet, P., Charnay, Y. & Rohner-Jeanrenaud, F. 2013. Improved Leptin Sensitivity as a Potential Candidate Responsible for the Spontaneous Food Restriction of the Lou/C Rat. *PLoS ONE*. 8(9):1–11.

Villaño, D., Pecorari, M., Testa, M.F., Raguzzini, A., Stalmach, A., Crozier, A., Tubili, C. & Serafini, M. 2010. Unfermented and fermented rooibos teas (*Aspalathus linearis*) increase plasma total antioxidant capacity in healthy humans. *Food Chemistry*. 123(3):679–683.

Virdis, A., Duranti, E., Rossi, C., Dell'Agnello, U., Santini, E., Anselmino, M., Chiarugi, M., Taddei, S., et al. 2015. Tumour necrosis factor-alpha participates on the endothelin-1/nitric oxide imbalance in small arteries from obese patients: role of perivascular adipose tissue. *European Heart Journal*. 36(13):784–794.

Viroonudomphol, D., Pongpaew, P., Tungtrongchitr, R., Phonrat, B., Supawan, V., Vudhivai, N. & Schelp, F.P. 2000. Erythrocyte antioxidant enzymes and blood pressure in relation to overweight and obese Thai in Bangkok. *Southeast Asian Journal of Tropical Medicine and Public Health*. 31(2):325–334.

Wang, J., Obici, S., Morgan, K., Barzilai, N., Feng, Z. & Rossetti, L. 2001. Overfeeding Rapidly Induces Leptin and Insulin Resistance. *Diabetes*. 50.

Wang, T.J., Larson, M.G., Levy, D., Benjamin, E.J., Leip, E.P., Wilson, P.W.F. & Vasan, R.S. 2004. Impact of Obesity on Plasma Natriuretic Peptide Levels. *Circulation*. 109(5):594–600.

Weil, B.R., Westby, C.M., Van Guilder, G.P., Greiner, J.J., Stauffer, B.L. & DeSouza, C.A. 2011. Enhanced endothelin-1 system activity with overweight and obesity. *American journal of physiology. Heart and circulatory physiology*. 301(3):H689-95.

Wells, W.W. & Xu, D.P. 1994. Dehydroascorbate reduction. *Journal of Bioenergetics and Biomembranes*. 26(4):369–377.

Weng, C.J. & Yen, G.C. 2012. Chemopreventive effects of dietary phytochemicals against cancer invasion and metastasis: Phenolic acids, monophenol, polyphenol, and their derivatives. *Cancer Treatment Reviews*. 38(1):76–87.

WHO, Federation, W.H. & World Stroke Organization. 2011. Global Atlas on cardiovascular disease prevention and control.

Wolin, M.S. 2000. Interactions of oxidants with vascular signaling systems. *Arteriosclerosis, thrombosis, and vascular biology*. 20(6):1430–42.

World Health Organisation. 2011. WHO | *About cardiovascular diseases*. [Online], Available: http://www.who.int/mediacentre/factsheets/fs317/en/ [2017, November 09].

World Health Organisation. 2017. *Noncommunicable diseases*. [Online], Available: http://www.who.int/mediacentre/factsheets/fs355/en/ [2017, October 24].

World Health Organization. 2017. WHO | *Noncommunicable diseases*. [Online], Available:

http://www.who.int/mediacentre/factsheets/fs355/en/ [2017, November 09].

World Health Organization. 2014. *Global status report on noncommunicable diseases 201 4 " Attaining the nine global noncommunicable diseases targets; a shared responsibility "* [Online], Available: http://apps.who.int/iris/bitstream/10665/148114/1/9789241564854_eng.pdf?ua=1 [2017, November 09].

World Health Organization. 2017. WHO | *Obesity and overweight*. [Online], Available: http://www.who.int/mediacentre/factsheets/fs311/en/ [2017, November 20].

Wozniak, S.E., Gee, L.L., Wachtel, M.S. & Frezza, E.E. 2009. Adipose tissue: The new endocrine organ? a review article. *Digestive Diseases and Sciences*. 54(9):1847–1856.

Xia, N. & Li, H. 2017. The role of perivascular adipose tissue in obesity-induced vascular dysfunction. *British Journal of Pharmacology*. 174(20):3425–3442.

Xia, N., Weisenburger, S., Koch, E., Burkart, M., Reifenberg, G., Förstermann, U. & Li, H. 2017. Restoration of perivascular adipose tissue function in diet-induced obese mice without changing bodyweight. *British Journal of Pharmacology*. 174(20):3443–3453.

Yanai, H., Tomono, Y., Ito, K., Furutani, N., Yoshida, H. & Tada, N. 2008. The underlying mechanisms for development of hypertension in the metabolic syndrome. *Nutrition Journal*. 7(1):1.

Yang, Y.-M., Huang, A., Kaley, G. & Sun, D. 2009. eNOS uncoupling and endothelial dysfunction in aged vessels. *American Journal of Physiology-Heart and Circulatory Physiology*. 297(5):H1829–H1836.

Zhang, H., Dellsperger, K.C. & Zhang, C. 2012. The link between metabolic abnormalities and endothelial dysfunction in type 2 diabetes: an update. *Basic research in cardiology*. 107(1):1–11.

Zhang, Y., Lee, T.-S., Kolb, E.M., Sun, K., Lu, X., Sladek, F.M., Kassab, G.S., Garland, T., et al. 2006. AMP-activated protein kinase is involved in endothelial NO synthase activation in response to shear stress. *Arteriosclerosis, thrombosis, and vascular biology*. 26(6):1281–7.

Zmijewski, J.W., Banerjee, S., Bae, H., Friggeri, A., Lazarowski, E.R. & Abraham, E. 2010. Exposure to hydrogen peroxide induces oxidation and activation of AMP-activated protein kinase. *Journal of Biological Chemistry*. 285(43):33154–33164.